EUROPEAN CENTRAL BANK
EUROSYSTEM

Working Paper Series

Andrea Caggese, Andrea Chiavari,
Sampreet Singh Goraya,
Carolina Villegas-Sanchez

Climate change, firms, and aggregate productivity

No 3084

Abstract: This paper uses a general equilibrium framework to examine the effects of temperature on firm-level demand, productivity, and input allocation efficiency, deriving an aggregate damage function for climate change. Using data from Italian firms and detailed climate data, it uncovers a sizable negative effect of extreme temperatures on firm-level productivity and revenue-based marginal product of capital. Based on these estimates, the model generates aggregate productivity losses from local temperature fluctuations that are higher than previously thought, ranging from 0.60 to 6.82 percent depending on the scenario and the extent of adaptation. Notably, these losses are approximately four times greater than those estimated by averaging firm-level losses in a representative firm model, which does not capture frictions that alter allocative efficiency in a heterogeneous firm setting. Therefore, incorporating our framework into Integrated Assessment Models is likely to revise upwards the estimated economic costs of climate change.

Keywords: Climate Change, Aggregate Productivity, Firms, Allocative Efficiency.

JEL Codes: Q54, D24, D22, O44

Non-Technical Summary

Climate change is altering global economic conditions, but its impact on firm productivity remains poorly understood. This study examines how rising temperatures affect businesses by linking firm-level data to aggregate economic damages. The central insight is that temperature influences firm productivity through two key channels: direct effects, such as lower worker efficiency or machinery performance, and indirect effects, which arise when firms face difficulties adjusting inputs like capital or labor in response to climate shifts.

A key contribution of the study is demonstrating that input adjustment frictions significantly amplify the productivity costs of climate change. For example, when firms cannot quickly scale down capital in response to lower productivity, they experience inefficiencies, leading to larger aggregate economic losses than previously estimated. This finding challenges traditional climate-economy models, which tend to underestimate the long-term economic costs of warming.

Using firm-level data from Italy (1999–2013) and high-resolution climate records, the study quantifies these effects. Results show an inverted U-shaped relationship between temperature and firm productivity: moderate temperatures have little impact, but extreme heat significantly lowers firm sales and input efficiency. Importantly, firms struggle to adjust capital in response to climate shocks, leading to indirect effects that double the estimated economic damages.

The study's findings have major policy implications. First, they suggest that existing climate damage estimates may be too low because they fail to account for input rigidity and misallocation. Second, because climate change affects regions differently, it may widen economic inequality, particularly between areas with different adaptation capacities. Third, policies that improve firms' ability to adjust inputs—such as investment in climate-resilient infrastructure—could mitigate productivity losses.

By integrating firm-level insights into macroeconomic models, this study provides a new approach to measuring the true economic cost of climate change. The results suggest that aggregate productivity losses from rising temperatures may be significantly larger than previously thought.

1 Introduction

The rising levels of CO_2 in the atmosphere are significantly increasing global temperatures and altering weather patterns, leading to climate change (IPCC, 2021). Since Nordhaus (1977), with its latest version in Barrage and Nordhaus (2023), the literature has relied on Integrated Assessment Models (IAMs) to quantify the aggregate costs of climate change, the social cost of carbon, and explore the potential for policy interventions. This approach extends the standard neoclassical growth model by incorporating climate-induced economic losses through an *aggregate damage function*, which links aggregate productivity to temperature changes within the standard aggregate production function. Despite the aggregate damage function being a key component of IAMs, no consensus has yet emerged regarding its measurement.

In this paper, we develop a microfounded aggregate damage function grounded in firm-level analysis, offering a framework for its measurement and making three contributions. First, we introduce a micro-to-macro framework that links firm-level damages from temperature increases to aggregate productivity, emphasizing two channels: a direct effect that reduces productivity and/or demand and an indirect effect arising from input adjustment frictions. Second, using standard firm-level data, we provide causal estimates of both direct and indirect effects. To the best of our knowledge, this is the first study to offer causal evidence of significant indirect effects driven by frictions in firm-level capital adjustment. Finally, we show that the channels identified in our framework result in substantial aggregate productivity damages. Both direct and indirect effects play equally important roles, with considerable heterogeneity in productivity damages, even within narrowly defined geographic regions.

Our framework models monopolistically competitive heterogeneous firms producing with capital, labor, and materials, with their scale of operations *directly* influenced by local temperature through its effects on productivity and demand. This relationship captures several well-documented channels through which temperature impacts firms. For instance, temperature may reduce labor efficiency via its effects on workers' performance, attendance, or health. Similarly, it may lower capital productivity as machinery and equipment operate less efficiently under extreme conditions. Additionally, temperature can shift consumer spending patterns and local demand, particularly for non-tradable goods consumed locally.[1]

However, these direct effects do not fully account for the total productivity losses incurred by firms. When frictions—such as adjustment costs or spatial and financial constraints—limit

[1]The demand-side impacts of temperature are underscored in Busse et al. (2015) for the case of durable goods, while its effects on productivity have been explored extensively (e.g., Seppanen et al., 2006; Zhang et al., 2018; Somanathan et al., 2021), as summarized in Heal and Park (2016) and Lai et al. (2023).

firms' ability to adjust their inputs in response to temperature changes, firms may be compelled to retain inputs they would otherwise discard. For example, frictions that constrain the adjustment of capital may lead some firms to hold excess capital while maintaining optimal levels of labor and materials. As a result, the revenue-based marginal product of capital declines due to the law of diminishing returns, as the excess capital contributes less output at the margin. Consequently, the direct effects of temperature changes can be amplified by the presence of such frictions. To fix ideas, consider the following illustrative example: an extreme temperature event hits half of the regions in a country, such that firms are unable to operate 20% of the time, and their output falls by 20%. In a hypothetical scenario where all firms can adjust their inputs costlessly and operate under constant returns to scale, aggregate productivity would remain unaffected. Conversely, in a scenario where unaffected firms can scale up to meet demand but affected firms are unable to reduce their inputs, aggregate productivity would decline by approximately 10%.[2] To capture this *indirect* effect, we introduce reduced-form, input-specific wedges, following Restuccia and Rogerson (2008) and Hsieh and Klenow (2009). These wedges, which we allow to vary with temperature, capture the gap between an input's revenue-based marginal product and its user cost, influencing the relative use of each input in response to temperature changes.

Our model shows that, at the firm level, productivity losses are driven by the temperature-semielasticity of two factors: firm sales and the revenue-based marginal product of inputs. Through the lens of the model, these semielasticities allow us to separately identify and quantify both direct and indirect effects. At the macro level, the model introduces a novel closed-form characterization of the aggregate productivity damage function, linking it to the firm-level temperature-semielasticities. Direct effects reflect how firm-level productivity contributes to aggregate productivity, while indirect effects emerge from frictions that distort input allocation within the economy. Crucially, our methodology does not rely on aggregate equilibrium prices, ensuring robustness to general equilibrium considerations.

We demonstrate how to implement our framework using the Italian case, which represents an ideal setting given its unique characteristics. Italy frequently experiences episodes of very high temperatures—with European temperatures rising at more than twice the global average over the past 30 years[3]—and exhibits substantial regional variation in both climate and economic development. The study merges firm-level data from Orbis (1999-2013), which

[2]Intuitively, affected firms, unable to reduce inputs, face a 20% productivity decline. Unaffected firms meet demand by scaling up their inputs, without a loss in productivity. Aggregate productivity then falls substantially, reflecting the weighted average of productivity across affected and unaffected firms.
[3]Source: Report on the State of the Climate in Europe, 2021, by the World Meteorological Organization.

covers approximately 75% of Italy's aggregate gross output (Kalemli-Özcan et al., 2024), with climate data from Copernicus Climate Change Services. The climate data provides daily temperature and rainfall measurements at an approximately 11x11 km grid resolution. Firms are matched to climate data based on their headquarters' postcode location.[4]

Empirically, we adopt the firm-level methodology of Somanathan et al. (2021), aggregating daily temperatures at each grid point to the annual level by counting the number of days within different temperature ranges, as in Deschênes and Greenstone (2011).[5] Our analysis reveals an inverted U-shaped effect of temperature on sales, where extremely high or low temperatures negatively impact firms. We also find that extreme temperatures reduce labor and material inputs but not capital usage among affected firms, suggesting more significant frictions to capital adjustment than to other inputs. As a result, we estimate an inverted U-shaped relationship between extreme temperatures and the revenue-based marginal product of capital, with no significant impact on the marginal products of other inputs. This captures the indirect effect of temperature on firms. Finally, while distinguishing between productivity and demand effects is not essential for the quantitative aggregation exercise, understanding their relative importance is valuable. To explore this, we assume, based on trade literature, that temperature impacts productivity similarly across tradable and non-tradable firms but affects demand for non-tradable goods more due to their local consumption.[6] Our findings show no significant differences in temperature effects between tradable and non-tradable sectors, suggesting that temperature primarily impacts firms through productivity rather than demand.

Quantitatively, we construct the aggregate damage function by integrating the closed-form characterization derived from our framework with the reduced-form causal estimates of the direct and indirect effects of temperature at the firm level, from the estimated semi-elasticities. Under a 2℃ rise in average yearly temperature, aggregate productivity declines by 1.68%, with direct effects contributing a 0.81% drop and indirect effects accounting for 0.87%. This indicates that both effects are quantitatively significant. Our approach reveals a highly nonlinear relationship between temperature and aggregate productivity, driven by the inverted U-shaped patterns observed at the firm level. In particular, for a 4℃ increase, productivity falls by 6.81%, more than four times the decline under 2℃. This non-linearity is

[4]Most of our sample comprises single-establishment small and medium-sized firms, and robustness checks confirm that the results are not influenced by larger firms or those with multiple establishments.
[5]Alternative approaches, such as the degree-day method or nonlinear average yearly temperature from Burke et al. (2015), yield similar results.
[6]For instance, Almunia et al. (2021) document lower demand sensitivity for tradable goods.

caused by a combination of the non-linear impact of temperature on firm-level productivity, and the wider geographic spread of extreme temperatures in the 4℃ increase scenario.

We highlight the added value of our micro-to-macro approach to measure the aggregate damage function by contrasting its predictions with those from firm-level studies and IAMs. Firm-level studies (e.g., Zhang et al., 2018; Somanathan et al., 2021) typically estimate firm-level losses based on simple average temperature scenarios using a representative firm framework. This approach, when applied to our firm-level estimates, predicts a decline in aggregate productivity of 0.39%, which is significantly less than our model-based estimate of 1.68%. We show that the novel indirect channel is quantitatively important, accounting for as much as 68% of this difference. The remaining difference stems from two key factors. First, the roundabout nature of material production, where materials are produced using output (Jones, 2011). Initial productivity losses reduce output, which in turn lowers material production, creating a feedback loop that amplifies the impact—a multiplier effect. Second, the covariance between efficient firm-level weights and estimated productivity losses. A higher covariance indicates that temperature-related productivity damages are concentrated in regions with larger firms.

How do our results contribute to the quantification of aggregate economic damages from climate change? Traditional IAMs incorporate temperature effects through aggregate damage functions that reduce productivity as temperatures rise (e.g. see Barrage and Nordhaus, 2023). The appropriate parametrization of these functions is key to evaluate the social cost of climate change. Among the recent literature advancing on this issue, the spatial integrated models (S-IAMs) pioneered by Desmet and Rossi-Hansberg (2015) have made important contributions by incorporating forward-looking agents and firms (e.g. see Conte et al., 2022, Cruz and Rossi-Hansberg, 2023 and Bilal and Rossi-Hansberg, 2023). These studies offer new insights into the relationship between climate change-induced extreme events and aggregate damages by considering reallocation effects across locations and adaptation through migration and capital accumulation. However, they do not address heterogeneous firm level effects. Our approach is complementary to this literature. First, we highlight new sources of productivity damages, including not only direct firm-level productivity effects but also indirect effects driven by adjustment frictions. Second, our methodology provides a closed-form solution that maps these firm-level outcomes to their aggregate implications, offering a framework that could be integrated into future IAMs. Our results suggest that incorporating these effects revises upwards the estimated economic costs of climate change and the social cost of carbon.[7] In

[7]Like the studies mentioned above, our paper estimates the effects of local temperature fluctuations on local economic outcomes. We view this approach as complementary to studying the effects of global temperature

particular, our methodology is likely to be especially important when using micro-level data to evaluate the aggregate productivity effects of climate shocks in less developed countries, where firm-level frictions—affecting both capital and labor—are typically more pronounced than in developed countries like Italy.

We conclude the analysis by examining two scenarios that could amplify or mitigate our main findings. First, we assess the role of firm-level adaptation in shaping our estimates. By comparing areas historically exposed to extreme temperatures—likely already adapted—to areas newly experiencing such extremes, we find that climate-mitigating technologies can reduce damages by 20–30%. Second, we construct aggregate damage functions at the NUTS3 level to explore the regional impact of climate change on productivity across Italian provinces. This analysis reveals heterogeneous effects, ranging from mildly positive to severely negative outcomes. Notably, as poorer southern regions are expected to face greater shifts toward extreme temperature ranges, climate change is likely to exacerbate existing regional inequalities in Italy. Our findings underscore this dynamic by showing a negative relationship between expected productivity losses and current GDP per capita.

Finally, we discuss some limitations of our framework and interpret the results. First, our static framework does not account for the extensive margin, such as firm entry and exit, which could influence the outcomes. For example, unproductive firms may exit affected regions, improving the selection of firms, or firms might relocate to cooler areas, enhancing allocative efficiency. While our sample provides limited evidence for the latter, our analysis lays the groundwork for future models to address these dynamics. Second, the long-run effects of temperature on productivity may be mitigated as short-term capital adjustment frictions ease, leading to improved allocative efficiency. Although estimating these dynamics within our short panel is challenging, our framework offers an upper bound for aggregate productivity losses, providing insight into the potential long-term impacts of fully adjustable capital.

Literature Review. This paper contributes to the literature on firm heterogeneity that uses the reduced-form wedge approach to evaluate the aggregate productivity impacts of shocks, frictions, and policies, including studies by Restuccia and Rogerson (2008), Hsieh and Klenow (2009), Gopinath et al. (2017), Osotimehin (2019), and Baqaee and Farhi (2020). Building on this foundation, we analyze aggregate productivity losses under climate scenarios. Our work is

changes on global GDP (e.g., Bilal and Känzig, 2024). The global approach captures broader climate damages, such as more frequent droughts, extreme winds, and precipitation, but faces challenges in identifying causal effects due to confounding global factors. In contrast, panel data approaches that estimate the effects of local temperature shocks on local productivity, combined with model-based restrictions, improve causal identification and help reveal the specific channels through which temperature affects economic activity.

related to Bau and Matray (2023), who develop a framework to assess the effects of observed policies on aggregate productivity but without enabling counterfactual analysis, and Sraer and Thesmar (2023), who incorporate counterfactual analysis but focus solely on changes in frictions. We extend this literature by introducing a novel decomposition of aggregate productivity changes that facilitates counterfactual analysis in general equilibrium, capturing changes in productivity and frictions caused by shocks, using causally estimated firm-level semi-elasticities as inputs.

This paper also contributes to the growing body of research that leverages granular data and quantitative macroeconomic models to study the economic impacts of climate change (e.g., Desmet and Rossi-Hansberg, 2015; Barrage, 2020; Conte et al., 2022; Fried, 2022; Nath, 2024; Balboni et al., 2024; Castro-Vincenzi, 2022; Castro-Vincenzi et al., 2024). Unlike studies that focus on specific policies or the sectoral and regional dynamics of climate change, our contribution lies in microfounding the aggregate damage function at the firm level and developing an empirical framework for its measurement. Therefore, our work is closely related to the macro-climate literature employing Integrated Assessment Models (IAMs), pioneered by Nordhaus (1977) and further expanded in dynamic versions by Golosov et al. (2014), Krusell and Smith (2022), and Barrage and Nordhaus (2023). These studies calibrate aggregate damage functions to ensure that output losses align with historical temperature-induced changes in aggregate estimates (see Nordhaus and Moffat (2017) for a review).[8]

More recent contributions by Cruz and Rossi-Hansberg (2023) and Bilal and Rossi-Hansberg (2023) expand IAMs to account for the spatial implications of climate change, employing structural models that incorporate migration and capital accumulation to match observed regional losses with historical temperature changes. These IAMs are critical for understanding the dynamic responses to climate change, aggregate consequences, and the social cost of carbon. However, estimating the aggregate damage function—a core component—at country or regional levels remains challenging due to standard identification issues in aggregate regressions. These challenges include isolating pure productivity effects from policy responses to temperature changes or other confounding factors that operate at similar levels of aggregation. Our framework addresses these issues by enabling an exploration of firm-level mechanisms, distinguishing between direct productivity effects and indirect effects caused by input adjustment frictions. To achieve this, we utilize the input-specific wedges approach, which

[8]Empirical studies measuring aggregate output losses through cross-country regressions include Dell et al. (2012, 2014); Burke et al. (2015); Hsiang et al. (2017); Burke and Tanutama (2019); Kalkuhl and Wenz (2020); Kahn et al. (2021); Newell et al. (2021); Bastien-Olvera et al. (2022); Casey et al. (2023); Nath et al. (2024); Leduc and Wilson (2023); and Bilal and Känzig (2024).

allows for a detailed decomposition of these effects and their aggregate implications.

Finally, we contribute to the empirical literature that addresses the challenges of aggregate regressions by estimating causal losses using firm-level data and historical temperature changes. Notable examples include Zhang et al. (2018), Addoum et al. (2020), Somanathan et al. (2021), and Ponticelli et al. (2023).[9] While these studies address the empirical identification challenges of aggregate analyses, they face limitations in informing aggregate counterfactuals. Specifically, all general equilibrium effects remain unmeasured, as they are absorbed into the intercept—a limitation referred to as the "missing intercept problem" (Moll, 2021). In addition, to the best of our knowledge, we are the first to provide causal evidence of firm-level indirect effects driven by input adjustment frictions and their implications for productivity.

In summary, our micro-to-macro methodology, which estimates aggregate damages from their firm-level origins by combining empirically estimated semielasticities with a structural model incorporating input adjustment frictions, complements both the empirical micro-level climate change literature and recent advances in quantifying aggregate macroeconomic effects using state-of-the-art IAMs. Two novel insights emerge from our approach: (i) compared to standard IAM methodologies, our framework reveals quantitatively larger aggregate damages, suggesting greater economic losses from climate change; and (ii) compared to firm-level approaches, we provide the first evidence of an inverted U-shaped relationship between the revenue-based marginal product of capital and temperature, uncovering a new indirect channel through which temperature impacts firms, with significant implications for aggregate productivity.

Outline. The rest of the article is organized as follows. Section 2 describes a theoretical model. Section 3 describes data and measurement. Section 4 lays the empirical strategy. Section 5 presents the main results. Section 6 provides the aggregate effects. Section 7 concludes.

2 Structural Framework

In this section, we present a framework to microfound the impact of temperature on aggregate productivity—the aggregate damage function central to IAMs—through the different effects of temperature on firms.

[9] Other studies exploring the micro-level impact of climate change on other outcomes include Deschênes and Greenstone (2011), Kala et al. (2012), Graff Zivin and Neidell (2014), Cohn and Deryugina (2018), Diffenbaugh and Burke (2019), Colmer (2021), Albert et al. (2021), Pankratz and Schiller (2024), Custodio et al. (2024), Cascarano et al. (2022), Liu and Xu (2024), Balboni (2025) and Acharya et al. (2023).

2.1 Firm-Level Variables

We build our framework on a closed-economy version of Melitz (2003).[10] We consider an economy at time t populated by a large number N of monopolistically competitive firms i, producing differentiated varieties, and operating in a grid-cell g.[11] In this economy, aggregate output Y is a CES aggregate of N firms:

$$Y_t = \left(\sum_{i=1}^{N_t} \left(e^{d_{it}(T_{g(i)t})} Y_{it} \right)^{\frac{\sigma-1}{\sigma}} \right)^{\frac{\sigma}{\sigma-1}}, \tag{1}$$

where Y_{it} is the output of firm i, $e^{d_{it}(T_{g(i)t})}$ is a *temperature-dependent demand shifter* with $T_{g(i)t}$ being the temperature in a grid-cell g, and σ denotes the elasticity of substitution between varieties. The notation $g(i)$ means that the grid-cell g varies for different firms i. The presence of a temperature-dependent demand shifter, $e^{d_{it}(T_{g(i)t})}$, suggests that temperature changes in a given grid-cell can influence the demand faced by firms within that cell. Note that, since temperature fluctuations are spatially correlated across grid-cells, in our empirical analysis we show that our results are robust to using spatially adjusted standard errors based on the method proposed by Conley (2010). Furthermore, the functional form assumed for $d_{it}(T_{g(i)t})$, along with other temperature-dependent variables in the model, allows for the possibility that factors beyond grid-cell-level temperature may also affect demand. Section 4 details the specific functional forms used in the empirical analysis.

We denote by P_{it} the price of firm i and by P_t the price of aggregate output Y_t.[12] The demand faced by each firm i is given by

$$Y_{it} = \left(e^{d_{it}(T_{g(i)t})} \right)^{\sigma-1} \left(\frac{P_{it}}{P_t} \right)^{-\sigma} Y_t. \tag{2}$$

The production function of each firm is Cobb-Douglas in productivity, capital, labor, and materials:

$$Y_{it} = e^{z_{it}(T_{g(i)t})} \prod_{X \in \mathcal{X}} X_{it}^{\alpha^X}, \quad \text{with} \quad \sum_{X \in \mathcal{X}} \alpha^X = 1, \tag{3}$$

where $e^{z_{it}(T_{g(i)t})}$ is the *temperature-dependent productivity* for firm i in grid-cell g and $\mathcal{X} \equiv$

[10] The model is static, and firm decisions at time t do not depend on past choices, nor they affect future outcomes. For convenience, we introduce the time subscript from the outset, as it will be useful in the empirical application where we will be using panel data.

[11] The grid-cell is the finest geographical unit for which we have data on temperatures. It coincides with an area of 0.1deg^2, which corresponds approximately to 121km^2. This is approximately the size of Turin (130km^2) and $1/10th$ the size of Rome ($1,285\text{km}^2$). Section 3 describes the data in more detail.

[12] P_t is a CES aggregate of firm level prices P_{it}, as defined by equation 50 in Appendix A

$\{K, L, M\}$ with K being capital, L being labor, and M being materials. The term, $e^{z_{it}(T_{g(i)t})}$, implies that temperature changes in a given grid-cell may impact the productivity of firms operating within that cell. Under the Cobb-Douglas production function assumption, this term captures different forms of productivity, including both labor-augmenting and capital-augmenting productivity.

The problem of a firm is given by

$$\begin{aligned} \Pi_i &= \max_{\{P_{it}, Y_{it}\}} P_{it} Y_{it} - \mathcal{C}(Y_{it}), \\ \text{s.t.} \quad Y_{it} &= \left(e^{d_{it}(T_{g(i)t})}\right)^{\sigma-1} \left(\frac{P_{it}}{P_t}\right)^{-\sigma} Y_t; \end{aligned} \tag{4}$$

where

$$\mathcal{C}(Y_{it}) = \min_{X} \left\{ \sum_{X \in \mathcal{X}} e^{\tau_{it}^{X}(T_{g(i)t})} P_t^X X_{it} \quad \middle| \quad Y_{it} - e^{z_{it}(T_{g(i)t})} \prod_{X \in \mathcal{X}} X_{it}^{\alpha^X} \right\}, \tag{5}$$

where $e^{\tau_{it}^{X}(T_{g(i)t})}$ are *temperature-dependent input-specific wedges* for firm i in grid-cell g and P_t^X is the price of input X.

The model highlights two types of temperature-related effects: direct and indirect. The *direct* effect of temperature is represented by the temperature-dependent demand and productivity terms. The former captures potential changes in demand patterns across firms, as reported in Busse et al. (2015) for the case of durable goods purchases. The latter encompasses a range of effects. For example, recent research reviewed by Heal and Park (2016) and Lai et al. (2023) demonstrates that extreme temperatures impair labor productivity by affecting health, labor supply, and concentration.[13] Extreme heat may also reduce capital productivity, as suggested by case studies indicating that machines such as cell phones, data centers, cars, and lithium-ion batteries become less efficient at high temperatures (e.g., Garimella et al., 2023).

The *indirect* effect of temperature in the model is summarized by reduced-form wedges, as in Restuccia and Rogerson (2008) and Hsieh and Klenow (2009), representing frictions that affect the marginal products or costs of specific inputs, such as adjustment costs, spatial, and financial frictions. These frictions may be directly influenced by temperature, affecting the reduced-form wedge. Even if not directly impacted, their presence can constrain the adjustment of inputs in response to temperature-induced changes in demand or productivity, which would still manifest as changes in the wedges. For instance, in response to the direct effect of

[13] Additional evidence is provided by Gould et al. (2024) and Filomena and Picchio (2024) for Italy, while Somanathan et al. (2021) shows reduced productivity and increased absenteeism in Indian manufacturing plants during hot days.

extreme temperatures reducing demand or productivity, frictions that limit capital adjustment may cause some firms to hold excess capital but not labor or materials, resulting in a higher capital wedge without corresponding increases in labor or material wedges. Our objective is to estimate how these wedges respond to temperature changes and quantify their impact on aggregate productivity.

Profit maximization yields the standard condition that the firm's output price is a fixed markup over its marginal cost:

$$P_{it} = \mathcal{M} \cdot \mathcal{C}'(Y_{it}), \tag{6}$$

where $\mathcal{M} \equiv \sigma/(\sigma - 1)$. The solution of the minimization problem is given by

$$\mathcal{C}(Y_{it}) = \prod_{X \in \mathcal{X}} \left(\frac{e^{\tau_{it}^X(T_{g(i)t})} P_t^X}{\alpha^X} \right)^{\alpha^X} \frac{Y_{it}}{e^{z_{it}(T_{g(i)t})}}. \tag{7}$$

Combining equations (2), (6), and (7), firm i sales can hence be expressed just as a function of the primitives of the model as

$$P_{it}Y_{it} = \left(e^{\tilde{z}_{it}(T_{g(i)t})}\right)^{\sigma-1} \left(\mathcal{M} \prod_{X \in \mathcal{X}} \left(\frac{e^{\tau_{it}^X(T_{g(i)t})} P_t^x}{\alpha^X} \right)^{\alpha^X} \right)^{-(\sigma-1)} P_t^\sigma Y_t, \tag{8}$$

with

$$e^{\tilde{z}_{it}(T_{g(i)t})} \equiv e^{d_{it}(T_{g(i)t})} e^{z_{it}(T_{g(i)t})}, \tag{9}$$

where $e^{\tilde{z}_{it}(T_{g(i)t})}$ is defined through the rest of the paper as the firm level *temperature-dependent demand-adjusted productivity*, and combines the firm productivity and the demand shifter responses to temperature. Taking logarithms in equation (8) we recover the following log-linear relation:

$$\begin{aligned} p_{it}y_{it} = (\sigma - 1) \quad & \tilde{z}_{it}(T_{g(i)t}) - \sum_{X \in \mathcal{X}} \alpha^X \tau_{it}^X(T_{g(i)t}) \Bigg) \\ & - (\sigma - 1) \quad \mu + \sum_{X \in \mathcal{X}} \alpha^X \left(p_t^X - \log \alpha^X \right) \Bigg) + \sigma p_t + y_t, \end{aligned} \tag{10}$$

with lowercase letters indicating logarithms. $p_{it}y_{it}$ is the logarithm of sales for firm i in period t. In Section 4, we explain how we estimate an empirical counterpart of equation (10). Unlike the existing literature that has conducted similar regressions, our theoretical framework has

the advantage of identifying the various channels through which temperature shocks impact firm-level revenues. More specifically, sales may respond to temperature because this can affect (i) the firm demand-adjusted productivity through $\tilde{z}_{it}(T_{g(i)t})$ or (ii) the input-specific wedges through $\tau_{it}^{X}(T_{g(i)t})$. Formally, the temperature-semielasticity of sales is given by

$$\frac{\partial p_{it} y_{it}}{\partial T_{g(i)t}} = (\sigma - 1) \quad \frac{\partial \tilde{z}_{it}(T_{g(i)t})}{\partial T_{g(i)t}} - \sum_{X \in \mathcal{X}} \alpha^{X} \frac{\partial \tau_{it}^{X}(T_{g(i)t})}{\partial T_{g(i)t}} \Bigg) \tag{11}$$

Equation (11) shows that, conditional on a measure of the elasticity of substitution between varieties, σ, and the production function elasticities, α^{X}, if one can measure the temperature-semielasticity of the input-specific wedges, $\frac{\partial \tau_{it}^{X}(T_{g(i)t})}{\partial T_{g(i)t}}$, then the temperature-semielasticity of the demand-adjusted productivity, $\frac{\partial \tilde{z}_{it}(T_{g(i)t})}{\partial T_{g(i)t}}$, can be recovered. If this is not the case, however, one would incorrectly attribute the effect of temperature on input-specific wedges to demand-adjusted productivity.

Thus, to estimate the effect of temperature on input-specific wedges we note that the optimality conditions of our model imply that individual input demand is given by:

$$e^{\tau_{it}^{X}(T_{g(i)t})} P_{t}^{X} X_{it} = \alpha^{X} \mathcal{C}(Y_{it}), \quad \forall X \in \mathcal{X}, \tag{12}$$

which can be rearranged, using equation (6), as

$$MRPX_{it} \equiv \alpha^{X} \frac{P_{it} Y_{it}}{X_{it}} = \mathcal{M} e^{\tau_{it}^{X}(T_{g(i)t})} P_{t}^{X}. \tag{13}$$

Taking logarithms in equation (13) we recover the following log-linear relation:

$$\log MRPX_{it} = \tau_{it}^{X}(T_{g(i)t}) + \mu + p_{t}^{X}. \tag{14}$$

Equations (13) and (14) have two important insights. First, conditional on the production function elasticity α^{X}, the revenue-based marginal product of input X ($MRPX$) of firm i can be measured just by observing firm-level sales $P_{it}Y_{it}$ and firm-level input quantities $X_{it} \in \{K_{it}, L_{it}, M_{it}\}$. Second, in equilibrium the effect of temperature on $\log MRPX_{it}$ only depends on its input-specific wedge $\tau_{it}^{X}(T_{g(i)t})$, and not on the other input-specific frictions.[14]

[14] It also depends on the logarithm of the markup, μ, and of the input price, p_{t}^{X}. Regarding the latter, to the extent that its variations are similar across all firms in a given industry, they are absorbed by sector-year effects in our empirical specification. Regarding the former, assuming a CES aggregator in our model rules out any direct effect of temperature on markups. However, while this channel might be accommodated by the temperate-dependent input-specific wedges, in the empirical analysis in Section 5 we find no *prima facie* effect

Hence, having the necessary data to empirically measure firm-level sales and $MRPX$, we can use equations (10) and (14) to estimate the temperature-semielasticity of sales and of input-specific wedges, and then use equation (11) to recover the temperature-semielasticity of the demand-adjusted productivity. We provide a detailed procedure for this in Section 4.

2.2 Aggregate Variables

To quantify the effects of temperature on aggregate productivity—and thereby trace the aggregate damage function central to IAMs—we use changes in the Solow residual as a proxy for changes in aggregate productivity. Appendix A reports the details of all the calculations.

Before introducing the Solow residual in our framework, we demonstrate that aggregate gross output TFP can be expressed as

$$TFP_t = \frac{Y_t}{\prod_{X\in\mathcal{X}} X_t^{\alpha^X}}, \tag{15}$$

$$= \sum_{i=1}^{N_t} \left(e^{\tilde{z}_{it}(T_{g(i)t})}\right)^{\sigma-1} \prod_{X\in\mathcal{X}} \left(e^{\tau_{it}^X(T_{g(i)t})}\right)^{-(\sigma-1)\alpha^X}\Bigg)^{\frac{\sigma}{\sigma-1}}$$

$$\times \prod_{X\in\mathcal{X}} \sum_{i=1}^{N_t} \frac{\left(e^{\tilde{z}_{it}(T_{g(i)t})}\right)^{\sigma-1}}{e^{\tau_{it}^X(T_{g(i)t})}} \prod_{X\in\mathcal{X}} \left(e^{\tau_{it}^X(T_{g(i)t})}\right)^{-(\sigma-1)\alpha^X}\Bigg)^{-\alpha^X}; \tag{16}$$

with $X_t = \sum_{i=1}^{N_t} X_{it}$ standing for real aggregate capital, labor, and materials.

Similarly to Hsieh and Klenow (2009) and Gopinath et al. (2017), we can use equation (16) to also recover the upper bound of aggregate gross output TFP in this economy. This is obtained by equalizing all input-specific wedges $e^{\tau_{it}^X(T_{g(i)t})}$ across firms. The resulting expression is given by

$$TFP_t^* = \sum_{i=1}^{N_t} \left(e^{\tilde{z}_{it}(T_{g(i)t})}\right)^{\sigma-1}\Bigg)^{\frac{1}{\sigma-1}}. \tag{17}$$

Equation (17) represents the upper bound of aggregate TFP in a counterfactual, frictionless scenario, reminiscent of the aggregate productivity in Melitz (2003). Throughout the paper, we refer to this counterfactual, frictionless measure of aggregate TFP as "efficient"—a

of temperature on the revenue-based marginal product of materials and labor (which are common measures of firm-level markups used by the literature; see Loecker and Warzynski, 2012), validating the CES assumption. Furthermore, the empirical specification of equation (14) will further generalize this formula to account for other potential factors.

term commonly used in the literature, albeit with some flexibility in its interpretation.[15]

Equations (16) and (17) show that conditional on the elasticity of substitution between varieties σ and the production function elasticities α^X, aggregate gross output TFP and its efficient counterpart are just a function of two measurable objects: $e^{\tilde{z}_{it}(T_{g(i)t})}$ and $e^{\tau_{it}^X(T_{g(i)t})}$. Given our framework, the firm-level demand-adjusted productivity $e^{\tilde{z}_{it}(T_{g(i)t})}$ can be expressed as

$$e^{\tilde{z}_{it}(T_{g(i)t})} = \left(\frac{(P_t Y_t)^{-\frac{1}{\sigma-1}}}{P_t} \right) \left(\frac{(P_{it} Y_{it})^{\frac{\sigma}{\sigma-1}}}{\prod_{X \in \mathcal{X}} X_{it}^{\alpha^X}} \right). \tag{18}$$

Thus, conditional on a measure of the elasticity of substitution between varieties σ and the production function elasticities α^X, equation (18) can be measured just with data on nominal aggregate output $P_t Y_t$, the aggregate price deflator P_t, firm-level sales $P_{it} Y_{it}$, and firm-level inputs X_{it}. Moreover, firm-level input-specific wedges $e^{\tau_{it}^X(T_{g(i)t})}$ can be measured using equation (13). Hence, using standard firm-level data and leveraging the structure of our framework, we can measure empirically each element in equations (16) and (17). By taking logs and fully differentiating equations (16) and (17), we derive expressions that relate changes in both aggregate gross output TFP and efficient aggregate gross output TFP to variations in grid-cell-level temperatures, resulting in:

$$\begin{aligned}
\Delta \log TFP_t &\equiv \Delta \log TFP_t \left(e^{\tilde{z}_{it}(T_{g(i)t})}, e^{\tau_{it}^X(T_{g(i)t})}, \Delta T_{g(i)t} \right) \\
&\approx \sum_{i=1}^{N_t} \lambda_{it} \sum_{X \in \mathcal{X}} \frac{\alpha^X}{e^{\tau_{it}^X(T_{g(i)t})}} \Omega_t^X \\
&\times \left[\left(\sigma \frac{e^{\tau_{it}^X(T_{g(i)t})}}{\Omega_t^X} - (\sigma - 1) \right) \frac{\partial \tilde{z}_{it}(T_{g(i)t})}{\partial T_{g(i)t}} - \sum_{X \in \mathcal{X}} \alpha^X \frac{\partial \tau_{it}^X(T_{g(i)t})}{\partial T_{g(i)t}} \right) + \frac{\partial \tau_{it}^X(T_{g(i)t})}{\partial T_{g(i)t}} \Bigg] \\
&\times \Delta T_{g(i)t},
\end{aligned} \tag{19}$$

and

$$\Delta \log TFP_t^* \equiv \Delta \log TFP_t^* \left(e^{\tilde{z}_{it}(T_{g(i)t})}, \Delta T_{g(i)t} \right) \approx \sum_{i=1}^{N_t} \lambda_{it}^* \frac{\partial \tilde{z}_{it}(T_{g(i)t})}{\partial T_{g(i)t}} \Delta T_{g(i)t}, \tag{20}$$

[15] While we label this counterfactual TFP as efficient, we refrain from using it for normative assessments. This is because it may not always lie within the set of achievable allocations. For instance, if some frictions in the data arise from technological constraints like adjustment costs, this counterfactual TFP would be unattainable.

where $\lambda_{it} \equiv \lambda_{it}\left(e^{\tilde{z}_{it}(T_{g(i)t})}, e^{\tau_{it}^X(T_{g(i)t})}\right)$ and $\lambda_{it}^* \equiv \lambda_{it}^*\left(e^{\tilde{z}_{it}(T_{g(i)t})}\right)$ are firm-level weights, and $\Omega_t^X \equiv \Omega_t^X\left(e^{\tilde{z}_{it}(T_{g(i)t})}, e^{\tau_{it}^X(T_{g(i)t})}\right)$ is an aggregate object, all detailed in Appendix A.1.

Equations (19) and (20) represent a novel contribution of this paper, playing a central role in our analysis. These equations enable the calculation of *counterfactual* changes in aggregate TFP and TFP^* resulting from temperature variations at the grid-cell level, affecting both demand-adjusted productivity and input-related frictions. Notably, while these equations hold in general equilibrium, they require only data on the distribution of demand-adjusted productivity, $e^{\tilde{z}_{it}(T_{g(i)t})}$, input-specific wedges, $e^{\tau_{it}^X(T_{g(i)t})}$, and their corresponding semielasticities, $\partial\tilde{z}_{it}(T_{g(i)t})/\partial T_{g(i)t}$ and $\partial\tau_{it}^X(T_{g(i)t})/\partial T_{g(i)t}$, without needing information on the effect of grid-cell-level temperatures on aggregate prices. Therefore, this approach avoids reliance on estimating the effects of grid-cell-level temperatures on aggregate prices, circumventing the well-known "missing intercept" problem in cross-sectional data. Finally, while the data requirements may appear substantial, the distributions of demand-adjusted productivity and input-specific wedges can be derived using equations (13) and (18), and the semielasticities, central to our empirical analysis, are detailed in Section 4.

We now have all the necessary elements to decompose the change in aggregate gross output TFP into two components: an efficient component and a component associated with input-related frictions. The final expression for the changes in aggregate gross output TFP is as follows:

$$\Delta \log TFP_t = \underbrace{\Delta \log TFP_t^*}_{\Delta \text{ Technology}} - \underbrace{\left(\Delta \log TFP_t^* - \Delta \log TFP_t\right)}_{\Delta \text{ Allocative Efficiency}}. \tag{21}$$

The Δ Technology term captures changes in TFP^*, as described in equation (20). Intuitively, it reflects the changes in aggregate TFP driven by the effect of temperature on demand-adjusted productivity, $e^{\tilde{z}it(Tg(i)t)}$, in an economy without allocative frictions—where aggregate output cannot be increased by reallocating inputs across firms. This term isolates the direct impact of temperature on firm-level demand and productivity.

The Δ Allocative Efficiency term captures deviations from the efficient allocation, reflecting the impact of temperature shocks on aggregate TFP through changes in allocative efficiency. This term is influenced by changes in both demand-adjusted productivity, $e^{\tilde{z}_{it}(T_{g(i)t})}$, and input-specific wedges, $e^{\tau_{it}^X(T_{g(i)t})}$. While changes in the latter directly indicate shifts in firm-level resource allocation relative to a counterfactual frictionless benchmark, and thus affect aggregate allocative efficiency, changes in the former impact aggregate allocative effi-

ciency only if the economy's initial allocation is distorted by frictions. For instance, if firms with inefficiently high levels of inputs experience a temperature shock that reduces their demand-adjusted productivity, it not only diminishes the Δ Technology term but also decreases the Δ Allocative Efficiency term by pushing their allocation of inputs even further from the frictionless optimum. However, this effect is not always negative. Temperature-induced changes in demand-adjusted productivity can either enhance or diminish aggregate allocative efficiency, depending on the initial distribution of input-specific wedges and inputs. Thus, this term is the outcome of the indirect effect due to the presence of frictions and echoes the covariance argument between wedges and productivity highlighted in the misallocation literature (e.g., Gopinath et al., 2017) and ultimately remains a quantitative question.

Until now, our analysis has not required explicit assumptions about the supply of aggregate inputs. However, because our focus is on the impact of climate change on the Solow residual—defined in terms of value-added—we modify (21) accordingly, as detailed in Appendix A.2. In brief, this adjustment assumes that aggregate labor and capital are in fixed supply, while the use of the final good as materials introduces a simple roundabout production structure, as described in Jones (2011) and Baqaee and Farhi (2020). This results in the following measure for changes in the Solow residual:

$$\Delta \log Solow_t \approx \frac{Y_t}{GDP_t} \left(\Delta \log TFP_t^* - \left(\Delta \log TFP_t^* - \Delta \log TFP_t \right) \right), \tag{22}$$

where Y_t is gross output and GDP_t is value-added, i.e., gross output net of materials.

Equation (22) shows that the impact of climate change on the Solow residual exceeds its effect on gross output TFP due to a multiplier effect equal to the ratio of gross output to GDP. This arises from the roundabout nature of material production, where materials are produced using output. Initial productivity losses reduce output, which subsequently lowers material production, further constraining output. This feedback loop amplifies the initial productivity losses, creating a multiplier mechanism.

Therefore, to compute the counterfactual impact of climate change on aggregate productivity and decompose it into a technology component and a component related to allocative efficiency, we simultaneously utilize equations (19), (20), and (22).

3 Data

This section presents the two main data sources used for the empirical analysis.

3.1 Firm-Level Data

The Italian firm-level data is obtained from Orbis, provided by Bureau van Dijk between the years 1999-2013. Orbis offers harmonized cross-country financial information for both private and public firms collected from various national data sources, primarily business registers. The dataset covers, on average, 75 percent of the official Italian gross output reported in Eurostat. One major advantage of Orbis over other datasets is that it includes many small private firms. In fact, Kalemli-Özcan et al. (2024) show that Orbis closely mimics the official size distribution reported in Eurostat Structural and Business Statistics (SBS). The cleaning process follows Kalemli-Özcan et al. (2024) and Gopinath et al. (2017) and is explained in Appendix B.

The final dataset includes information on approximately 4.3 million observations corresponding to 1 million firms. We measure sales (PY) by operating revenue, materials (M) by expenditure on materials, labor (L) by the cost of employment, and capital (K) by the book value of tangible fixed assets. All monetary values are deflated using Eurostat two-digit industry price deflators, and capital is deflated using the country-specific price of investment from the World Development Indicators. The dataset also includes the primary sector of economic activity at the four-digit industry level and, importantly, firm-level zip codes, enabling geolocation. This geolocation is used to link the data to the climate variables.

We compute the marginal revenue product of input $X \in L, M, K$ using equation (13), with α^X, the elasticity of output with respect to X, measured via the cost shares approach (Foster et al., 2008) and taking the median firm-level cost share within each four-digit industry (De Loecker et al., 2020) to address measurement error and adjustment frictions.[16] The production function elasticities are given by $\alpha^M = \text{med}\left\{\frac{P_t^M M_{it}}{r_t K_{it}+W_t L_{it}+P_t^M M_{it}}\right\}$, $\alpha^L = \text{med}\left\{\frac{W_t L_{it}}{r_t K_{it}+W_t L_{it}+P_t^M M_{it}}\right\}$, $\alpha^K = 1-\alpha^L-\alpha^M$, where $r_t K_{it}$ is the rental cost of tangible capital, $W_t L_{it}$ is the wage bill, and $P_t^M M_{it}$ is the expenditure on materials.[17] We recover median production function elasticities $\{\alpha^X\}_{X\in\{M,L,K\}}$ equal to $\{0.53,\ 0.36,\ 0.11\}$, well within the range found by the literature.[18] For instance, Gandhi et al. (2020) reports values for materials, labor, and capital ranging from 0.50-0.67, 0.22-0.52, and 0.04-0.16, respectively.

[16] We use the production function elasticities both to calculate the aggregate counterfactual based on equation (19) and to compute the revenue-based marginal products in equation (13). For the latter, since our regression framework includes firm and sector-time fixed effects, these elasticities are absorbed into the error term and are therefore not required to identify the temperature-semielasticity of each revenue-based marginal product.

[17] We measure the user cost of capital as $r_t = i_t - \mathbb{E}_t\pi_{t+1} + \delta + RP$. We use the real interest, $i_t - \mathbb{E}_t\pi_{t+1}$, from Gopinath et al. (2017), a depreciation rate, δ, of 10% as usually done in the literature, and a risk premium, RP, of 5% as calculated in Caballero et al. (2017).

[18] The inclusion of aggregate median elasticities in the text serves the sole purpose of facilitating a meaningful comparison with the existing literature. However, in the calculations, only the sector-level elasticities are used.

3.2 Climate Data

The meteorological data are sourced from Copernicus, the European Union's flagship Earth Observation Programme, using E-OBS, a daily gridded land-only observational dataset for Europe.[19] For further details, see Cornes et al. (2018) and Appendix B.2.1. This dataset is constructed using observations from National Meteorological and Hydrological Services (NMHSs) and other data-holding institutions across Europe. It incorporates contributions from 84 organizations and includes data collected from over 23,000 meteorological stations. Additional information on the dataset's high station coverage is provided in Appendix B.2.2.

Figure 1: Average Yearly Temperature

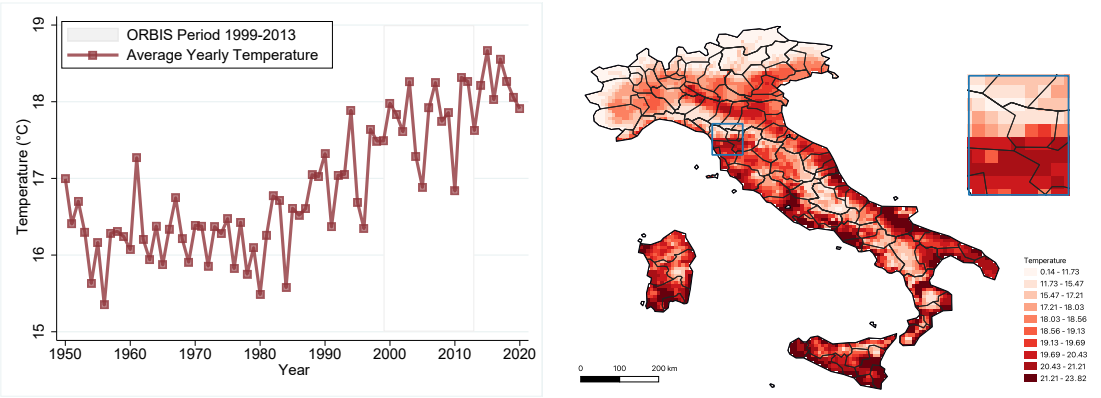

(a) 1950-2020 Trend **(b) 1999 Cross Section**

Note. Figure 1a shows the evolution of the average yearly temperature in Italy between 1950-2020. The grey areas show the time frame (1999-2013) for which Orbis data is available. Figure 1b shows the average yearly temperature across all the grid-cells in Italy in 1999. It also plots regional boundaries at the NUTS 3 level.

We use daily temperature and rainfall data with a horizontal grid resolution of 0.1° (approximately 11 km × 11 km, or 121 km^2), covering the period 1950–2020. Temperatures are recorded in degrees Celsius (°C), and rainfall is measured in millimeters (mm). Following Somanathan et al. (2021), daily temperature is represented by the maximum temperature, which typically occurs during working hours and serves as a proxy for heat exposure during peak economic activity. Rainfall is recorded as total daily precipitation, including rain, snow, and hail, expressed as the equivalent height of liquid water per square meter. While our primary variable of interest is temperature, rainfall is included as a control variable in the empirical analysis, as detailed in Section 4.

Figure 1a shows the evolution of the average yearly maximum temperature over the entire sample period. The average yearly maximum temperature is volatile and rising over time.

[19] See https://doi.org/10.24381/cds.151d3ec6.

Table 1 presents summary statistics for our climate data during the period 1999–2013, which corresponds to the subperiod for which firm-level data is available and forms the basis of our analysis. Summary statistics for the entire sample period are provided in Table B.2 in Appendix B.2.3. Additionally, Figure 1b illustrates the average yearly temperature in 1999 for each grid cell, overlaid with the boundaries of NUTS 3 regions in Italy. The average yearly temperature ranges from 0.14°C to 23.82°C, highlighting substantial variation across grid cells and regions. This pronounced temperature heterogeneity makes Italy an exceptional setting for studying the economic impacts of climate change. The coexistence of wide temperature gradients and diverse locations of economic activity—from production sites in colder areas like the Alps to warmer coastal regions—provides a unique opportunity to analyze firm responses to varying climatic conditions.

Table 1: Summary Statistics of Climate Data (1999-2013)

	Overall		Within Grid-Cell	
	Temperatures (°C)	Rainfalls (mm)	Temperatures (°C)	Rainfalls (mm)
Mean	17.74	2.28	17.74	2.28
Median	17.65	0.00	17.51	1.01
Min	-24.94	0.00	0.35	0.00
Max	43.71	258.40	33.62	26.99

Note. Table 1 shows summary statistics of temperature in degrees Celsius (°C) and rainfalls in millimeters (mm) for the period 1999-2013. The first two columns report statistics for the overall sample. The last two columns report statistics on the variation within the average grid-cell, that is, they show the average temperature distribution among the different grid-cells.

Our main empirical specification follows Somanathan et al. (2021), aggregating daily temperatures to the annual level by counting the number of days falling within specific temperature bins, as introduced by Deschênes and Greenstone (2011). We use the following bins: $\{(-\infty, 0°\text{C}], (0°\text{C}, 30°\text{C}], (30°\text{C}, 35°\text{C}], (35°\text{C}, 40°\text{C}], (40°\text{C}, +\infty)\}$. To summarize the yearly temperature distribution, we construct a vector $\boldsymbol{T} = \{T^1, T^2, T^3, T^4, T^5\}$, which counts the number of days in each bin for every grid cell and year. These non-overlapping bins fully capture the observed temperature distribution, with more bins at the high end to assess the economic impact of future climate change. In Section 5, we present a robustness exercise using a smaller benchmark bin, specifically $(15°\text{C}, 30°\text{C}]$. Additionally, we consider two alternative specifications for daily maximum temperatures: one based on a degree-day approach and another using a quadratic formulation of daily maximum temperatures.

Figure 2 shows the distribution of days within each temperature bin of the vector $\boldsymbol{T}$ averaged across grid-cells and years. Most of the days clearly belong to the $[0°\text{C}, 30°\text{C})$ range, which we will use as the reference bin in the regression framework. Importantly, all tem-

Figure 2: Average Distribution of Days Within Temperature Bins

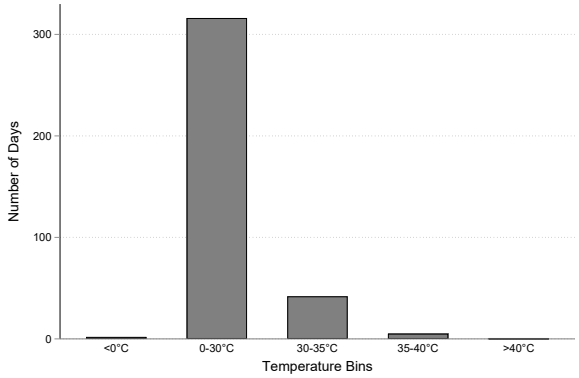

Note. Figure 2 shows the number of days per year within each temperature bin of the vector $\boldsymbol{T}$. We construct this figure averaging across all grid-cells and years.

perature bins have a non-zero average number of days. Table B.3 in Appendix B.3 reports summary statics for the distribution of days within each temperature bin across grid-cells.

3.3 Main Combined Data

To construct our final dataset, we merge firm-level data from Orbis with temperature data from Copernicus by assigning each firm to a specific grid cell in the Copernicus dataset. The Copernicus data includes latitude and longitude for its grid cells. We determine each firm's geographical coordinates in Orbis using their reported postcode to the business registry. Postcodes act as unique identifiers for specific locations, enabling precise localization. To convert postcodes into geographical coordinates, we use the Python package "pgeocode."[20] Using the firms' coordinates and the latitude and longitude of the Copernicus grid cells, we assign each firm to its nearest grid cell by calculating the minimum distance between the two.

One limitation of our data is that we only have information on the firm's headquarters address, with no details about production plant locations. For firms whose headquarters are in a different grid cell than their production plants, temperature data may be incorrectly assigned—a scenario more likely for large, multi-plant firms. However, in our sample of Orbis-Italian firms, only 1% are publicly listed, 3–4% are foreign-owned, and 2% have consolidated financial statements, suggesting that such firms represent a small minority. Robustness checks confirm that these cases do not drive our results. Furthermore, if production locations are misassigned to grid cells, the firm's response to the incorrectly assigned temperature would likely be weaker or negligible, biasing our results downward. This implies a conservative bias in our

[20]The pgeocode package (https://pypi.org/project/pgeocode/) utilizes data from GeoNames (https://www.geonames.org), an open-source project providing detailed postal code and location information.

estimates, offering a more benign interpretation of this potential source of mismeasurement.

4 Empirical Strategy

This section outlines our empirical approach to identifying the effects of temperature on firm-level demand-adjusted productivity and input-specific wedges.

In Section 2, we left the temperature-dependent factors as unspecified functions. Here, we specify the functional forms used in the empirical analysis for demand-adjusted productivity and input-specific wedges. Specifically, we assume that firm-level outcomes and input-specific wedges consist of a temperature-dependent component, $F(T_{g(i)t})$, and a temperature-independent component, $\boldsymbol{W}_{it}$, such that:

$$e^{\tilde{z}_{it}(T_{g(i)t})} \equiv e^{F^{\tilde{z}}(T_{g(i)t})+G^{\tilde{z}}(\mathbf{W}_{it})}, \tag{23}$$

$$e^{\tau^X_{it}(T_{g(i)t})} \equiv e^{F^{\tau^X}(T_{g(i)t})+G^{\tau^X}(\mathbf{W}_{it})}, \quad \text{with} \quad \forall X \in \mathcal{X}; \tag{24}$$

where $F(\cdot)$ is a non-linear function of temperature in the grid-cell to which firm i belongs and $G(\mathbf{W}_{it})$ is a function of alternative explanatory variables.

Thus, to measure the effect of changes in temperature on firm-level outcomes, we estimate the following equation:

$$Outcome_{it} = \sum_{\ell} \beta_\ell T^{\ell}_{g(i)t} + \delta Rain_{g(i)t} + \boldsymbol{\lambda}'\mathbf{X}_{r(i)t} + \gamma_{s(i)t} + \alpha_i + \varepsilon_{it}, \tag{25}$$

where i denotes a firm, t stands for year and $g(i)$ denotes the grid-cell to which firm i belongs. $Outcome_{it}$ denotes log firm-level outcomes or log revenue-based marginal product of a given input X, $\log MRPX_{it}$. We approximate the non-linear temperature function $F(\cdot)$ by the variable $T^{\ell}_{g(i)t}$, denoting the number of days in temperature bin ℓ, that each grid cell $g(i)$ experienced during a given year (see Section 3.2 for a description). We set the interval $[0°\text{C}, 30°\text{C})$ as the reference temperature bin since it covers the average range of temperature faced by most grid-cells in our data. For robustness, as detailed in Section 5, we use two alternative specifications for $F(\cdot)$: a degree-day measure and a quadratic specification of daily maximum temperatures.

$G(\mathbf{W}_{it})$ includes potential confounding factors at the firm, grid-cell, region, and sector level. Outcome variables may also respond to other climate factors related to temperature. To address this, we include $Raing(i)t$, which represents the average yearly rainfall in each grid

cell. For robustness, Section 5 introduces a nonlinear specification of rainfall, similar to $F(\cdot)$, to account for rainfall nonlinearity and the potential effects of floods, the primary extreme weather event in Italy caused by heavy precipitation. We include firm fixed effects (α_i) to control for unobserved time-invariant characteristics at the firm level. To account for regional shocks, we add regional trends, $\mathbf{X}r(i)t$, which include time trends at the NUTS 2 regional level ($r(i)$ indicates the region of firm i) and dummies for the Great Recession (2008–2009) and the Sovereign Debt Crisis (2012–2013), reflecting the uneven regional impact of these crises in Italy. Similarly, to control for sectoral and aggregate productivity trends, we include sector-time fixed effects ($\gamma s(i)t$), where $s(i)$ denotes the NACE 4 sector of firm i. These fixed effects capture sector-specific and broader economic fluctuations. Standard errors are clustered at the grid-cell level to account for potential serial correlation that could downwardly bias the estimates. To further address spatial autocorrelation in weather patterns, as highlighted by Auffhammer et al. (2013), we include a robustness check in Section 5 using spatially adjusted standard errors based on the method proposed by Conley (2010).

The regression specification given by equation (25) is the empirical counterpart of equations (10) and (14). The coefficient of interest is β_ℓ, which captures the effect of an extra day into the temperature bin ℓ relative to the reference temperature bin. Thus, $\beta_\ell < 0$ implies that the given firm-level outcome declines β_ℓ percent for each extra day into the temperature bin ℓ relative to the reference temperature bin. Our coefficient of interest, β_ℓ, is identified by comparing firms with similar time-invariant characteristics that experience the same grid-cell rainfall levels, regional development trends, exposure to the Great Recession (GR) and Sovereign Debt Crisis (SDC), and sectoral dynamics but are exposed to different grid-cell temperature changes over time. The key identification assumption is that, after controlling for regional and sectoral fixed effects, temperature fluctuations are exogenous to any other time-varying factors influencing demand, productivity, or inputs.

There are at least three potential challenges to the validity of our results, but as we explain below, these challenges do not fully align with our findings and would likely bias our estimates downward. First, there is the possibility of a contemporaneous shock that affects both temperatures and productivity simultaneously. For example, regions experiencing a surge in economic activity might face increased congestion or pollution, leading to both a rise in temperatures and a decline in productivity. However, this explanation does not fully align with our findings, as we observe output decreases directly linked to elevated temperatures. A second identification challenge arises from shocks that influence both productivity and its responsiveness to temperature. For instance, higher firm unionization might lead to tougher

bargaining discussions, including grievances about working under extreme temperatures. In this scenario, there is a potential for overestimating the impact of temperatures, as it may also encompass the effects of unionization itself. However, by controlling for sector-year fixed effects and considering that these phenomena are widespread across all firms in a sector, concerns should be mitigated. Third, if firms could accurately anticipate temperature increases at the grid-cell level and choose their locations accordingly, this could introduce selection bias. To address this, we include regional trends in our analysis, allowing us to estimate deviations from these trends and capture the effects of unanticipated temperature shocks. This approach suggests that our estimates are best interpreted as short- to medium-run elasticities.

5 Results

In this section, we present the firm-level effects of temperature on several objects of interest and we discuss potential channels and heterogenous effects.

5.1 Sales, Inputs, and Marginal Revenue Products

We estimate the effect of temperature on firm-level outcomes using the regression specification outlined in equation (25). We estimate the effect of temperature on sales and its impact on firms' inputs—materials, labor, and capital—to better understand the response of marginal revenue products of inputs. Table 2 reports the results.

The estimates reveal that temperature has an inverted U-shaped effect on sales, materials, and labor, indicating that extreme temperatures, whether high or low, tend to suppress these firm-level outcomes. For instance, one additional day above 40 degrees Celsius is estimated to reduce sales by 0.807%, while one extra day below 5 degrees Celsius decreases sales by 0.094%.[21] These losses are measured relative to the reference temperature bin $[0°\text{C}, 30°\text{C})$. The response of capital, however, is notably weaker, particularly at higher temperatures. This is significant for our analysis, as it suggests that while materials and, to a lesser extent, labor exhibit substantial and meaningful responses to extreme temperatures, capital adjustments are minimal, consistent with the widely recognized view that capital is subject to greater adjustment frictions compared to materials and labor.

[21] Assuming production is evenly distributed across all effective working days in a year (approximately 220 in Italy, accounting for 250 working days minus 30 holidays), an extra day above 40 degrees Celsius equates to nearly a two-day loss in sales ($100 \times 2/220 \approx 0.807$), and an extra day below 5 degrees Celsius corresponds to about a one-third-day loss in sales ($100 \times 0.3/220 \approx 0.094$).

Table 2: Average Effect of Temperature on Sales and Inputs

Dependent Variable	**Sales** (1)	**Materials** (2)	**Labor** (3)	**Capital** (4)
Temperature Bins				
$(-\infty, 0°C]$	-0.094***	-0.068**	-0.070***	-0.036*
	(0.019)	(0.029)	(0.019)	(0.021)
$(30°C, 35°C]$	-0.017*	-0.022	0.002	0.003
	(0.009)	(0.014)	(0.007)	(0.010)
$(35°C, 40°C]$	-0.046***	-0.060**	-0.003	0.004
	(0.017)	(0.025)	(0.016)	(0.019)
$(40°C, +\infty]$	-0.807***	-0.557**	-0.369**	0.033
	(0.194)	(0.242)	(0.187)	(0.217)
Fixed Effects				
Firm	✓	✓	✓	✓
Sector × Year	✓	✓	✓	✓
GR and SDC × Region	✓	✓	✓	✓
Controls				
Rainfalls	✓	✓	✓	✓
Region Trends	✓	✓	✓	✓
Observations	4,687,524	4,687,524	3,767,578	4,328,710

Note. All dependent variables are in logs. Temperature bins are constructed as explained in Section 3.2. Rows 1-4 present the effect on the log of the dependent variable of adding an extra day in the given temperature range respectively. Standard errors are clustered at the grid-cell level and reported in parentheses. *, **, and *** denote 10, 5, and 1% statistical significance respectively.

Table 3: Average Effect of Temperature on Revenue-Based Marginal Product of Inputs

Dependent Variable	**MRPM** (1)	**MRPL** (2)	**MRPK** (3)
Temperature Bins			
$(-\infty, 0°C]$	-0.018	0.008	-0.030
	(0.019)	(0.013)	(0.022)
$(30°C, 35°C]$	0.006	-0.012**	-0.014
	(0.008)	(0.006)	(0.010)
$(35°C, 40°C]$	0.011	-0.021	-0.045**
	(0.014)	(0.013)	(0.021)
$(40°C, +\infty)$	-0.209	-0.019	-0.578**
	(0.156)	(0.145)	(0.231)
Fixed Effects			
Firm	✓	✓	✓
Sector × Year	✓	✓	✓
GR and SDC × Region	✓	✓	✓
Controls			
Rainfalls	✓	✓	✓
Region Trends	✓	✓	✓
Observations	4,687,524	3,767,578	4,328,710

Note. All dependent variables are in logs. Temperature bins are constructed as explained in Section 3.2. Rows 1-4 present the effect on the log of the dependent variable of adding an extra day in the given temperature range respectively. Standard errors are clustered at the grid-cell level and reported in parentheses. *, **, and *** denote 10, 5, and 1% statistical significance respectively.

We next estimate the effect of temperature on the firm-level revenue-based marginal product of each input using the regression specification in equation (25). The results, shown in Table 3, reveal an inverted U-shaped relationship between temperature and revenue-based

marginal products, which is statistically significant and substantial only for $MRPK$. This indicates that extreme temperatures—whether high or low—reduce the revenue-based marginal product of capital. Specifically, an additional day above 40℃ decreases $MRPK$ by 0.578%, while an extra day below 5℃ reduces it by 0.030%. These findings are consistent with the patterns reported in Table 2. The results further show that $MRPM$ and $MRPL$ remain unaffected by temperature fluctuations, as materials and labor adjust in response to temperature changes to align with sales. In contrast, $MRPK$ is significantly impacted because capital adjustments are constrained, leaving firms with excess capital that cannot be reallocated effectively. This finding highlights the unique role of capital adjustment frictions and represents a novel contribution of our paper.[22]

The finding that materials are flexible to adjust aligns with a large body of literature in firm dynamics, which identifies materials as the most flexible input. Moreover, the minimal impact of temperature on the $MRPL$ suggests that, despite Italy's traditionally rigid labor market institutions, firms demonstrate considerable flexibility in adjusting their labor input. This adaptability operates through both intensive margins (adjusting hours worked) and extensive margins (utilizing fixed-term contracts), the latter facilitated by labor market reforms since the mid-1990s (Caggese and Cuñat, 2008). This labor input flexibility allows firms to maintain optimal labor allocation even when facing temperature shocks. The finding that capital is difficult to adjust aligns with the extensive literature on capital adjustment costs (e.g., Cooper and Haltiwanger, 2006). Our analysis shows a significant decline in $MRPK$ during high-temperature episodes. While factors such as increased cooling needs or temporary shutdowns might be expected to raise $MRPK$, we observe the opposite. This reflects the quasi-fixed nature of capital investments and the associated adjustment costs: firms are unable to efficiently scale down capital inputs during temporary production declines, leading to a reduced output-to-capital cost ratio.

Our main results are robust to various concerns and alternative specifications. Table C.4 in Appendix C.1 demonstrates that splitting the $(0°\text{C}, 30°\text{C}]$ range into smaller bins—$(0°\text{C}, 15°\text{C}]$ and $(15°\text{C}, 30°\text{C}]$—produces estimates consistent with the benchmark specification. Tables C.5 and C.6 in Appendix C.1 confirm the robustness of our findings under alternative regression specifications. First, we control for firm age, a well-documented determinant of firm heterogeneity (Fort et al., 2013), and find no changes to our results. Second, we test alternative tem-

[22] The model assumes no unemployed inputs. Thus, when firms reduce labor and material inputs due to temperature shocks, these inputs are assumed to be reallocated to more productive uses within the year. While some inputs may remain temporarily unemployed in reality, affecting aggregate output, this has less relevance for aggregate productivity, which is the primary focus of our analysis.

perature specifications, including a piecewise linear model based on degree days (Somanathan et al., 2021) and a quadratic model of daily maximum temperatures (Dell et al., 2012; Burke et al., 2015). Third, we include a specification with nonlinear rainfall controls to account for the effects of precipitation and floods. Finally, we address spatial autocorrelation by adjusting standard errors using the method of Conley (2010), allowing for dependence within radii of 80 km and 150 km.[23] Across all robustness checks, our findings remain consistent with the benchmark results reported in this section.

Finally, we show that our results are robust across various sample cuts. First, Tables C.7 and C.8 in Appendix C.2 present additional specifications to evaluate the sensitivity of our estimates to firms potentially assigned incorrect temperatures, as discussed in Section 3.3. These specifications exclude specific types of firms, such as foreign firms, listed firms, firms reporting consolidated accounts, and large firms, with the exclusion criteria detailed in Appendix C.2. Crucially, our analysis shows that the inclusion or exclusion of these firms does not affect our estimates, indicating that the concerns raised in Section 3.3 about potentially misclassified firms do not materially impact our findings. Second, we address the issue of differing sample sizes due to limited data availability for employment measures. As shown in Tables C.7 and C.8 in Appendix C.2, ensuring consistency in the number of observations across variables does not alter the patterns presented in this section.

5.2 Demand-Adjusted Productivity

Having estimated the effects of temperature on both sales and the revenue-based marginal product of inputs, we leverage the structural framework and equation (11) to recover the impact of temperature on firm-level demand-adjusted productivity. In Section 5.3.1, we further detail how we disentangle demand effects from productivity effects. Importantly, the effect of temperature on the revenue-based marginal product not only offers novel evidence of a previously underexplored channel through which extreme temperatures affect firms but also enables a more accurate measurement of demand-adjusted productivity. Neglecting this channel would lead to an underestimation of the temperature effect, as noted in equation (11).

To compute these estimates, we require the elasticity of substitution across varieties, denoted as σ, and the production function elasticities, α^X. For the latter, we use the elasticities described in Section 2, and we assume an elasticity of substitution $\sigma = 4$ between varieties. This value implies an average cost-weighted markup of 33 percent, which is consistent with

[23] These radii are a conservative choice, as Italy spans approximately 549 km x 549 km, totaling 301,340 km^2.

the estimates from De Loecker et al. (2020) and our own estimates for Italy, where we find a materials cost-weighted markup of 27 percent. It also aligns with the mean value reported by Broda and Weinstein (2006).[24] This elasticity estimate is further supported by both firm-level and macroeconomic studies. For instance, Bernard et al. (2003) report a value of $\sigma = 3.79$ in a firm-level export model, while Christiano et al. (2015), using a New-Keynesian model with financial frictions, estimate $\sigma = 3.78$. Additionally, we obtain the temperature-semielasticities of sales and revenue-based marginal products from Tables 2 and 3, and we set the temperature-semielasticity of $MRPM$ and $MRPL$ to zero as they are statistically insignificant and small.[25]

Table 4 summarizes the effect of temperature on demand-adjusted productivity, under the parameters specified above. Notice that the temperature-semielasticities of the demand-adjusted productivity vary across sectors as production function elasticities are sector-specific. Thus, we report both an unweighted average and a sales-weighted average across sectors.[26]

Table 4: Average Effect of Temperature on Demand-Adjusted Productivity

	Temperature Bins			
	$(-\infty, 0°C]$	$(30°C, 35°C]$	$(35°C, 40°C]$	$(40°C, \infty)$
Variable				
β_ℓ^z, unweighted	-0.031	-0.005	-0.021	-0.337
β_ℓ^z, weighted	-0.031	-0.005	-0.019	-0.321

Note. Table 4 reports the temperature-semielasticity for demand-adjusted wedges for each temperate bin. Temperature bins are constructed as explained in Section 3.2. Row 1 reports the unweighted average across sectors. Row 2 reports the sales-weighted average across sectors.

We observe that the temperature-semielasticity of demand-adjusted productivity exhibits the previously identified inverted U-shaped pattern. This result is not entirely unexpected, as equation (11) shows that this semielasticity is a linear combination of the earlier ones, subject to rescaling. Quantitatively, our analysis indicates that an additional day with temperatures exceeding 40 degrees Celsius decreases demand-adjusted productivity by 0.337 percent, while an additional day with temperatures below 0 degrees Celsius reduces it by 0.031 percent. These findings highlight the significant impact of extreme temperatures—both high and low—on demand-adjusted productivity as reflected in the data.

[24] Based on three-digit goods (SITC-3) data over the period 1990–2001.
[25] We do the same for the calculation implemented in Section 6.
[26] Table C.9 in the appendix C.3 shows how the effect of temperature on demand-adjusted productivity varies across sectors. High capital intensive sectors experience larger losses.

5.3 The Demand Channel and Adaptation Effects

This section investigates potential differences between tradable and non-tradable sectors, shedding light on the roles of demand versus efficiency. Additionally, it explores the possibility of firm adaptation to climate change.

5.3.1 Demand versus Productivity

Although the model does not require separating demand from productivity to conduct the aggregate counterfactual analysis in equation (21), we aim to understand which of these two margins is more affected by temperature. To this end, we extend our empirical strategy to disentangle the effects of temperature on firms' demand and productivity. While firms operating in a specific area are likely to experience similar productivity impacts from extreme temperatures, we observe that firms producing tradable goods are less exposed to local temperature-related demand shocks, as a significant portion of their demand originates from outside the local market, potentially from abroad.[27] Therefore, if temperature changes occur in the grid cell where their production is located, these firms' productivity will be affected. However, their demand will remain either unaffected or less affected, as they do not rely heavily on sales within that grid cell.

Thus, we set to identify the effect of temperature on demand and productivity separately using the following regression specification:

$$\begin{aligned} Outcome_{it} = &\sum_{\ell} \beta_{1,\ell} T^{\ell}_{g(i)t} + \delta_1 Rain_{g(i)t} + \boldsymbol{\lambda_1'} \mathbf{X}_{r(i)t} \\ &+ \left(\sum_{\ell} \beta_{2,\ell} T^{\ell}_{g(i)t} + \delta_2 Rain_{g(i)t} + \boldsymbol{\lambda_2'} \mathbf{X}_{r(i)t} \right) \times I^{NT}_{s(i)} + \gamma_{s(i)t} + \alpha_i + \varepsilon_{it}, \end{aligned} \tag{26}$$

where $I^{NT}_{s(i)}$ is an indicator function that takes the value of one if firm i belongs to sectors s selling non-tradable goods, as described below, and the other variables are described in the main specification in Section 4. In this specification, the estimated coefficients $\beta_{1,\ell}$ capture the temperature-semielasticity of sales, which is common to firms both in the tradable and non-tradable sectors and that therefore captures common productivity effects. Instead, the coefficients $\beta_{2,\ell}$ reflect the differential impact of temperature on firms in the non-tradable

[27] For instance, the lower demand sensitivity of sales for firms producing tradable goods has been empirically documented by Almunia et al. (2021) during the Great Recession. Furthermore, examining this dimension in our data is a natural choice, given that a significant proportion of Italian firms engage in the production of tradable goods and exporting, as highlighted by Caggese and Cuñat (2013).

sector, which we interpret as the semielasticity of the demand effect.

We employ three distinct measures to classify firms into tradable and non-tradable sectors. First, based on the World Input-Output Database (WIOD), we identify tradable sectors as those where the proportion of exports in total value-added for each NACE 2-digit sector in Italy exceeds the median. Recognizing that tradability involves more than international trade, we further identify firms whose goods and services are predominantly locally demanded. To achieve this, we employ two additional metrics. First, we use the classification provided by Gervais and Jensen (2019) which utilizes a dataset on the distribution of output and demand across regions of the United States to construct measures of trade costs for nearly a thousand service and manufacturing industries.[28] Secondly, we adapt the tradability measure from Mian and Sufi (2014), which links high regional employment concentration to greater tradability. Using a similar approach, we measure the geographical (NUTS 2) concentration of each NACE 2 sector in Italy, defining a sector as tradable if its wage bill concentration exceeds the median.

Table 5 presents the results. Column 1 reports the estimated average effect of temperature on sales, as shown in Table 2. Columns 2 to 4 provide (i) the coefficient for the common effect of temperature on sales across both tradable and non-tradable sectors and (ii) the coefficients for the additional effect of temperature on sales in non-tradable sectors, capturing the demand effect. In Column 2, tradable sectors are defined as those with a proportion of exports in total value-added above the median, based on WIOD data for each NACE 2-digit sector. Column 3 uses the tradability measure from Gervais and Jensen (2019), while Column 4 applies the tradability measure from Mian and Sufi (2014) using Italian data.

We observe that the interaction coefficient is largely insignificant and modest across intervals, except for the $(35°\text{C}, 40°\text{C}]$ interval, where it is negative in two out of three specifications. Conversely, the common coefficient for extreme temperatures is highly significant, substantial in size, and similar to the average effect. These findings suggest that non-tradable firms are only slightly more affected by temperature, indicating a minor but nonzero role of temperature in demand and a more substantial impact on productivity. This does not contradict the view that customer demand for certain goods, particularly durables, varies with daily weather (e.g., Busse et al., 2015), but suggests that such variations may be offset over the year, reducing the annual effect. Consequently, our results indicate that most of the temperature effect on the demand-adjusted productivity wedge stems from its impact on productivity.[29]

[28] We thank Antoine Gervais for sharing his data with us.

[29] This aligns with existing literature highlighting the influence of temperature on labor productivity, as reviewed by Pankratz and Schiller (2024) and Lai et al. (2023), with additional evidence for Italy provided by Gould et al. (2024) and Filomena and Picchio (2024).

Table 5: Effect of Temperature on Sales of Tradable versus Non-Tradable Sectors

Dependent Variable	**Sales** (1)	**Sales** (2)	**Sales** (3)	**Sales** (4)
Temperature Bins				
$(-\infty, 0°C]$	-0.094***	-0.090***	-0.096***	-0.113***
	(0.019)	(0.024)	(0.024)	(0.026)
$(30°C, 35°C]$	-0.017*	-0.006	-0.006	-0.025**
	(0.009)	(0.009)	(0.011)	(0.010)
$(35°C, 40°C]$	-0.046***	-0.017	-0.013	-0.024
	(0.017)	(0.019)	(0.020)	(0.021)
$(40°C, +\infty)$	-0.807***	-0.758***	-0.835***	-1.046***
	(0.194)	(0.260)	(0.297)	(0.310)
Temperature Bins$\times I^{NT}_{s(i)}$				
$(-\infty, 5°C]$		-0.006	0.005	0.032
		(0.030)	(0.026)	(0.029)
$(30°C, 35°C]$		-0.019	-0.016	0.014
		(0.015)	(0.012)	(0.012)
$(35°C, 40°C]$		-0.049*	-0.046*	-0.036
		(0.027)	(0.023)	(0.023)
$(40°C, +\infty)$		-0.087	0.022	0.385
		(0.352)	(0.357)	(0.383)
Fixed Effects				
Firm	✓	✓	✓	✓
Sector × Year	✓	✓	✓	✓
GR and SDC × Region	✓	✓	✓	✓
Controls				
Rainfalls	✓	✓	✓	✓
Region Trends	✓	✓	✓	✓
Observations	4,687,524	4,684,661	4,593,020	4,687,524

Note. All dependent variables are in logs. Temperature bins are constructed as explained in Section 3.2. The variable $I^{NT}_{s(i)}$ is an indicator set to one if firm i belongs to a non-tradable sector s, as described in Section 3. Column 2 defines tradable sectors using WIOD, where exports exceed the median proportion of total value-added for NACE 2-digit sectors. Column 3 applies the tradability measure from Gervais and Jensen (2019), while Column 4 adapts Mian and Sufi (2014)'s measure to Italy using wage bill data. Rows 1-4 show the effect on log sales of an additional day in each temperature range. Rows 5-8 show the additional effect on log sales for non-tradable goods. Standard errors are clustered at the grid-cell level and reported in parentheses. *, **, and *** denote 10, 5, and 1% statistical significance respectively.

5.3.2 Adaptation

In the next section, we use the estimates presented in Section 5.1 to predict the aggregate productivity effects of temperature increases due to climate change. For this purpose, considering adaptation is important, as neglecting the fact that firms adopt climate-mitigating measures in response to climate change may lead to overestimating the overall effect.[30]

We build on recent literature on adaptation, including Auffhammer (2018), Heutel et al. (2021), Carleton et al. (2022), and Nath (2024), by exploiting variation in long-term climate

[30]Note that our model and empirical strategy already incorporate two aspects of adaptation. First, the model allows for input reallocation, with empirical evidence showing materials and labor respond to temperature changes, while capital does not. Second, since firm-level data are annual and temperature measures are daily, actions firms take to boost production in response to temperature increases during the year, such as extending working hours during cooler periods, are already captured in our semielasticities.

exposure. Firms in different regions experience distinct climates, not only in average temperature but also in variability. Greater exposure to extreme temperatures may lead to differing adaptation patterns and temperature semielasticities. We examine the impact of operating in grid cells with varying exposure to extreme temperatures, arguing that regional adaptation is better modeled based on temperature variability rather than averages. This is very relevant in Italy, where coastal areas often have higher average temperatures but fewer extreme heat events compared to inland regions. Our findings align with earlier estimates showing that firms are more affected by extreme temperatures than by small deviations from the average. To test this hypothesis we estimate the following regression:

$$\begin{aligned} Outcome_{it} = & \sum_{\ell} \beta_{1,\ell} T^{\ell}_{g(i)t} + \delta_1 Rain_{g(i)t} + \boldsymbol{\lambda_1'} \mathbf{X}_{r(i)t} \\ & + \left(\sum_{\ell} \beta_{2,\ell} T^{\ell}_{g(i)t} + \delta_2 Rain_{g(i)t} + \boldsymbol{\lambda_2'} \mathbf{X}_{r(i)t} \right) \times I^{H}_{g(i)} + \gamma_{s(i)t} + \alpha_i + \varepsilon_{it}, \end{aligned} \tag{27}$$

where $I^{H}_{g(i)}$ is an indicator set to one if firm i operates in adapted grid-cells g, defined as those experiencing more extreme temperatures during the year, and the other variables are described in equation (25).[31] Columns 2 and 5 of Table 6 use an indicator variable set to one if the number of extreme temperature days in a grid-cell exceeds the national mean, while columns 3 and 6 use the national median as the threshold. In this specification, the estimated coefficients $\beta_{1,\ell}$ represent the temperature-semielasticity of sales common to firms in regions with both high and low exposure to extreme temperatures. In contrast, the coefficients $\beta_{2,\ell}$ capture the differential effect of temperature on firms in more adapted grid-cells.

Results in Table 6, columns 2 and 3, show that this differential effect is positive for the number of days above 40 degrees. In other words, firms in more adapted regions experience a less negative effect of extremely high temperatures on output compared to firms in less adapted regions. They also experience a lower fall in their marginal return to capital, although this coefficient is imprecisely estimated. Conversely, we find smaller and insignificant effects of adaptation regarding the exposure to high but less extreme temperatures. Overall, we take these results as suggestive evidence of relatively small adaptation effects, broadly in line with those found in the literature (Nath, 2024).

[31] Specifically, we define extreme days as those with maximum temperatures above 30 degrees or below 0 degrees. For each location and year, we calculate the ratio of days with extreme temperatures to days with moderate temperatures (maximum daily temperatures between 0 and 30 degrees). Adapted locations are those with an average yearly ratio over the sample period exceeding the national mean or median.

Table 6: Effect of Temperature on Sales and MRPK Conditional on Adaptation

Dependent Variable	**Sales** (1)	**Sales** (2)	**Sales** (3)	**MRPK** (4)	**MRPK** (5)	**MRPK** (6)
Temperature Bins						
$(-\infty, 0°C]$	-0.094***	-0.080***	-0.079***	-0.030	-0.004	-0.001
	(0.019)	(0.021)	(0.021)	(0.022)	(0.027)	(0.028)
$(30°C, 35°C]$	-0.017*	-0.029***	-0.023**	-0.014	-0.019	-0.018
	(0.009)	(0.010)	(0.009)	(0.010)	(0.012)	(0.013)
$(35°C, 40°C]$	-0.046***	-0.035	-0.024	-0.045**	-0.049	-0.061
	(0.017)	(0.033)	(0.037)	(0.021)	(0.036)	(0.042)
$(40°C, +\infty)$	-0.807***	-1.864***	-2.039***	-0.578**	-1.225**	-1.393***
	(0.194)	(0.505)	(0.524)	(0.231)	(0.536)	(0.551)
Temperature Bins$\times I^H_{g(i)}$						
$(-\infty, 0°C]$		-0.019	-0.019		-0.039	-0.041
		(0.028)	(0.027)		(0.031)	(0.031)
$(30°C, 35°C]$		0.018	0.009		0.017	0.019
		(0.011)	(0.011)		(0.014)	(0.013)
$(35°C, 40°C]$		-0.003	-0.012		0.025	0.042
		(0.032)	(0.036)		(0.038)	(0.043)
$(40°C, +\infty)$		1.146**	1.344**		0.653	0.826
		(0.540)	(0.559)		(0.581)	(0.595)
Fixed Effects						
Firm	✓	✓	✓	✓	✓	✓
Sector × Year	✓	✓	✓	✓	✓	✓
GR and SDC × Region	✓	✓	✓	✓	✓	✓
Controls						
Rainfalls	✓	✓	✓	✓	✓	✓
Region Trends	✓	✓	✓	✓	✓	✓
Observations	4,687,524	4,687,503	4,687,503	4,328,710	4,328,689	4,328,689

Note. All dependent variables are in logs. Temperature bins are constructed as explained in Section 3.2. In columns 2 and 5 the variable $I^H_{g(i)}$ is an indicator function that takes the value of one if firm i belongs to a grid-cell g with the number of extreme days above the national mean. In columns 3 and 6 the variable $I^H_{g(i)}$ is an indicator function that takes the value of one if firm i belongs to a grid-cell g with the number of extreme days above the national median. Rows 1-4 present the effect on the log of sales of adding an extra day in the given temperature range respectively. Rows 5-12 present the extra effect coming from being exposed to extreme temperatures. Standard errors are clustered at the grid-cell level and reported in parentheses. *, **, and *** denote 10, 5, and 1% statistical significance respectively.

6 Aggregate Effects

This section documents the aggregate productivity losses resulting from various warming scenarios and highlights their heterogeneous regional impact.

6.1 Aggregate Productivity Loss

While our reduced-form estimates indicate that climate change reduces firm-level productivity and the revenue-based marginal product of capital, they do not reveal whether these effects significantly impact aggregate productivity. To assess this, we estimate the effect of climate change on the Solow residual, a proxy for aggregate productivity, using equations (19), (20),

and (22), which we restate compactly as:

$$\Delta \log Solow_t \approx \frac{Y_t}{GDP_t} \underbrace{\Delta \log TFP_t^* \left(e^{\tilde{z}_{it}(T_{g(i)t})}, \Delta T_{g(i)t} \right)}_{\Delta \text{Technology}} - \underbrace{\left(\Delta \log TFP_t^* \left(e^{\tilde{z}_{it}(T_{g(i)t})}, \Delta T_{g(i)t} \right) - \Delta \log TFP_t \left(e^{\tilde{z}_{it}(T_{g(i)t})}, e^{\tau_{it}^X(T_{g(i)t})}, \Delta T_{g(i)t} \right) \right)}_{\Delta \text{Allocative Efficiency}}. \tag{28}$$

Equation (28) indicates that to quantify the counterfactual effect of climate change on aggregate productivity, we require: (i) the demand-adjusted productivity $e^{\tilde{z}_{it}(T_{g(i)t})}$ and the temperature-semielasticity; (ii) input-specific wedges $e^{\tau_{it}^X(T_{g(i)t})}$ and the temperature-semielasticity; and (iii) counterfactual changes in grid-cell-level temperatures $\Delta T_{g(i)t}$. For the elasticity of substitution between the varieties σ and the production function elasticities α^X we use the same values as in Section 5.2. We next turn to explain how we use the empirical results from Section 5 to measure each of these elements.

6.1.1 Measurement and Identification

Demand-adjusted productivity. We compute demand-adjusted productivity in the data using equation (18). For the temperature-semielasticity of the demand-adjusted productivity, we follow the calculations in Section 5.2 as reported in Table 4.

Input-specific wedges. We compute input-specific wedges with our firm-level data using equation (13) as explained in Section 3. To calculate the temperature-semielasticity of the input-specific wedges we use the findings from Section 5.1 and proceed as follows: (i) we set the temperature-semielasticity of labor and materials inputs to zero, as no significant effects of temperature were observed (see Table 3), and (ii) we use the estimated temperature-semielasticity of capital input from Table 3.

Counterfactual changes in grid-cell-level temperatures. The final component for calculating productivity losses from climate change under various warming scenarios is the counterfactual change in grid-cell-level temperatures. We derive these changes for different scenarios, including mean temperature increases of 1, 2 (baseline), and 4 degrees Celsius. A 2-degree Celsius increase serves as our benchmark, aligning with the Paris Agreement goals, while other scenarios are used for robustness checks.[32] Additionally, we include the RCP4.5 and RCP8.5 scenarios from the Copernicus climate models as robustness checks, representing average

[32] https://unfccc.int/process-and-meetings/the-paris-agreement.

temperature increases of approximately 2 and 4 degrees Celsius, respectively.[33] These scenarios offer the advantage of capturing non-linear and heterogeneous temperature increases across different regions (NUTS3), aligning closely with realistic climate change models.

Figure 3: Counterfactual Average Distribution of Days Within Temperature Bins

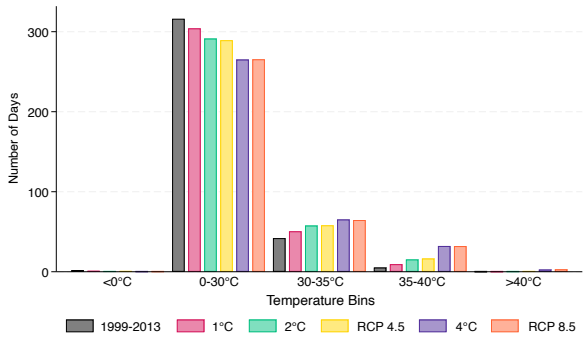

Note. Figure 3 shows the average number of days per year within each temperature bin of the vector $\boldsymbol{T}$. The number of days within each bin is an average across grid-cells. The first column (grey) reports the data for the period 1999-2013. The second column (pink) reports the warming scenario where the daily temperature increases by 1-degree Celsius. The third column (green) reports the warming scenario where the daily temperature increases by 2-degrees Celsius. The fourth column (orange) reports the warming scenario from the RCP4.5 where temperature increases by approximately 2-degrees Celsius. The fifth column (blue) reports the warming scenario where the daily temperature increases by 4-degrees Celsius. The sixth column (red) reports the warming scenario from the RCP8.5 where temperature increases by approximately 4-degrees Celsius.

To calculate the counterfactuals for different warming scenarios, we add the specified temperature increase to each grid-cell's daily temperatures throughout the year. This produces a new distribution of days within each temperature range for each grid-cell under each scenario. We then partition these distributions into temperature bins, as outlined in Section 3.2, represented by the vector $\boldsymbol{T_c} = \{T_c^\ell\}_\ell$. Figure 3 illustrates the average counterfactual distributions of days within each bin across grid-cells, while Table D.10 in Appendix D.1 provides the complete distribution for all grid-cells and scenarios. Using these partitions, we compute the counterfactual changes in the number of days per temperature bin relative to those in Section 3.2, which form the basis of our analysis. Table D.11 in Appendix D.1 presents the full distribution of changes across grid-cells under each warming scenario.

6.1.2 Results

In this section, we quantify the aggregate productivity losses resulting from climate change across various climate scenarios, distinguishing between the effects of pure technology and changes in allocative efficiency.

[33] https://climate.copernicus.eu/sites/default/files/2021-01/infosheet3.pdf.

Baseline. Under the baseline warming scenario of a 2-degree Celsius increase in average temperature, we estimate an aggregate productivity loss of 1.68 percent (Table 7, row 1).[34] This loss is driven by two factors: 48 percent is due to firm-level productivity reductions, and 52 percent results from decreased allocative efficiency. In economic terms, this equates to a GDP loss of approximately 35.37 billion USD in 2021, based on Italy's GDP of approximately 2.108 trillion USD that year.[35]

Alternative scenarios and robustness. To better understand the relationship between the magnitude of temperature shocks and their economic impacts, as well as to test the robustness of our findings, we examine five alternative scenarios outlined in Table 7. These include 1-degree and 4-degree Celsius increases in average temperature, the RCP4.5 and RCP8.5 scenarios from the Copernicus climate model, and the baseline 2-degree Celsius scenario with adaptation forces accounted for. In the 1-degree Celsius scenario (row 2), aggregate productivity losses are 0.77 percent, with 40 percent due to firm-level productivity reductions and 60 percent to decreased allocative efficiency. In contrast, the 4-degree Celsius scenario (row 4) shows productivity losses rising to 6.82 percent, with 49 percent stemming from firm-level reductions and 51 percent from decreased allocative efficiency. These scenarios correspond to GDP losses of 16.27 billion USD and 143.88 billion USD, respectively.

Table 7: Effect of Climate Change on Aggregate Productivity

		Aggregate Productivity Loss		
		Δ*Total*	Δ*Technology*	Δ*Allocative Efficiency*
Baseline	2°C	1.68%	0.81%	0.87%
	1°C	0.77%	0.31%	0.46%
	2°C, Adaptation	1.21%	0.53%	0.68%
Robustness	4°C	6.82%	3.33%	3.49%
	RCP4.5	1.64%	0.85%	0.79%
	RCP8.5	5.35%	2.75%	2.60%

Note. This table reports the productivity losses due to climate change. Column 1 reports the total losses, column 2 reports the losses due to due to reductions in firm-level productivity, and column 3 reports the losses due to allocative efficiency. Row 1 reports the losses under the baseline scenario of a 2-degree Celsius increase in average temperature. Rows 2 to 6 report the robustness exercises. Row 2 reports the losses under the scenario of 1 degrees Celsius increase in average temperature. Row 3 reports the losses under the scenario of a 2-degrees Celsius increase in average temperature conditional on adaptation as explained in the main text. Row 4 reports the losses under the scenario of a 4-degrees Celsius increase in average temperature. Row 5 reports the losses under the scenario of an approximately 2-degrees Celsius increase from the RCP4.5 climate model. Row 6 reports the losses under the scenario of an approximately 4-degrees Celsius from the RCP8.5 climate model.

[34]To reduce the impact of short-term temperature volatility (as shown in Figure 1a for 1999–2013), we calculate the counterfactual aggregate productivity loss for each sample year and compute a weighted average based on the number of observations.

[35]To calculate the GDP loss, we multiply the 2021 Italian GDP in US dollars (2.108 trillion US dollars) by the percentage loss (1.56 percent): 0.0168$\times$2.108 trillion US dollars = 35.37 billion US dollars.

These alternative scenarios underscore the nonlinear and convex nature of climate change's impact on productivity losses. This is partly driven by the inverted U-shaped relationship between temperature and firm-level economic outcomes identified in Section 5, where a linear increase in hot days results in a convex rise in productivity losses. Additionally, climate change exponentially increases the number of regions exposed to extreme temperatures as average temperatures rise. As shown in Table D.10 in the appendix, the average number of +40℃ days per year rises from 0.04 to 0.41 in the 2-degree Celsius scenario and surges to 2.55 in the 4-degree scenario. In Section 6.2, we compare these findings to losses derived from damage functions used in Integrated Assessment Models.

In the RCP4.5 scenario (row 5) and RCP8.5 scenario (row 6), corresponding to average temperature increases of 2 and 4 degrees Celsius, aggregate productivity losses are 1.64 percent and 5.35 percent, respectively, with 48 percent and 49 percent due to decreased allocative efficiency, and the remainder to firm-level productivity losses. These scenarios translate to GDP losses of 34.58 billion USD and 112.72 billion USD, respectively. Thus, counterfactual temperature changes from realistic climate models yield similar aggregate productivity losses to those from simpler scenarios.

Finally, we evaluate how firm-level adaptation influences our aggregate findings. Using the estimates from Table 6 in Section 5.3.2, we find that for the baseline 2-degree Celsius temperature increase (row 3), aggregate productivity losses amount to 1.21 percent—28 percent lower than in the baseline scenario. Of this reduction, 57 percent is due to declining allocative efficiency, with the remainder from firm-level productivity losses. This corresponds to a GDP loss of 25.44 billion USD. The effects of adaptation under other scenarios are detailed in Appendix D.2.[36]

6.2 Discussion

In this section, we highlight the benefits of a model-based approach for estimating the aggregate effects of temperature on productivity. We compare our findings with existing literature and address the main caveats of our approach, acknowledging its limitations and suggesting areas for future research.

[36] Adaptation mitigates damages less in higher-temperature scenarios (4-degree Celsius and RCP8.5) than in the baseline. This is because 81 percent of firms in less adapted regions (i.e., grid-cells with below-median extreme temperature days) are projected to adapt under the 2-degree Celsius scenario, leaving limited room for additional adaptation as temperatures rise further. Alternative adaptation models, based on the historical relationship between average temperatures and their dispersion, yield similar results. These estimates are available upon request.

6.2.1 Advantage of Theory-Based Aggregation of Firm-Level Climate Damages

As discussed, a key advantage of our approach is its closed-form expression, which links micro-level temperature effects to aggregate productivity outcomes.

To illustrate the added value of our framework in assessing aggregate productivity losses from climate change, we compare our results with best practices from firm-level studies (e.g., Zhang et al., 2018, Somanathan et al., 2021). These studies typically apply estimated firm-level productivity losses directly to the temperature change assumed in the counterfactual scenario, calculating the following simple average:

$$\overline{\widehat{\Delta \tilde{z}_{it}}} = \sum_{i=1}^{N_t} \frac{\widehat{\Delta \tilde{z}_{it}}}{N_t}, \quad \text{where} \quad \widehat{\Delta \tilde{z}_{it}} \equiv \frac{\partial \tilde{z}_{it}(T_{g(i)t})}{\partial T_{g(i)t}} \Delta T_{g(i)t}. \tag{29}$$

For a 2-degree Celsius temperature increase, applying this approach to our estimates results in a productivity decline of 0.39 percent. In contrast, our theory-based aggregation yields a decline of 1.68 percent—more than three times larger. This discrepancy can be understood through the following decomposition within our framework:

$$\begin{aligned} \Delta \log Solow_t - \overline{\widehat{\Delta \tilde{z}_{it}}} = & \underbrace{\left(\frac{Y_t}{GDP_t} - 1\right) \overline{\widehat{\Delta \tilde{z}_{it}}}}_{\text{Roundabout material production}} + \underbrace{\frac{Y_t}{GDP_t} \mathbb{C}\left(\lambda_{it}^*, \widehat{\Delta \tilde{z}_{it}}\right)}_{\text{Size and losses covariance}} \\ & - \underbrace{\frac{Y_t}{GDP_t} \left(\Delta \log TFP_t^* - \Delta \log TFP_t\right)}_{\Delta \text{ Allocative Efficiency}}, \end{aligned} \tag{30}$$

where $\overline{\widehat{\Delta \tilde{z}_{it}}}$ and $\widehat{\Delta \tilde{z}_{it}}$ are defined in equation (29), and λ_{it}^* is defined in Section 2.

Three factors account for the difference between our theory-based approach and the reduced-form approach. First, the roundabout nature of material production acts as a multiplier, as described in Section 2. Greater material usage in the economy increases the ratio of Y_t/GDP_t, amplifying the difference between the two approaches. Second, the covariance between efficient firm-level weights and estimated productivity losses plays a role. When firm-level losses positively covary with firms' initial efficient sizes, the divergence becomes more pronounced. Finally, changes in allocative efficiency further amplify the difference, as this factor has not been accounted for in previous empirical studies. Overall, we find that the first term explains 29 percent of the difference, the second term 3 percent, and the third term 68 percent. In summary, while causal estimates of firm-level damages are valuable, a

theory-based aggregation that incorporates multiple channels, general equilibrium effects, and amplification mechanisms is essential for accurately capturing the significant impact of climate change on aggregate productivity losses.

6.2.2 Comparison with the Literature

Figures 4a and 4b compare our aggregate productivity losses, with and without adaptation, to the damage functions used in the latest iteration of the DICE model by Barrage and Nordhaus (2023).[37] This model serves as a benchmark, representing the standard calibration approach in the literature (e.g., Golosov et al., 2014, Krusell and Smith, 2022, Hassler et al., 2016, Fernández-Villaverde et al., 2024). Its global damage function is given by $0.003467 \times \Delta T^2$. To compare with our Europe-based estimates, we adjust their calibration by multiplying the world damage function by 0.677.[38] This adjustment reflects findings from aggregate studies (e.g., Nordhaus and Yang, 1996; Dell et al., 2012) that Europe typically experiences lower aggregate productivity damages. Details of our productivity loss calculations are provided in Section 6.1.1.

Figure 4: Differences Across Productivity Loss Functions

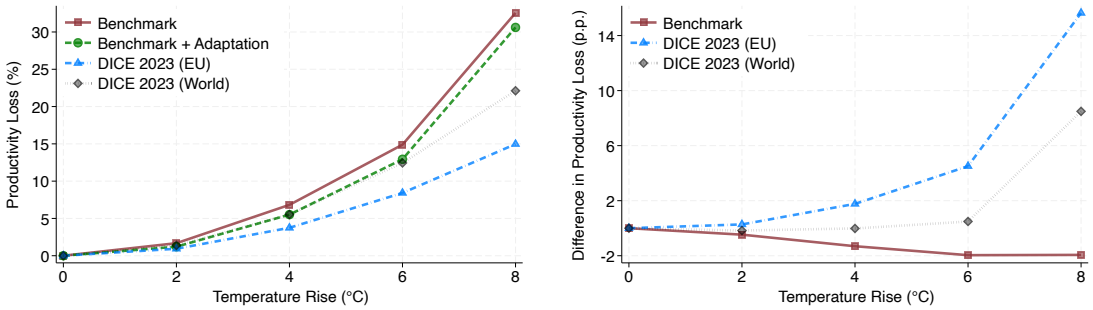

(a) Productivity Loss Across Models

(b) Difference in Productivity Loss Across Models

Note. Figure 4a compares productivity losses (in percent) due to temperature increases across four models: our model without adaptation (red line with squares), our model with adaptation (dashed green line with circles), the European-adjusted losses from the DICE model (dash-dotted blue line with triangles), and the global losses from the DICE model (dotted gray line with diamonds). Figure 4b illustrates the percentage point differences in productivity losses between our benchmark model , the DICE model adjusted for Europe, and the world DICE model, with respect to our benchmark model with adaptation. The DICE model used as a reference is from Barrage and Nordhaus (2023).

The left figure shows productivity losses across different models, while the right figure highlights the differences between losses in our benchmark model, as well as the losses for

[37] We include losses with and without adaptation to ensure a fair comparison, as DICE model calibrations typically account for adaptation adjustments.

[38] This adjustment uses the regional damages reported in Nordhaus and Yang (1996), specifically the ratio of European to global damages. The ratio is derived from GDP-weighted averages of regional damages listed in Table 2 on page 746.

Europe and the world from the DICE model, relative to our model with adaptation. All models display a convex, nonlinear relationship that steepens with higher temperature increases. Recasting our results into the functional form of an aggregate damage function, our model implies a loss of $0.00444 \times \Delta T^2$. This indicates that productivity losses are larger in our framework, especially under more extreme climate change scenarios.

It is important to interpret the evidence presented here accurately. Our estimated losses are not intended as a superior proxy for the loss functions modeled in the above-mentioned studies. Those works aim to assess the overall economic impact of temperature increases across various channels, including changes in mortality, crop yields, coastal erosion, and labor supply. In contrast, our findings highlight significant losses from a single, largely independent channel, emphasizing the value of detailed micro-data in reassessing the total economic costs of climate change. However, we acknowledge that integrating all these effects into a unified framework and evaluating their relative importance lies beyond the scope of this study.

6.2.3 Interpretation of the Results

Our findings are subject to potential caveats. Like much of the literature that uses micro-data to estimate the effects of local temperature fluctuations, we focus on short-run effects. However, these may differ from long-run effects due to technological adaptation. Over time, firms may become better equipped to manage extreme temperatures through technological advancements or increased investment in climate-mitigating technologies. While quantifying the former remains challenging, we show in Sections 5.3.2 and 6.1.2 that accounting for the latter reduces our estimated productivity losses of climate change by roughly 20–30 percent.

Furthermore, long-run effects may diminish due to improvements in allocative efficiency as short-term capital reallocation frictions ease. While estimating these dynamics is challenging within our short panel, our framework provides an upper bound on this potential bias in aggregate productivity losses. Assuming firm-level productivity losses persist but all capital reallocation frictions are resolved in the long run, the frictionless term in equation (20) estimates the minimum aggregate productivity loss achievable under full capital mobility.

Additionally, our framework is static. While this choice has advantages, it does not account for the extensive margin, such as firm entry and exit, due to limited data on these dynamics. Neglecting this margin likely biases our results through two channels. First, unproductive firms in affected regions may exit, improving firm selection. Second, firms in these regions might close and relocate their capital to cooler areas, enhancing long-term allocative efficiency (although we find limited evidence for this in our sample). Despite this limitation,

our findings on the relative importance of different channels and wedges offer valuable inputs for future models incorporating extensive margin effects.[39]

6.3 Regional Heterogeneity

This section examines the impact of climate change on productivity losses at the province level (NUTS 3) in Italy. Using the methodology described in Section 2, we apply equation (22) to each province to estimate the magnitude and spatial distribution of these losses under the baseline warming scenario of 2-degrees Celsius.

Figure 5: Regional Productivity Losses for 2°C Warming Scenario

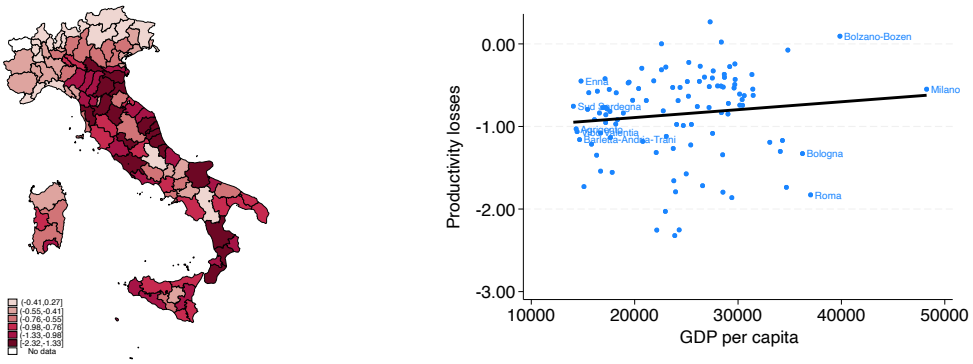

(a) Regional Productivity Losses **(b) Regional Losses and GDP Per Capita**

Note. Figure 5a shows the productivity losses across NUTS 3 regions due to a 2-degrees Celsius increase in temperature, calculated using equation (19), adjusted with the ratio of gross output to value added. Productivity losses are in percent, and darker colors represent larger losses. Figure 5b plots the same regional losses against average GDP per capita in our sample, showing a negative correlation of 0.232.

The results in Figure 5a reveal significant regional variations in productivity losses across Italian provinces under the 2-degree Celsius warming scenario. While climate change negatively impacts productivity overall, the effects are uneven. Some regions see modest productivity gains of up to 0.27 percent, whereas others experience substantial losses, with reductions as high as 2.32 percent.

Our analysis highlights regional disparities in climate change-induced productivity losses between southern and northern Italy. Southern regions face significant negative impacts due to an increase in extreme heat days, while northern alpine areas benefit from fewer days below 0 degrees Celsius, leading to moderate productivity losses or even modest gains. Appendix D.3, Figures D.2a-D.2b, illustrates regional productivity losses across the four alter-

[39] This is particularly relevant as the misallocation literature highlights that input wedges and productivity factors, like those quantified here, influence firms' entry and exit decisions in different ways (Restuccia and Rogerson, 2017).

native warming scenarios. Overall, we find that the most severe impacts of climate change persist in southern regions across all scenarios. The RCP4.5 and RCP8.5 scenarios, which provide more accurate predictions of local temperature changes and project greater temperature increases in the south compared to the north, indicate even wider disparities in productivity losses between northern and southern regions.

These findings highlight how firm-level losses, characterized by an inverted U-shaped pattern, translate into significant regional differences based on historical temperatures. To further examine the relationship between predicted productivity losses and inequality, Figure 5b plots productivity losses against GDP per capita. While some wealthy northern regions experience considerable productivity losses, as noted in Section 6.2.1, we observe an overall positive correlation, indicating that climate change is likely to exacerbate regional inequality in Italy. Notably, this correlation is much stronger under the more accurate RCP4.5 and RCP8.5 scenarios (see Figures D.3d and D.3e in Appendix D.3).

7 Conclusion

We present a novel micro-to-macro framework to quantify the aggregate productivity impacts of climate change, rooted in firm-level data and a general equilibrium model. Our findings underscore the importance of incorporating both direct productivity effects and indirect effects stemming from input adjustment frictions. These mechanisms amplify the economic costs of climate change, with aggregate productivity losses estimated to be significantly larger than those derived from representative firm models or standard IAM methodologies.

Our analysis reveals a highly nonlinear relationship between temperature increases and aggregate productivity losses, driven by firm-level dynamics and geographic variation in temperature extremes. Using Italian firm-level data combined with detailed climate information, we identify an inverted U-shaped effect of temperature on firm sales, with extreme high or low temperatures significantly reducing productivity. Extreme temperatures decrease labor and material inputs but leave capital usage largely unchanged, reflecting greater frictions in capital adjustment compared to other inputs. As a result, we find an inverted U-shaped relationship between extreme temperatures and the revenue-based marginal product of capital, while the marginal products of other inputs remain unaffected.

These findings underscore the importance of indirect effects, driven by input adjustment frictions, in amplifying the overall impact of temperature on firms. Using the estimated semi-elasticities from our empirical analysis, we quantify these impacts in a general equilibrium

model. We estimate that indirect effects account for half of the aggregate productivity losses. Under a 2℃ warming scenario, aggregate productivity losses reach 1.68%, while a 4℃ scenario leads to a sharp increase to 6.81%, illustrating the compounding effects of temperature on economic outcomes. Moreover, we uncover heterogeneous regional impacts across Italy, highlighting how extreme temperatures disproportionately affect productivity in areas with limited adaptation capacity.

This research contributes to the broader climate economics literature by complementing existing approaches and addressing some of their limitations. First, we show that indirect effects—driven by input frictions and allocative inefficiencies—are quantitatively significant, accounting for a substantial share of total losses. Second, our closed-form aggregate damage function, derived from firm-level semi-elasticities, provides a robust methodology for integrating these findings into IAMs, offering a more comprehensive assessment of climate-related damages. Notably, our framework predicts higher aggregate losses compared to traditional IAMs, emphasizing the need to revise upward the economic costs of climate change and the social cost of carbon. In conclusion, this paper highlights the importance of a microfounded approach, leveraging firm-level data and structural modeling, to inform existing aggregate models of the economics of climate change. Our complementary framework could be easily integrated to enhance assessments of climate change's economic impacts.

References

Acharya, V. V., A. Bhardwaj, and T. Tomunen (2023): "Do Firms Mitigate Climate Impact on Employment? Evidence from U.S. Heat Shocks," NBER Working Paper no.31967.

Addoum, J. M., D. T. Ng, and A. Ortiz-Bobea (2020): "Temperature Shocks and Establishment Sales," *The Review of Financial Studies*, 33, 1331–1366.

Albert, C., P. Bustos, and J. Ponticelli (2021): "The Effects of Climate Change on Labor and Capital Reallocation," NBER Working Paper no.28995.

Almunia, M., P. Antràs, D. Lopez-Rodriguez, and E. Morales (2021): "Venting out: Exports During a Domestic Slump," *American Economic Review*, 111, 3611–62.

Auffhammer, M. (2018): "Quantifying Economic Damages from Climate Change," *Journal of Economic Perspectives*, 32, 33–52.

Auffhammer, M., S. M. Hsiang, W. Schlenker, and A. Sobel (2013): "Using weather data and climate model output in economic analyses of climate change," *Review of Environmental Economics and Policy*, 7(2), 181–198.

Balboni, C. (2025): "In Harm's Way? Infrastructure Investments and the Persistence of Coastal Cities," *American Economic Review*, 115, 77–116.

Balboni, C., J. Boehm, and M. Waseem (2024): "Firm adaptation and production networks: Structural evidence from extreme weather events in Pakistan," PEDL Working Paper.

Baqaee, D. R. and E. Farhi (2020): "Productivity and Misallocation in General Equilibrium," *The Quarterly Journal of Economics*, 135, 105–163.

Barrage, L. (2020): "The Fiscal Costs of Climate Change," in *AEA Papers and Proceedings*, vol. 110, 107–112.
Barrage, L. and W. D. Nordhaus (2023): "Policies, Projections, and the Social Cost of Carbon: Results from the DICE-2023 Model," NBER Working Paper no.31112.
Bastien-Olvera, B. A., F. Granella, and F. C. Moore (2022): "Persistent Effect of Temperature on GDP Identified from Lower Frequency Temperature Variability," *Environmental Research Letters*, 17, 084038.
Bau, N. and A. Matray (2023): "Misallocation and Capital Market Integration: Evidence From India," *Econometrica*, 91, 67–106.
Bernard, A. B., J. Eaton, J. B. Jensen, and S. Kortum (2003): "Plants and Productivity in International Trade," *American Economic Review*, 93, 1268–1290.
Bilal, A. and D. R. Känzig (2024): "The Macroeconomic Impact of Climate Change: Global vs. Local Temperature," NBER Working Paper no.32450.
Bilal, A. and E. Rossi-Hansberg (2023): "Anticipating Climate Change Across the United States," NBER Working Paper no.31323.
Broda, C. and D. E. Weinstein (2006): "Globalization and the Gains from Variety," *The Quarterly Journal of Economics*, 121, 541–585.
Burke, M., S. M. Hsiang, and E. Miguel (2015): "Global Non-Linear Effect of Temperature on Economic Production," *Nature*, 527, 235–239.
Burke, M. and V. Tanutama (2019): "Climatic Constraints on Aggregate Economic Output," NBER Working Paper no.25779.
Busse, M. R., D. G. Pope, J. C. Pope, and J. Silva-Risso (2015): "The Psychological Effect of Weather on Car Purchases," *The Quarterly Journal of Economics*, 130, 371–414.
Caballero, R. J., E. Farhi, and P.-O. Gourinchas (2017): "Rents, Technical Change, and Risk Premia Accounting for Secular Trends in Interest Rates, Returns on Capital, Earning Yields, and Factor Shares," *American Economic Review*, 107, 614–620.
Caggese, A. and V. Cuñat (2008): "Financing Constraints and Fixed-Term Employment Contracts," *The Economic Journal*, 118, 2013–2046.
——— (2013): "Financing Constraints, Firm Dynamics, Export Decisions, and Aggregate Productivity," *Review of Economic Dynamics*, 16, 177–193.
Carleton, T., A. Jina, M. Delgado, M. Greenstone, T. Houser, S. Hsiang, A. Hultgren, R. E. Kopp, K. E. McCusker, I. Nath, et al. (2022): "Valuing the Global Mortality Consequences of Climate Change Accounting for Adaptation Costs and Benefits," *The Quarterly Journal of Economics*, 137, 2037–2105.
Cascarano, M., F. Natoli, and A. Petrella (2022): "Entry, Exit and Market Structure in a Changing Climate," Banca d'Italia Working Paper No.1418.
Casey, G., S. Fried, and E. Goode (2023): "Projecting the Impact of Rising Temperatures: The Role of Macroeconomic Dynamics," *IMF Economic Review*, 1–31.
Castro-Vincenzi, J. (2022): "Climate hazards and resilience in the global car industry," *Princeton University manuscript*.
Castro-Vincenzi, J., G. Khanna, N. Morales, and N. Pandalai-Nayar (2024): "Weathering the storm: Supply chains and climate risk," NBER Working Paper no.32218.
Christiano, L. J., M. S. Eichenbaum, and M. Trabandt (2015): "Understanding the Great Recession," *American Economic Journal: Macroeconomics*, 7, 110–167.
Cloyne, J., C. Ferreira, M. Froemel, and P. Surico (2023): "Monetary Policy, Corporate Finance, and Investment," *Journal of the European Economic Association*, 21, 2586–2634.
Cohn, J. and T. Deryugina (2018): "Firm-level Financial Resources and Environmental Spills,"

NBER Working Paper no.24516.
Colciago, A., V. Lindenthal, and A. Trigari (2019): "Who Creates and Destroys Jobs over the Business Cycle?" De Nederlandsche Bank Working Paper No. 628.
Colmer, J. (2021): "Temperature, Labor Reallocation, and Industrial Production: Evidence from India," *American Economic Journal: Applied Economics*, 13, 101–24.
Conley, T. G. (2010): "Spatial Econometrics," in *Microeconometrics*, ed. by A. C. Cameron and P. K. Trivedi, New York: Springer, 303–328.
Conte, B., K. Desmet, and E. Rossi-Hansberg (2022): "On the Geographic Implications of Carbon Taxes," NBER Working Paper no.30678.
Cooper, R. W. and J. C. Haltiwanger (2006): "On the nature of capital adjustment costs," *The Review of Economic Studies*, 73, 611–633.
Cornes, R. C., G. van der Schrier, E. J. van den Besselaar, and P. D. Jones (2018): "An Ensemble Version of the E-OBS Temperature and Precipitation Data Sets," *Journal of Geophysical Research: Atmospheres*, 123, 9391–9409.
Cruz, J.-L. and E. Rossi-Hansberg (2023): "The Economic Geography of Global Warming," *The Review of Economic Studies*, 91, 899–939.
Custodio, C., M. A. Ferreira, E. Garcia-Appendini, and A. Lam (2024): "Does Climate Change Affect Firm Output? Identifying Supply Effects," Available at SSRN: https://ssrn.com/abstract=3724940.
De Loecker, J., J. Eeckhout, and G. Unger (2020): "The Rise of Market Power and the Macroeconomic Implications," *The Quarterly Journal of Economics*, 135, 561–644.
Dell, M., B. F. Jones, and B. A. Olken (2012): "Temperature Shocks and Economic Growth: Evidence from the Last Half Century," *American Economic Journal: Macroeconomics*, 4, 66–95.
——— (2014): "What Do We Learn from the Weather? The New Climate-Economy Literature," *Journal of Economic Literature*, 52, 740–98.
Deschênes, O. and M. Greenstone (2011): "Climate Change, Mortality, and Adaptation: Evidence from Annual Fluctuations in Weather in the U.S." *American Economic Journal: Applied Economics*, 3, 152–185.
Desmet, K. and E. Rossi-Hansberg (2015): "On the Spatial Economic Impact of Global Warming," *Journal of Urban Economics*, 88, 16–37.
Diffenbaugh, N. S. and M. Burke (2019): "Global Warming has Increased Global Economic Inequality," *Proceedings of the National Academy of Sciences*, 116, 9808–9813.
Fernández-Villaverde, J., K. Gillingham, and S. Scheidegger (2024): "Climate Change through the Lens of Macroeconomic Modeling," NBER Working Paper no.32963.
Filomena, M. and M. Picchio (2024): "Unsafe Temperatures, Unsafe jobs: The Impact of Weather Conditions on Work-Related Injuries," *Journal of Economic Behavior & Organization*, 224, 851–875.
Fort, T. C., J. Haltiwanger, R. S. Jarmin, and J. Miranda (2013): "How Firms Respond to Business Cycles: The Role of Firm Age and Firm Size," *IMF Economic Review*, 61, 520–559.
Foster, L., J. Haltiwanger, and C. Syverson (2008): "Reallocation, Firm Turnover, and Efficiency: Selection on Productivity or Profitability?" *American Economic Review*, 98, 394–425.
Fried, S. (2022): "Seawalls and Stilts: A Quantitative Macro Study of Climate Adaptation," *The Review of Economic Studies*, 89, 3303–3344.
Gandhi, A., S. Navarro, and D. A. Rivers (2020): "On the Identification of Gross Output Production Functions," *Journal of Political Economy*, 128, 2973–3016.
Garimella, S., M. T. Hughes, and The Conversation US (2023): "Physicists Explain How

Heat Kills Machines and Electronics," .
Gervais, A. and J. B. Jensen (2019): "The Tradability of Services: Geographic Concentration and Trade Costs," *Journal of International Economics*, 118, 331–350.
Golosov, M., J. Hassler, P. Krusell, and A. Tsyvinski (2014): "Optimal taxes on fossil fuel in general equilibrium," *Econometrica*, 82, 41–88.
Gopinath, G., Ş. Kalemli-Özcan, L. Karabarbounis, and C. Villegas-Sanchez (2017): "Capital Allocation and Productivity in South Europe," *The Quarterly Journal of Economics*, 132, 1915–1967.
Gould, C. F., S. Heft-Neal, A. K. Heaney, E. Bendavid, C. W. Callahan, M. Kiang, J. S. G. Zivin, and M. Burke (2024): "Temperature Extremes Impact Mortality and Morbidity Differently," NBER Working Paper no.32195.
Graff Zivin, J. and M. Neidell (2014): "Temperature and the Allocation of Time: Implications for Climate Change," *Journal of Labor Economics*, 32, 1–26.
Hassler, J., P. Krusell, and A. A. Smith Jr (2016): "Environmental Macroeconomics," in *Handbook of Macroeconomics*, Elsevier, vol. 2, 1893–2008.
Heal, G. and J. Park (2016): "Reflections—Temperature Stress and the Direct Impact of Climate Change: A Review of an Emerging Literature," *Review of Environmental Economics and Policy*, 10, 347–362.
Heutel, G., N. H. Miller, and D. Molitor (2021): "Adaptation and the Mortality Effects of Temperature across U.S. Climate Regions," *Review of Economics and Statistics*, 103, 740–753.
Hsiang, S., R. Kopp, A. Jina, J. Rising, M. Delgado, S. Mohan, D. Rasmussen, R. Muir-Wood, P. Wilson, M. Oppenheimer, et al. (2017): "Estimating Economic Damage from Climate Change in the United States," *Science*, 356, 1362–1369.
Hsieh, C.-T. and P. J. Klenow (2009): "Misallocation and Manufacturing TFP in China and India," *The Quarterly Journal of Economics*, 124, 1403–1448.
IPCC (2021): "IPCC, 2021: Summary for Policymakers," .
Jones, C. I. (2011): "Misallocation, Economic Growth, and Input-Output Economics," NBER Working Paper no.16742.
Kahn, M. E., K. Mohaddes, R. N. Ng, M. H. Pesaran, M. Raissi, and J.-C. Yang (2021): "Long-term Macroeconomic Effects of Climate Change: A Cross-country Analysis," *Energy Economics*, 104, 105624.
Kala, N., P. Kurukulasuriya, and R. Mendelsohn (2012): "The Impact of Climate Change on Agro-Ecological Zones: Evidence from Africa," *Environment and Development Economics*, 17, 663–687.
Kalemli-Özcan, S., B. E. Sørensen, C. Villegas-Sanchez, V. Volosovych, and S. Yeşiltaş (2024): "How to Construct Nationally Representative Firm-Level Data from the Orbis Global Database: New Facts on SMEs and Aggregate Implications for Industry Concentration," *American Economic Journal: Macroeconomics*, 16, 353–74.
Kalkuhl, M. and L. Wenz (2020): "The Impact of Climate Conditions on Economic Production. Evidence from a Global Panel of Regions," *Journal of Environmental Economics and Management*, 103, 102360.
Klein Tank, A., J. Wijngaard, G. Können, R. Böhm, G. Demarée, A. Gocheva, M. Mileta, S. Pashiardis, L. Hejkrlik, C. Kern-Hansen, et al. (2002): "Daily dataset of 20th-century surface air temperature and precipitation series for the European Climate Assessment," *International Journal of Climatology: A Journal of the Royal Meteorological Society*, 22, 1441.
Krusell, P. and A. A. Smith (2022): "Climate Change around the World," NBER Working Paper no.30338.

Lai, W., Y. Qiu, Q. Tang, C. Xi, and P. Zhang (2023): "The effects of temperature on labor productivity," *Annual Review of Resource Economics*, 15, 213–232.
Leduc, S. and D. J. Wilson (2023): "Climate Change and the Geography of the US Economy," Federal Reserve Bank of San Francisco, Working Paper Series 2023-17.
Liu, T. and Z. Xu (2024): "The (Mis)Allocation Channel of Climate Change: Evidence from Global Firm-level Microdata," Working Paper.
Loecker, J. D. and F. Warzynski (2012): "Markups and Firm-level Export Status," *American Economic Review*, 102, 2437–2471.
Melitz, M. J. (2003): "The impact of trade on intra-industry reallocations and aggregate industry productivity," *Econometrica*, 71, 1695–1725.
Mian, A. and A. Sufi (2014): "What Explains the 2007–2009 Drop in Employment?" *Econometrica*, 82, 2197–2223.
Moll, B. (2021): "The Missing Intercept in Cross-Section Regressions," Available at https://benjaminmoll.com/wp-content/uploads/2021/02/missing_intercept.pdf.
Nath, I. (2024): "Climate Change, the Food Problem, and the Challenge of Adaptation through Sectoral Reallocation," *Accepted for publication Journal of Political Economy*.
Nath, I. B., V. A. Ramey, and P. J. Klenow (2024): "How Much Will Global Warming Cool Global Growth?" NBER Working Paper no.32761.
Newell, R. G., B. C. Prest, and S. E. Sexton (2021): "The GDP-Temperature Relationship: Implications for Climate Change Damages," *Journal of Environmental Economics and Management*, 108, 102445.
Nordhaus, W. D. (1977): "Economic Growth and Climate: The Carbon Dioxide Problem," *The American Economic Review*, 67, 341–346.
Nordhaus, W. D. and A. Moffat (2017): "A survey of global impacts of climate change: replication, survey methods, and a statistical analysis," NBER Working Paper no.23646.
Nordhaus, W. D. and Z. Yang (1996): "A Regional Dynamic General-Equilibrium Model of Alternative Climate-Change Strategies," *The American Economic Review*, 741–765.
Osotimehin, S. (2019): "Aggregate Productivity and the Allocation of Resources over the Business Cycle," *Review of Economic Dynamics*, 32, 180–205.
Pankratz, N. M. and C. M. Schiller (2024): "Climate Change and Adaptation in Global Supply-Chain Networks," *The Review of Financial Studies*, 37, 1729–1777.
Ponticelli, J., X. Qiping, and S. Zeume (2023): "Temperature, Adaptation, and Local Industry Concentration," NBER Working Paper no.31533.
Restuccia, D. and R. Rogerson (2008): "Policy Distortions and Aggregate Productivity with Heterogeneous Establishments," *Review of Economic Dynamics*, 11, 707–720.
——— (2017): "The Causes and Costs of Misallocation," *Journal of Economic Perspectives*, 31, 151–174.
Seppanen, O., W. J. Fisk, and Q. Lei (2006): "Room Temperature and Productivity in Office Work," Tech. rep., Lawrence Berkeley National Lab.(LBNL), Berkeley, CA (United States).
Solow, R. M. (1957): "Technical Change and the Aggregate Production Function," *The Review of Economics and Statistics*, 312–320.
Somanathan, E., R. Somanathan, A. Sudarshan, and M. Tewari (2021): "The Impact of Temperature on Productivity and Labor Supply: Evidence from Indian Manufacturing," *Journal of Political Economy*, 129, 1797–1827.
Sraer, D. and D. Thesmar (2023): "How to Use Natural Experiments to Estimate Misallocation," *American Economic Review*, 113, 906–938.
Zhang, P., O. Deschenes, K. Meng, and J. Zhang (2018): "Temperature Effects on Productiv-

ity and Factor Reallocation: Evidence from a Half Million Chinese Manufacturing Plants," *Journal of Environmental Economics and Management*, 88, 1–17.

Online Appendix

Contents

A Structural Framework

In this section, we show the derivations of the equations in Section 2.2.

A.1 Aggregate Gross Output TFP

To derive the equations (19) and (20), we start from the definition of aggregate gross output TFP, given by

$$TFP_t = \left(\frac{\prod_{X \in \mathcal{X}} X_t^{\alpha^X}}{Y_t} \right)^{-1}, \tag{31}$$

$$= \prod_{X \in \mathcal{X}} \left(\frac{X_t}{Y_t} \right)^{-\alpha^X}; \tag{32}$$

where aggregate real inputs are defined as

$$X_t = \sum_{i=1}^{N_t} X_{it}. \tag{33}$$

To characterize aggregate real inputs X_t, we now need to derive the demand for each input X_{it}. We start recalling that the minimized cost function is given by

$$\mathcal{C}(Y_{it}) = \frac{Y_{it}}{e^{z_{it}(T_{g(i)t})}} \prod_{X \in \mathcal{X}} \left(\frac{e^{\tau_{it}^X (T_{g(i)t})} P^X}{\alpha^X} \right)^{\alpha^X}, \tag{34}$$

$$= \prod_{X \in \mathcal{X}} \left(\frac{P_t^X}{\alpha^X} \right)^{\alpha^X} \frac{Y_{it}}{e^{z_{it}(T_{g(i)t})}} \prod_{X \in \mathcal{X}} \left(e^{\tau_{it}^X (T_{g(i)t})} \right)^{\alpha^X}, \tag{35}$$

$$= C_t \frac{Y_{it}}{e^{z_{it}(T_{g(i)t})}} \prod_{X \in \mathcal{X}} \left(e^{\tau_{it}^X (T_{g(i)t})} \right)^{\alpha^X}; \tag{36}$$

where

$$C_t = \prod_{X \in \mathcal{X}} \left(\frac{P_t^X}{\alpha^X} \right)^{\alpha^X}. \tag{37}$$

Given that the first-order conditions for each input are given by

$$e^{\tau_{it}^X(T_{g(i)t})} P_t^X X_{it} = \alpha^X \mathcal{C}(Y_{it}), \tag{38}$$

$$= \alpha^X C_t \frac{Y_{it}}{e^{z_{it}(T_{g(i)t})}} \prod_{X \in \mathcal{X}} \left(e^{\tau_{it}^X(T_{g(i)t})} \right)^{\alpha^X}; \tag{39}$$

we obtain the following input demand function:

$$X_{it} = \alpha^X \frac{C_t}{P_t^X} \frac{Y_{it}}{e^{\tau_{it}^X(T_{g(i)t})} e^{z_{it}(T_{g(i)t})}} \prod_{X \in \mathcal{X}} \left(e^{\tau_{it}^X(T_{g(i)t})} \right)^{\alpha^X}, \tag{40}$$

This implies the following aggregate level for each input X_t:

$$X_t = \alpha^X \frac{C_t}{P_t^X} \sum_{i=1}^{N_t} \frac{Y_{it}}{e^{\tau_{it}^X(T_{g(i)t})} e^{z_{it}(T_{g(i)t})}} \prod_{X \in \mathcal{X}} \left(e^{\tau_{it}^X(T_{g(i)t})} \right)^{\alpha^X}. \tag{41}$$

Substituting equation (41) back into equation (32) we obtain the following:

$$TFP_t = \prod_{X \in \mathcal{X}} \left(\alpha^X \frac{C_t}{P_t^X} \sum_{i=1}^{N_t} \frac{1}{e^{\tau_{it}^X(T_{g(i)t})} e^{z_{it}(T_{g(i)t})}} \frac{Y_{it}}{Y_t} \prod_{X \in \mathcal{X}} \left(e^{\tau_{it}^X(T_{g(i)t})} \right)^{\alpha^X} \right)^{-\alpha^X}, \tag{42}$$

$$= \prod_{X \in \mathcal{X}} \left(\alpha^X \frac{C_t}{P_t^X} \right)^{\alpha^X} \left(\sum_{i=1}^{N_t} \frac{1}{e^{\tau_{it}^X(T_{g(i)t})} e^{z_{it}(T_{g(i)t})}} \frac{Y_{it}}{Y_t} \prod_{X \in \mathcal{X}} \left(e^{\tau_{it}^X(T_{g(i)t})} \right)^{\alpha^X} \right)^{-\alpha^X}, \tag{43}$$

$$= \prod_{X \in \mathcal{X}} \left(\sum_{i=1}^{N_t} \frac{1}{e^{\tau_{it}^X(T_{g(i)t})} e^{z_{it}(T_{g(i)t})}} \frac{Y_{it}}{Y_t} \prod_{X \in \mathcal{X}} \left(e^{\tau_{it}^X(T_{g(i)t})} \right)^{\alpha^X} \right)^{-\alpha^X}; \tag{44}$$

where the last equality holds because of the definition of C_t in equation (37). Notice that now aggregate gross output TFP in equation (44) depends only on wedges and on each firm relative size Y_{it}/Y_t. Hence, to obtain an expression for aggregate gross output TFP that depends only on wedges, we need to express the relative size of each firm as a function of wedges only. We start by defining a firm's relative size using the demand function:

$$\frac{Y_{it}}{Y_t} = \left(e^{d_{it}(T_{g(i)t})} \right)^{\sigma-1} \left(\frac{P_{it}}{P_t} \right)^{-\sigma}. \tag{45}$$

Now, recall that the firms' prices are given by

$$P_{it} = \mathcal{MC}'(Y_{it}), \tag{46}$$

$$= \mathcal{MC}_t \frac{1}{e^{z_{it}(T_{g(i)t})}} \prod_{X \in \mathcal{X}} \left(e^{\tau_{it}^X (T_{g(i)t})} \right)^{\alpha^X}; \tag{47}$$

Moreover, we can substitute firm-level prices from equation (47) into the aggregate price index and obtain

$$P_t = \left(\sum_{i=1}^{N_t} \left(\frac{P_{it}}{e^{d_{it}(T_{g(i)t})}} \right)^{1-\sigma} \right)^{\frac{1}{1-\sigma}}, \tag{48}$$

$$= \left(\sum_{i=1}^{N_t} \left(\mathcal{MC}_t \frac{1}{e^{d_{it}(T_{g(i)t})} e^{z_{it}(T_{g(i)t})}} \prod_{X \in \mathcal{X}} \left(e^{\tau_{it}^X (T_{g(i)t})} \right)^{\alpha^X} \right)^{1-\sigma} \right)^{\frac{1}{1-\sigma}}, \tag{49}$$

$$= \mathcal{MC}_t \left(\sum_{i=1}^{N_t} \left(\frac{1}{e^{\tilde{z}_{it}(T_{g(i)t})}} \prod_{X \in \mathcal{X}} \left(e^{\tau_{it}^X (T_{g(i)t})} \right)^{\alpha^X} \right)^{1-\sigma} \right)^{\frac{1}{1-\sigma}}; \tag{50}$$

Finally, substituting equations (47) and (50) into equation (45), we obtain an expression for firms' relative size as a function of wedges only, given by

$$\frac{Y_{it}}{Y_t} = \left(e^{d_{it}(T_{g(i)t})} \right)^{\sigma-1} \left(\frac{\frac{1}{e^{z_{it}(T_{g(i)t})}} \prod_{X \in \mathcal{X}} \left(e^{\tau_{it}^X (T_{g(i)t})} \right)^{\alpha^X}}{\left(\sum_{i=1}^{N_t} \left(\frac{1}{e^{\tilde{z}_{it}(T_{g(i)t})}} \prod_{X \in \mathcal{X}} \left(e^{\tau_{it}^X (T_{g(i)t})} \right)^{\alpha^X} \right)^{1-\sigma} \right)^{\frac{1}{1-\sigma}}} \right)^{-\sigma} \tag{51}$$

Now, we can substitute equation (51) into equation (44) to obtain the following:

$$TFP_t = \prod_{X\in\mathcal{X}} \left(\sum_{i=1}^{N_t} \frac{\left(e^{d_{it}(T_{g(i)t})}\right)^{\sigma-1}}{e^{\tau_{it}^X(T_{g(i)t})} e^{z_{it}(T_{g(i)t})}} \left(\frac{\frac{1}{e^{z_{it}(T_{g(i)t})}} \prod_{X\in\mathcal{X}} \left(e^{\tau_{it}^X(T_{g(i)t})}\right)^{\alpha^X}}{\left(\sum_{i=1}^{N_t} \left(\frac{1}{e^{\tilde{z}_{it}(T_{g(i)t})}} \prod_{X\in\mathcal{X}} \left(e^{\tau_{it}^X(T_{g(i)t})}\right)^{\alpha^X}\right)^{1-\sigma}\right)^{\frac{1}{1-\sigma}}} \right)^{-\sigma} \prod_{X\in\mathcal{X}} \left(e^{\tau_{it}^X(T_{g(i)t})}\right)^{\alpha^X} \right)^{-\alpha^X}, \tag{52}$$

$$= \left(\sum_{i=1}^{N_t} \left(e^{\tilde{z}_{it}(T_{g(i)t})}\right)^{\sigma-1} \prod_{X\in\mathcal{X}} \left(e^{\tau_{it}^X(T_{g(i)t})}\right)^{-(\sigma-1)\alpha^X} \right)^{\frac{\sigma}{\sigma-1}}$$

$$\times \prod_{X\in\mathcal{X}} \left(\sum_{i=1}^{N_t} \frac{\left(e^{\tilde{z}_{it}(T_{g(i)t})}\right)^{\sigma-1}}{e^{\tau_{it}^X(T_{g(i)t})}} \prod_{X\in\mathcal{X}} \left(e^{\tau_{it}^X(T_{g(i)t})}\right)^{-(\sigma-1)\alpha^X} \right)^{-\alpha^X}. \tag{53}$$

Hence, taking logs in equation (53) we obtain the following:

$$\log TFP_t = \frac{\sigma}{\sigma-1} \log \left(\sum_{i=1}^{N_t} \left(e^{\tilde{z}_{it}(T_{g(i)t})}\right)^{\sigma-1} \prod_{X\in\mathcal{X}} \left(e^{\tau_{it}^X(T_{g(i)t})}\right)^{-(\sigma-1)\alpha^X} \right)$$

$$- \sum_{X\in\mathcal{X}} \alpha^X \log \left(\sum_{i=1}^{N_t} \frac{\left(e^{\tilde{z}_{it}(T_{g(i)t})}\right)^{\sigma-1}}{e^{\tau_{it}^X(T_{g(i)t})}} \prod_{X\in\mathcal{X}} \left(e^{\tau_{it}^X(T_{g(i)t})}\right)^{-(\sigma-1)\alpha^X} \right). \tag{54}$$

Equation 54 shows that aggregate gross output TFP in this framework can be expressed as just a function of (i) firm-level wedges, $e^{\tilde{z}_{it}(T_{g(i)t})}$ and $e^{\tau_{it}^X}(T_{g(i)t})$; (ii) the elasticity of substitution across goods σ; and (iii) the production function elasticities α^X.

Notice that if the revenue-based marginal products equalize across firms, i.e., if $e^{\tau_{it}^X(T_{g(i)t})} = 1$, then equation (54) reduces to the efficient aggregate gross output TFP, given by

$$\log TFP_t^* = \frac{1}{\sigma-1} \log \left(\sum_{i=1}^{N_t} \left(e^{\tilde{z}_{it}(T_{g(i)t})}\right)^{\sigma-1} \right). \tag{55}$$

This concludes the derivations to get equations (16) and (17), which define respectively the inefficient and the efficient aggregate gross output TFP. Using these two equations, we can now derive equations (19) and (20). We start by differentiating equation (54) to obtain a relation linking changes in aggregate gross output TFP to changes in grid-cell-level temperatures,

given by

$$d\log TFP_t = \sigma \sum_{i=1}^{N_t} \underbrace{\left(\frac{\left(e^{\tilde{z}_{it}(T_{g(i)t})}\right)^{\sigma-1} \prod_{X\in\mathcal{X}} \left(e^{\tau_{it}^X(T_{g(i)t})}\right)^{-(\sigma-1)\alpha^X}}{\sum_{i=1}^{N_t} \left(e^{\tilde{z}_{it}(T_{g(i)t})}\right)^{\sigma-1} \prod_{X\in\mathcal{X}} \left(e^{\tau_{it}^X(T_{g(i)t})}\right)^{-(\sigma-1)\alpha^X}} \right)}_{\equiv \lambda_{it}\left(e^{\tilde{z}_{it}(T_{g(i)t})}, e^{\tau_{it}^X(T_{g(i)t})}\right)}$$

$$\times \left(\frac{\partial \tilde{z}_{it}(T_{g(i)t})}{\partial T_{g(i)t}} - \sum_{X\in\mathcal{X}} \alpha^X \frac{\partial \tau_{it}^X(T_{g(i)t})}{\partial T_{g(i)t}} \right) dT_{g(i)t}$$

$$- \sum_{X\in\mathcal{X}} \alpha^X \sum_{i=1}^{N_t} \left(\frac{\frac{\left(e^{\tilde{z}_{it}(T_{g(i)t})}\right)^{\sigma-1}}{e^{\tau_{it}^X(T_{g(i)t})}} \prod_{X\in\mathcal{X}} \left(e^{\tau_{it}^X(T_{g(i)t})}\right)^{-(\sigma-1)\alpha^X}}{\sum_{i=1}^{N_t} \frac{\left(e^{\tilde{z}_{it}(T_{g(i)t})}\right)^{\sigma-1}}{e^{\tau_{it}^X(T_{g(i)t})}} \prod_{X\in\mathcal{X}} \left(e^{\tau_{it}^X(T_{g(i)t})}\right)^{-(\sigma-1)\alpha^X}} \right)$$

$$\times \left((\sigma-1) \frac{\partial \tilde{z}_{it}(T_{g(i)t})}{\partial T_{g(i)t}} - \frac{\partial \tau_{it}^X(T_{g(i)t})}{\partial T_{g(i)t}} - \sum_{X\in\mathcal{X}} (\sigma-1)\alpha^X \frac{\partial \tau_{it}^X(T_{g(i)t})}{\partial T_{g(i)t}} \right) dT_{g(i)t}, \tag{56}$$

$$= \sigma \sum_{i=1}^{N_t} \lambda_{it}\left(e^{\tilde{z}_{it}(T_{g(i)t})}, e^{\tau_{it}^X(T_{g(i)t})}\right)$$

$$\times \left(\frac{\partial \tilde{z}_{it}(T_{g(i)t})}{\partial T_{g(i)t}} - \sum_{X\in\mathcal{X}} \alpha^X \frac{\partial \tau_{it}^X(T_{g(i)t})}{\partial T_{g(i)t}} \right) dT_{g(i)t}$$

$$- \sum_{X\in\mathcal{X}} \alpha^X \sum_{i=1}^{N_t} \underbrace{\left(\frac{\sum_{i=1}^{N_t} \left(e^{\tilde{z}_{it}(T_{g(i)t})}\right)^{\sigma-1} \prod_{X\in\mathcal{X}} \left(e^{\tau_{it}^X(T_{g(i)t})}\right)^{-(\sigma-1)\alpha^X}}{\sum_{i=1}^{N_t} \frac{\left(e^{\tilde{z}_{it}(T_{g(i)t})}\right)^{\sigma-1}}{e^{\tau_{it}^X(T_{g(i)t})}} \prod_{X\in\mathcal{X}} \left(e^{\tau_{it}^X(T_{g(i)t})}\right)^{-(\sigma-1)\alpha^X}} \right)}_{\equiv \Omega_t^X\left(e^{\tilde{z}_{it}(T_{g(i)t})}, e^{\tau_{it}^X(T_{g(i)t})}\right)} \lambda_{it}\left(e^{\tilde{z}_{it}(T_{g(i)t})}, e^{\tau_{it}^X(T_{g(i)t})}\right)$$

$$\times \frac{1}{e^{\tau_{it}^X(T_{g(i)t})}} \left((\sigma-1) \frac{\partial \tilde{z}_{it}(T_{g(i)t})}{\partial T_{g(i)t}} - \frac{\partial \tau_{it}^X(T_{g(i)t})}{\partial T_{g(i)t}} - \sum_{X\in\mathcal{X}} (\sigma-1)\alpha^X \frac{\partial \tau_{it}^X(T_{g(i)t})}{\partial T_{g(i)t}} \right) dT_{g(i)t}, \tag{57}$$

$$= \sum_{i=1}^{N_t} \lambda_{it}\left(e^{\tilde{z}_{it}(T_{g(i)t})}, e^{\tau_{it}^X(T_{g(i)t})}\right) \left[\sigma \left(\frac{\partial \tilde{z}_{it}(T_{g(i)t})}{\partial T_{g(i)t}} - \sum_{X\in\mathcal{X}} \alpha^X \frac{\partial \tau_{it}^X(T_{g(i)t})}{\partial T_{g(i)t}} \right) dT_{g(i)t} \right.$$

$$- \sum_{X\in\mathcal{X}} \frac{\alpha^X}{e^{\tau_{it}^X(T_{g(i)t})}} \Omega_t^X\left(e^{\tilde{z}_{it}(T_{g(i)t})}, e^{\tau_{it}^X(T_{g(i)t})}\right)$$

$$\left. \times \left((\sigma-1) \frac{\partial \tilde{z}_{it}(T_{g(i)t})}{\partial T_{g(i)t}} - \frac{\partial \tau_{it}^X(T_{g(i)t})}{\partial T_{g(i)t}} - \sum_{X\in\mathcal{X}} (\sigma-1)\alpha^X \frac{\partial \tau_{it}^X(T_{g(i)t})}{\partial T_{g(i)t}} \right) dT_{g(i)t} \right], \tag{58}$$

$$= \sum_{i=1}^{N_t} \lambda_{it}\left(e^{\tilde{z}_{it}(T_{g(i)t})}, e^{\tau_{it}^X(T_{g(i)t})}\right) \sum_{X\in\mathcal{X}} \frac{\alpha^X}{e^{\tau_{it}^X(T_{g(i)t})}} \Omega_t^X\left(e^{\tilde{z}_{it}(T_{g(i)t})}, e^{\tau_{it}^X(T_{g(i)t})}\right)$$

$$\times \left[\left(\sigma \frac{e^{\tau_{it}^X(T_{g(i)t})}}{\Omega_t^X\left(e^{\tilde{z}_{it}(T_{g(i)t})}, e^{\tau_{it}^X(T_{g(i)t})}\right)} - (\sigma-1) \right) \left(\frac{\partial \tilde{z}_{it}(T_{g(i)t})}{\partial T_{g(i)t}} - \sum_{X\in\mathcal{X}} \alpha^X \frac{\partial \tau_{it}^X(T_{g(i)t})}{\partial T_{g(i)t}} \right) + \frac{\partial \tau_{it}^X(T_{g(i)t})}{\partial T_{g(i)t}} \right]$$

$$\times dT_{g(i)t}; \tag{59}$$

which is exactly the expression in equation (19) in Section (2). We can now follow the strategy as above and differentiate equation (55) to obtain a relation linking changes in efficient aggregate gross output TFP to changes in grid-cell-level temperatures, given by

$$d\log TFP_t^* = \sum_{i=1}^{N_t} \underbrace{\left(\frac{\left(e^{\tilde{z}_{it}(T_{g(i)t})}\right)^{\sigma-1}}{\sum_{i=1}^{N_t}\left(e^{\tilde{z}_{it}(T_{g(i)t})}\right)^{\sigma-1}} \right)}_{\equiv \lambda_{it}^*\left(e^{\tilde{z}_{it}(T_{g(i)t})}\right)} \frac{\partial \tilde{z}_{it}(T_{g(i)t})}{\partial T_{g(i)t}} dT_{g(i)t}, \tag{60}$$

$$= \sum_{i=1}^{N_t} \lambda_{it}^*\left(e^{\tilde{z}_{it}(T_{g(i)t})}\right) \frac{\partial \tilde{z}_{it}(T_{g(i)t})}{\partial T_{g(i)t}} dT_{g(i)t}; \tag{61}$$

which is exactly the expression in equation (20) in Section (2).

A.2 Solow Residual

The model presented in Section 2 has three productive inputs: capital, labor, and materials. This implies that its notion of output is a gross measure, hence, its implied TFP is defined on gross output. However, when normally thinking about productivity as defined by Solow (1957), we think of a concept related to net output, i.e., to GDP. Here, we show how to adjust our measurement to be able to study the effect of climate change on aggregate net output TFP, i.e., on the Solow residual. Our strategy is reminiscent of the insights from Jones (2011).

We start by the definition of GDP, given by

$$GDP_t = Y_t - \frac{P_t^M}{P_t} M_t, \tag{62}$$

$$= TFP_t K^{\alpha^K} L^{\alpha^L} M^{\alpha^M} - \frac{P_t^M}{P_t} M_t; \tag{63}$$

i.e., GDP is defined as gross output net of the aggregate real value of materials. Given equation (63), we can defined the Solow residual as

$$Solow_t = \frac{TFP_t K^{\alpha^K} L^{\alpha^L} M^{\alpha^M} - \frac{P_t^M}{P_t} M_t}{K^{\widehat{\alpha}^K} L^{\widehat{\alpha}^L}}, \tag{64}$$

where $\widehat{\alpha}^K$ and $\widehat{\alpha}^L$ are the aggregate capital and labor elasticities of value added. Taking logs gives

$$\log Solow_t = \log\left(TFP_t K^{\alpha^K} L^{\alpha^L} M^{\alpha^M} - \frac{P_t^M}{P_t} M_t \right) - \log\left(K^{\widehat{\alpha}^K} L^{\widehat{\alpha}^L} \right). \tag{65}$$

Since we are interested in a counterfactual that assesses the implications of a medium- or long-run phenomenon such as climate change, we abstract from the fluctuations in aggregate capital and labor due to it and assume that these two aggregate quantities are fixed in the medium- or long-run, i.e., $K_t = \overline{K}$ and $L_t = \overline{L}$. Notice that this assumption is coherent with the model being in general equilibrium, it just implies that aggregate capital and labor supplies are supplied inelastically. Under these two assumptions, we can differentiate equation (65) and obtain the following:

$$d\log Solow_t = \frac{1}{GDP_t} TFP_t K^{\alpha K} L^{\alpha L} M^{\alpha M} \frac{dTFP_t}{TFP_t} + \frac{\alpha^M}{GDP_t} TFP_t K^{\alpha K} L^{\alpha L} M^{\alpha M} \frac{dM_t}{M_t} - \frac{\frac{P_t^M}{P_t} M_t}{GDP_t} \frac{dM_t}{M_t}, \tag{66}$$

$$= \frac{Y_t}{GDP_t} d\log TFP_t + \alpha^M \frac{Y_t}{GDP_t} d\log M_t - \frac{\frac{P_t^M}{P_t} M_t}{Y_t} \frac{Y_t}{GDP_t} d\log M_t, \tag{67}$$

$$= \frac{Y_t}{GDP_t} \left(d\log TFP_t + \left(\alpha^M - \frac{\frac{P_t^M}{P_t} M_t}{Y_t} \right) d\log M_t \right). \tag{68}$$

The equation (68) says that a percentage change in the Solow residual is proportional to the linear combination of the percentage changes in aggregate gross output TFP and aggregate materials. We further approximate equation (68) by assuming that $\alpha^M - P^M M_t / P_t Y_t$ is close to zero. This assumption is convenient since it allows us to solve the model in closed form.[40] We emphasize two things about this additional assumption: (i) In the likely scenario where the general equilibrium temperature-semielasticity of the aggregate materials is negative, this assumption should be considered conservative because it goes against the effect of temperature on the Solow residual; and (ii) when we test this hypothesis empirically by measuring the difference between α^M and $P^M M_t / P_t Y_t$, we find that it is less than 0.1 in our data.[41] Hence, with this additional assumption at hand, we can derive the following adjustment to our gross

[40] Notice that, while aggregate gross output TFP does not depend on aggregate prices, aggregate materials do depend on them. Therefore, to know their response to changes in temperature we would have to infer the general equilibrium effect of temperature, i.e., their effect on the user cost of capital and wages, which is beyond the scope of our analysis and difficult because of the constraints imposed by the short time frame of our data.

[41] This implies that, even if the temperature-semielasticity of aggregate materials is x, which we consider an unlikely upper bound, given that this is our estimate of partial equilibrium temperature-semielasticity found in Table 2 and that normally general equilibrium effects dampen partial equilibrium estimates, we would lose at *most* 0.1^*x percentage points relative to our main results.

output TFP measure:

$$d \log Solow_t = \frac{Y_t}{GDP_t} d \log TFP_t, \tag{69}$$

which is exactly equation (22) in Section (2).

B Data

B.1 Firm-Level Data

To ensure data quality, we employ firm-level balance sheet information from Orbis, following the data construction and cleaning methodologies outlined by Kalemli-Özcan et al. (2024) and Gopinath et al. (2017). The following steps are implemented: (1) Removal of Missing Information: We drop firm-year observations that have missing data on total assets, operating revenue, sales, and employment. (2) Exclusion of Negative Values: Firms reporting negative values for assets, tangible fixed assets, employment, or sales are excluded from the analysis. (3) Limiting Extreme Values: To enhance the robustness of our findings, we compute three ratios: sales to total assets, employment to total assets, and employment to sales. We then remove observations that fall below the 0.1 percentile or above the 99.9 percentile of the distribution of these ratios. By doing so, we mitigate the potential influence of extreme values on our analysis.

For this specific project, we apply additional filters and exclusions. (1) Removal of Missing Zipcode Information: Firms with missing zipcode information are dropped from the dataset. This ensures that we can accurately associate firms with specific geographic regions. (2) Exclusion of Finance, Insurance, and Utility Sectors: To maintain focus on the sectors relevant to our analysis, we exclude firms operating in the finance and insurance sectors, as well as the utility sector. (3) Exclusion of Firms with Negative Age or Exceeding 100: Firms with negative age or those exceeding 100 years are excluded from the analysis. (4) Time Period Selection: We keep observations from 1999 to 2013.

The final sample used for our analysis consists of approximately 4.3 million observations, representing 1 million unique firms. To account for changes in prices and maintain comparability over time, we deflate operating revenue, material expenditure, and wage bill using gross output price indices at the two-digit industry level, with the base year of 2005 (sourced from the Eurostat database). Additionally, the capital stock is deflated using the economy-wide price of investment goods obtained from the World Development Indicators database. Table B.1 provides an overview of the main variables in our analysis, based on the final Orbis

dataset.

Table B.1: Summary Statistics (1999-2013)

	Sales	Materials	Wage Bill	Employees	Capital	MRPM	MRPL	MRPK
Mean	13.33	11.61	11.66	1.88	11.14	1.72	2.03	2.30
Median	13.34	12.02	11.82	1.79	11.05	1.01	1.77	2.39
Min	5.92	3.55	4.35	0	5.51	-0.04	-0.05	-4.26
Max	17.78	17.32	16.08	5.76	16.68	8.09	7.52	7.27
No. Obs.	4,823,392	4,823,392	3,875,031	2,545,857	4,444,668	4,823,392	3,875,031	4,444,668

Note. Summary statistics of cleaned Orbis dataset between 1999 and 2013. All variables are in logs. All monetary values are deflated using Eurostat two-digit industry price deflators, and capital is deflated using the country-specific price of investment from the World Development Indicators.

B.2 Climate Data

B.2.1 Description of E-OBS data

E-OBS is a land-only gridded daily observational dataset that provides information on precipitation, temperature, sea level pressure, global radiation, wind speed, and relative humidity in Europe.[42] The dataset is derived from meteorological observations collected by the National Meteorological and Hydrological Services (NMHSs) and other data-holding institutes across Europe.

E-OBS is presented on regular latitude-longitude grids with spatial resolutions of 0.1°. It covers a significant portion of the European continent, spanning from northern Scandinavia to southern Spain and extending from Iceland to 40°E in the Russian Federation. Over time, the coverage of E-OBS has progressively expanded since its inception in the 1950s, encompassing a larger area of the European continent due to an increasing number of contributing meteorological stations. The dataset undergoes comprehensive updates twice a year, with provisional monthly updates accessible through the E-OBS website.[43]

Originally developed in 2008 as a validation tool for Europe-wide climate model simulations within the European Union ENSEMBLES project, E-OBS has evolved into a resource for monitoring climate conditions across Europe (Klein Tank et al., 2002). The position of E-OBS in Europe is unique due to its relatively high spatial resolution, daily temporal resolution, multiple variables, and the extensive length of the dataset. The station-level data on which E-OBS is based can be accessed through the webpages of the European Climate Assessment

[42] Official E-OBS website: https://cds.climate.copernicus.eu.
[43] E-OBS monthly updates: http://surfobs.climate.copernicus.eu/dataaccess/access_eobs_months.php.

& Dataset (ECA&D), subject to data permissions.[44]

The dataset is daily, meaning the observations cover a 24-hour period per time step. The specific 24-hour period may vary across regions and data providers. The reason for this is that some data providers measure between midnight to midnight while others might measure from morning to morning. Since E-OBS is an observational dataset, no attempts have been made to adjust the time series for this 24-hour offset. However, it ensures that the largest part of the measured 24-hour period corresponds to the day attached to the time step in E-OBS and ECA&D

B.2.2 Distribution of Meteorological Stations

The station data used in the E-OBS dataset are sourced from 84 participating institutions and encompass over 23,000 meteorological stations. For a considerable number of countries, the number of stations used in the E-OBS dataset represents their complete national network, resulting in a much higher density compared to the station network routinely shared among NMHSs, which forms the basis of other gridded datasets.

Figure B.1: Distribution of Meteorological Station Used by E-OBS

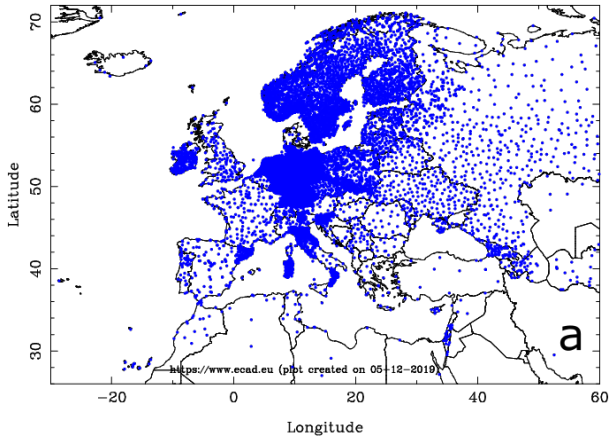

Note. Figure B.1 shows the map with the station coverage in ECA&D which is the basis for the E-OBS precipitation dataset v20.0e.

Figure B.1 presents the distribution of meteorological stations used by E-OBS. This map showcases the station coverage in ECA&D, which serves as the basis for the E-OBS precipitation dataset v20.0e., regardless of their start or stop dates. The figure illustrates the high density of stations in many parts of Europe.

[44]ECA&D website: www.ecad.eu.

B.2.3 Climate Data Summary Statistics

Table B.2 displays the distribution of temperatures and rainfall across Italy and within the average grid-cell of Italy. It reveals significant variation in temperature throughout Italy, ranging from a minimum of -25 degrees Celsius to a maximum of 45 degrees Celsius, with an average temperature of 17 degrees Celsius.

Table B.2: Summary Statistics of Climate Data (1950-2020)

	Overall		Within Grid-Cell	
	Temperatures (°C)	Rainfalls (mm)	Temperatures (°C)	Rainfalls (mm)
Mean	16.88	2.28	16.88	2.28
Median	16.73	0.00	16.50	1.09
Min	-25.43	0.00	-2.60	0.00
Max	45.82	308.20	35.02	31.71

Note. Table 1 shows summary statistics of temperature in degrees Celsius (°C) and rainfalls in millimeters (mm) for the period 1999-2013. The first two columns report statistics for the overall sample. The last two columns report statistics on the variation within the average grid-cell, i.e., they show the average temperature distribution among the different grid-cells.

Examining the variation within grid-cells, which is the crucial one to identify our effects, we find slightly lower but still significant temperature variation. Specifically, the average minimum temperature within grid-cells is -3 degrees Celsius, and the average maximum is 35 degrees Celsius, with an average temperature within grid-cells of 17 degrees Celsius.

B.3 Temperature bins

Table B.3 reports summary statistics on the distribution of the number of days across grid-cells within each temperature bin for the period 1999-2013. Several points can be highlighted from these statistics.

Table B.3: Summary Statistics of Days Within Temperature Bins (1999-2013)

	Temperature Bins				
	$(-\infty, 0°C]$	$(0°C, 30°C]$	$(30°C, 35°C]$	$(35°C, 40°C]$	$(40°C, \infty)$
Mean	1.90	316.10	41.87	5.19	0.04
Median	0	317	43	3	0
Min	0	201	0	0	0
Max	164	365	95	56	10

Note. Table B.3 shows the summary statistics on the number of days across grid-cells within each temperature bin for the period 1999-2013.

First, despite the considerable variation in the data, all temperature bins have a positive number of days on average, with the exception of the bin capturing temperatures above 40

degrees Celsius. This shows that there is some representation for each bin across the grid-cells. Second, there is significant variation within each temperature bin across different grid cells. Even in the reference temperature bin $(0°C, 30°C]$, the number of days ranges from a minimum of 201 to a maximum of 365. This observation underscores the substantial variability present across grid-cells, which is important for our regression analysis. Third, it is worth noting that certain grid-cells exhibit a particularly high number of days with temperatures that are typically considered extreme. For instance, the maximum number of days below 0 degrees Celsius can reach as high as 164. This is not surprising considering Italy's diverse geography, which includes areas in the Alps (in the northern part of Italy) that frequently experience subzero temperatures. Additionally, some grid-cells experience a significant number of days with temperatures above 40 degrees Celsius, with some areas recording up to 10 such days.

C Empirical Results

C.1 Additional Controls and Alternative Independent Variables

In this section of the appendix, we present additional regression models to further validate the extent of the robustness of our results obtained from equation (25).

We start by splitting the $(0°C, 30°C]$ range into two bins: $(0°C, 15°C]$ and $(15°C, 30°C]$. We estimate the effects of temperature relative to the $(15°C, 30°C]$ range and report the results in Table C.4. Our findings indicate that one additional day in the $(0°C, 15°C]$ range increases sales by 0.015%. For the bins common to both distributions, we observe similar semielasticities.

Further, we augment the regression framework in equation (25) with a quadratic control for age. Age it has been shown empirically to be an important predictor of firm-level differences related to demand, productivity, and differences in financial frictions (see Fort et al., 2013; Cloyne et al., 2023; and Colciago et al., 2019). Columns 1, 5, 9, and 13 of Table C.5 and columns 1, 5, and 9 of Table C.6 present the estimates of this specification.

Moreover, we also use alternative functions of daily maximum temperatures over the year, such as the piece-wise linear degree days measure used in Somanathan et al. (2021). The calculation of degree days is best explained with an example. A day with a temperature of 35 degrees Celsius contributes 30 degrees Celsius to the first bin (0°C,30°C], 5 degrees Celsius to the third bin (30°C, 35°C], and 0 degree Celsius to the fourth bin (35°C, 40°C]. Thus, when a single day moves from 35 degrees Celsius to 40 degrees Celsius there is an increase of 5

Table C.4: Average Effect of Temperature on Sales and Inputs

Dependent Variable	**Sales** (1)	**Materials** (2)	**Labor** (3)	**Capital** (4)	**MRPL** (5)	**MRPM** (6)	**MRPK** (7)
Temperature Bins							
$(-\infty, 0°C]$	-0.076***	-0.049**	-0.058**	-0.026	-0.003	-0.012	-0.034
	(0.018)	(0.020)	(0.028)	(0.024)	(0.014)	(0.020)	(0.023)
$(0°C, 15°C]$	0.015*	0.017**	0.009	0.008	-0.009	0.004	-0.003
	(0.009)	(0.007)	(0.012)	(0.008)	(0.006)	(0.007)	(0.010)
$(30°C, 35°C]$	-0.014*	0.006	-0.020	0.004	-0.013**	0.006	-0.015
	(0.009)	(0.008)	(0.013)	(0.011)	(0.006)	(0.008)	(0.010)
$(35°C, 40°C]$	-0.043**	0.001	-0.059**	0.006	-0.023*	0.012	-0.046**
	(0.017)	(0.016)	(0.025)	(0.019)	(0.0125)	(0.014)	(0.021)
$(40°C, +\infty]$	-0.806***	-0.369*	-0.557**	0.034	-0.020	-0.209	-0.579**
	(0.1945)	(0.188)	(0.241)	(0.217)	(0.145)	(0.156)	(0.231)
Fixed Effects							
Firm	✓	✓	✓	✓	✓	✓	✓
Sector × Year	✓	✓	✓	✓	✓	✓	✓
GR and SDC × Region	✓	✓	✓	✓	✓	✓	✓
Controls							
Rainfalls	✓	✓	✓	✓	✓	✓	✓
Region Trends	✓	✓	✓	✓	✓	✓	✓
Observations	4,587,926	4,635,108	3,692,934	4,260,946	3,692,934	4,587,926	4,260,946

Note. All dependent variables are in logs. Temperature bins are defined with greater granularity than in the baseline specification. Rows 1-5 present the effect on the log of the dependent variable of adding an extra day in the given temperature range respectively. Standard errors are clustered at the grid-cell level and reported in parentheses. *, **, and *** denote 10, 5, and 1% statistical significance respectively.

degrees Celsius in the fourth-degree-day bin and no change in other bins.

More formally, denote the endpoints of our five temperature bins by $[T^{1\ell}, T^{2\ell})$, ℓ = 1,2,. . . , 5. A daily temperature T contributes positive degree days to all those bins for which $T > T^{1\ell}$ and zero to all others. If $T \geq T^{2\ell}$, the day contributes $T^{2\ell} - T^{1\ell}$ to bin ℓ. If $T^{1\ell} < T \leq T^{2\ell}$, it contributes $T - T^{1\ell}$ to bin ℓ. We now sum the degree days in each bin over the year to obtain D^{ℓ}_{it} for each unit i and estimate the following model:

$$Outome_{it} = \sum_{\ell} \beta_{\ell} D^{\ell}_{it} + \delta Rain_{g(i)t} + \boldsymbol{\lambda}' \mathbf{X}_{r(i)t} + \gamma_{s(i)t} + \alpha_i + \varepsilon_{it}. \tag{70}$$

Columns 2, 6, 10, and 14 of Table C.5 and columns 2, 6, and 10 of Table C.6 present the estimates of this specification.

Furthermore, we present results from an additional model of daily temperatures where the dependent variable depends on polynomial functions of daily maximum temperature, summed over the year. Denoting by T_{dit} the maximum temperature for firm i on day d of year t, the polynomial specification takes the following form:

$$Outome_{it} = \sum_{d}^{365} \beta_1 T_{dit} + \sum_{d}^{365} \beta_2 T^2_{dit} + \delta Rain_{g(i)t} + \boldsymbol{\lambda}' \mathbf{X}_{r(i)t} + \gamma_{s(i)t} + \alpha_i + \varepsilon_{it}. \tag{71}$$

Columns 3, 9, 15, and 21 of Table C.5 provide and columns 3, 9, and 15 of Table C.6 present the estimates of this specification. Overall, we find patterns qualitatively consistent with our baseline estimates. However, this specification, due to its restrictive parametric assumptions, misses at times some additional effects, particularly for extreme temperatures, highlighting the value added by our semiparametric approach.

Additionally, we also estimate equation (25) allowing for a semiparametric specification of rainfalls instead of the linear baseline one. This allows us to capture the nonlinear effects of rainfall, including the impacts of floods caused by extreme precipitation. We use ten different bins, capturing P10, P20, ..., P100. Columns 4, 10, 16, and 20 of Table C.5 and Columns 4, 10, and 16 of Table C.6 present the estimates of this specification.

Finally, we also estimate equation (25) using the same benchmark definition for temperature bins, but constructing standard errors following Conley (2010) with a radius of 80km and 150km, corresponding to the size of largest NUTS3 and NUTS2 region. Columns 5, 11, 17, and 23 and columns 6, 12, 18, and 2 of Table C.5 and columns 5, 11, and 17 and 6, 12, and 18 of Table C.6 present the estimates of this specification. Estimates remain statistically significant in most cases, even with the very conservative distance of 150 km, considering that Italy covers an area of 301,340km^2, suggesting that our results are robust to considerations of spatial serial correlation.

Tables C.5 and C.6 consistently confirm our main findings through the outlined robustness exercises. Specifically, we observe that extreme temperatures harm sales, materials, and labor, while they do not affect capital substantially. Consequently, the revenue-based marginal products of materials and labor exhibit much sensitivity to extreme temperatures, whereas that of capital does.

Table C.5: Average Effect of Temperature on Sales and Inputs—Robustness

Dependent Variable	Sales						Materials						Labor						Capital					
	(1)	(2)	(3)	(4)	(5)	(6)	(7)	(8)	(9)	(10)	(11)	(12)	(13)	(14)	(15)	(16)	(17)	(18)	(19)	(20)	(21)	(22)	(23)	(24)
Temperature Bins																								
$(-\infty, 0°C]$	-0.088***	0.011**	-0.215***	-0.084***	-0.094***	-0.094***	-0.063**	0.010	-0.228***	-0.061**	-0.068***	-0.068**	-0.065***	0.006	-0.063**	-0.065***	-0.070**	-0.070**	-0.034	-0.001	0.007	-0.035	-0.036	-0.36
	(0.019)	(0.005)	(0.033)	(0.018)	(0.030)	(0.034)	(0.028)	(0.007)	(0.046)	(0.028)	(0.025)	(0.033)	(0.019)	(0.004)	(0.027)	(0.019)	(0.033)	(0.029)	(0.021)	(0.005)	(0.033)	(0.022)	(0.040)	(0.036)
$(30°C, 35°C]$	-0.019**	-0.011***	0.005	-0.013	-0.017	-0.017	-0.024*	-0.012***	-0.007	-0.018	-0.022	-0.022	-0.000	0.001	0.010	0.005	0.002	0.002	0.002	-0.000	0.003	0.004	0.003	0.003
	(0.009)	(0.003)	(0.012)	(0.008)	(0.014)	(0.012)	(0.014)	(0.004)	(0.017)	(0.013)	(0.018)	(0.025)	(0.008)	(0.003)	(0.012)	(0.008)	(0.008)	(0.010)	(0.010)	(0.004)	(0.014)	(0.010)	(0.012)	(0.015)
$(35°C, 40°C]$	-0.043**	-0.019*	-0.018	-0.042**	-0.046*	-0.046	-0.058**	-0.027*	-0.038	-0.055**	-0.060*	-0.060	0.002	-0.006	0.007	0.002	-0.003	-0.003	0.005	-0.008	0.005	0.007	0.004	0.004
	(0.017)	(0.010)	(0.019)	(0.017)	(0.025)	(0.032)	(0.025)	(0.014)	(0.027)	(0.025)	(0.031)	(0.048)	(0.016)	(0.009)	(0.018)	(0.017)	(0.022)	(0.028)	(0.019)	(0.011)	(0.021)	(0.020)	(0.022)	(0.028)
$(40°C, +\infty)$	-0.722***	-0.969***	-0.075**	-0.720***	-0.807**	-0.807**	-0.473**	-0.519*	-0.106**	-0.467*	-0.557	-0.557**	-0.257	-0.438**	-0.004	-0.374*	-0.369**	-0.369*	0.063	0.128	0.009	-0.020	0.033	0.034
	(0.190)	(0.250)	(0.033)	(0.196)	(0.368)	(0.339)	(0.236)	(0.297)	(0.047)	(0.246)	(0.370)	(0.246)	(0.197)	(0.206)	(0.030)	(0.197)	(0.159)	(0.194)	(0.221)	(0.198)	(0.035)	(0.227)	(0.174)	(0.211)
Fixed Effects																								
Firm	✓	✓	✓	✓	✓	✓	✓	✓	✓	✓	✓	✓	✓	✓	✓	✓	✓	✓	✓	✓	✓	✓	✓	✓
Sector × Year	✓	✓	✓	✓	✓	✓	✓	✓	✓	✓	✓	✓	✓	✓	✓	✓	✓	✓	✓	✓	✓	✓	✓	✓
GR and SDC × Region	✓	✓	✓	✓	✓	✓	✓	✓	✓	✓	✓	✓	✓	✓	✓	✓	✓	✓	✓	✓	✓	✓	✓	✓
Controls																								
Rainfalls	✓	✓	✓	✓	✓	✓	✓	✓	✓	✓	✓	✓	✓	✓	✓	✓	✓	✓	✓	✓	✓	✓	✓	✓
Region Trends	✓	✓	✓	✓	✓	✓	✓	✓	✓	✓	✓	✓	✓	✓	✓	✓	✓	✓	✓	✓	✓	✓	✓	✓
Age^2	✓						✓						✓						✓					
Observations	4,687,503	4,687,503	4,687,503	4,687,503	4,687,503	4,687,503	4,687,503	4,687,503	4,687,503	4,687,503	4,687,503	4,687,503	3,767,558	3,767,558	3,767,558	3,767,558	3,767,558	3,767,558	4,328,689	4,328,689	4,328,689	4,328,689	4,328,689	4,328,689

Note. All dependent variables are in logs. Columns 1, 6, 11, and 16 provide estimates from the baseline specification in equation (25), with temperature bins constructed as explained in Section 3.2, augmented with a quadratic age control. Columns 2, 7, 12, and 17 present estimates from the degree-day model in equation (70). Columns 3, 9, 15, and 21 provide estimates from the quadratic specification in equation (71). Columns 4, 10, 16, and 22 provide estimates from the baseline specification in equation (25), with temperature bins constructed as explained in Section 3.2, where rainfall controls are defined semiparametrically by ten bins instead of the linear specification in the benchmark case. Columns 5, 11, 17, and 23 provide estimates from the baseline specification in equation (25), with temperature bins constructed as explained in Section 3.2 but standard errors constructed following Conley (2010) with a radious of 80km. Columns 6, 12, 18, and 24 provide estimates from the baseline specification in equation (25), with temperature bins constructed as explained in Section 3.2 but standard errors constructed following Conley (2010) with a radious of 150km. Rows 1-4 present the effect on the log of the dependent variable of adding an extra day in the given temperature range respectively. Standard errors are clustered at the grid-cell level and reported in parentheses. *, **, and *** denote 10, 5, and 1% statistical significance respectively.

Table C.6: Average Effect of Temperature on Revenue-Based Marginal Products of Inputs—Robustness

Dependent Variable	MRPM						MRPL						MRPK					
	(1)	(2)	(3)	(4)	(5)	(6)	(7)	(8)	(9)	(10)	(11)	(12)	(13)	(14)	(15)	(16)	(17)	(18)
Temperature Bins																		
$(-\infty, 0°C]$	-0.018	-0.000	0.018	-0.016	-0.018	-0.018	0.007	0.000	-0.037*	0.007	0.008	0.008	-0.026	0.005	-0.159***	-0.023	-0.030	-0.030
	(0.019)	(0.005)	(0.024)	(0.019)	(0.020)	(0.019)	(0.013)	(0.003)	(0.021)	(0.013)	(0.015)	(0.007)	(0.022)	(0.004)	(0.036)	(0.022)	(0.038)	(0.030)
$(30°C, 35°C]$	0.006	0.001	0.012	0.006	0.006	0.006	-0.011*	-0.006***	-0.002	-0.012**	-0.012	-0.012	-0.015	-0.008**	0.008	-0.012	-0.014	-0.014
	(0.008)	(0.003)	(0.009)	(0.007)	(0.006)	(0.004)	(0.006)	(0.002)	(0.008)	(0.006)	(0.008)	(0.010)	(0.011)	(0.004)	(0.013)	(0.010)	(0.015)	(0.015)
$(35°C, 40°C]$	0.011	0.005	0.019	0.010	0.011	0.011	-0.022*	-0.002	-0.007	-0.025*	-0.021	-0.021	-0.044**	-0.009	-0.008	-0.046**	-0.045*	-0.045*
	(0.014)	(0.008)	(0.014)	(0.015)	(0.013)	(0.011)	(0.013)	(0.007)	(0.012)	(0.013)	(0.015)	(0.016)	(0.022)	(0.013)	(0.021)	(0.022)	(0.026)	(0.028)
$(40°C, +\infty)$	-0.209	-0.412**	0.032	-0.212	-0.209	-0.209	-0.049	-0.034	-0.018	0.060	-0.019	-0.019	-0.523**	-0.803***	-0.048	-0.443**	-0.578**	-0.578***
	(0.156)	(0.179)	(0.024)	(0.157)	(0.229)	(0.212)	(0.148)	(0.169)	(0.021)	(0.138)	(0.204)	(0.156)	(0.225)	(0.246)	(0.036)	(0.227)	(0.290)	(0.203)
Fixed Effects																		
Firm	✓	✓	✓	✓	✓	✓	✓	✓	✓	✓	✓	✓	✓	✓	✓	✓	✓	✓
Sector × Year	✓	✓	✓	✓	✓	✓	✓	✓	✓	✓	✓	✓	✓	✓	✓	✓	✓	✓
GR and SDC × Region	✓	✓	✓	✓	✓	✓	✓	✓	✓	✓	✓	✓	✓	✓	✓	✓	✓	✓
Controls																		
Rainfalls	✓	✓	✓	✓	✓	✓	✓	✓	✓	✓	✓	✓	✓	✓	✓	✓	✓	✓
Region Trends	✓	✓	✓	✓	✓	✓	✓	✓	✓	✓	✓	✓	✓	✓	✓	✓	✓	✓
Age^2	✓					✓					✓							
Observations	4,687,503	4,687,503	4,687,503	4,687,503	4,687,503	4,687,503	3,767,558	3,767,558	3,767,558	3,767,558	3,767,558	3,767,558	4,328,689	4,328,689	4,328,689	4,328,689	4,328,689	4,328,689

Note. All dependent variables are in logs. Columns 1, 7, and 13 provide estimates from the baseline specification in equation (25), with temperature bins constructed as explained in Section 3.2, augmented with a quadratic age control. Columns 2, 8, and 14 present estimates from the degree-day model in equation (70). Columns 3, 9, and 15 provide estimates from the quadratic specification in equation (71). Columns 4, 10, and 16 provide estimates from the baseline specification in equation (25), with temperature bins constructed as explained in Section 3.2, where rainfall controls are defined semiparametrically by ten bins instead of the linear specification in the benchmark case. Columns 5, 11, and 17 provide estimates from the baseline specification in equation (25), with temperature bins constructed as explained in Section 3.2 but standard errors constructed following Conley (2010) with a radious of 80km. Columns 6, 12, and 18 provide estimates from the baseline specification in equation (25), with temperature bins constructed as explained in Section 3.2 but standard errors constructed following Conley (2010) with a radious of 150km. Rows 1-4 present the effect on the log of the dependent variable of adding an extra day in the given temperature range respectively. Standard errors are clustered at the grid-cell level and reported in parentheses. *, **, and *** denote 10, 5, and 1% statistical significance respectively.

C.2 Additional Sample Cuts

In this section, we present additional sample custs. To mitigate concerns associated with the presence of multiplant firms, as discussed in Section 3.3, we conduct regression analysis where we exclude specific subsets of firms from our sample. First, we exclude all foreign firms, as presented in Columns 1, 6, 11, and 16 of Table C.7 and Columns 1, 6, and 11 of Table C.8. Next, we exclude all listed firms, as displayed in Columns 2, 7, 12, and 17 of Table C.7 and Columns 2, 7, and 12 of Table C.8. Furthermore, we exclude all firms that report consolidated accounts, as illustrated in Columns 3, 8, 13, and 18 of Table C.7 and Columns 3, 8, and 13 of Table C.8. Finally, we drop firms within the top 5 percent of the sales distribution, as depicted in Columns 4, 9, 14, and 19 of Table C.7 and Columns 4, 9, 14 of Table C.8.

Tables C.7 and C.8 consistently indicate that extreme temperatures adversely affect sales, materials, and labor, but not capital. Consequently, the revenue-based marginal products of materials and labor display no systematic sensitivity to extreme temperature fluctuations, in contrast to capital. Notably, our estimates are if anything larger, confirming the downward bias produced by firms more likely to be multiplant. Nevertheless, the consistency of results across these specifications underscores that the presence of multiplant firms does not significantly impact our fundamental conclusions.

Finally, Columns 5, 10, 15, and 20 of Table C.7 and Columns 5, 10, and 15 of Table C.8 include only firm-year observations where none of the revenues, wage bill, material costs, or capital are missing. Although the results are qualitatively similar, the lower number of observations introduces some quantitative differences, particularly with the revenue semi-elasticity for days above 40°C appearing slightly lower.

Table C.7: Average Effect of Temperature on Sales and Inputs—Robustness II

Dependent Variable	**Sales**					**Materials**					**Labor**					**Capital**				
	(1)	(2)	(3)	(4)	(5)	(6)	(7)	(8)	(9)	(10)	(11)	(12)	(13)	(14)	(15)	(16)	(17)	(18)	(19)	(20)
Temperature Bins																				
$(-\infty, 0°C]$	-0.095***	-0.095***	-0.092***	-0.085***	-0.047***	-0.070**	-0.069**	-0.065**	-0.057*	-0.058***	-0.070***	-0.070***	-0.069***	-0.069***	-0.063***	-0.033	-0.036*	-0.037*	-0.035	-0.024
	(0.020)	(0.019)	(0.019)	(0.020)	(0.015)	(0.022)	(0.029)	(0.029)	(0.031)	(0.019)	(0.021)	(0.019)	(0.020)	(0.020)	(0.021)	(0.022)	(0.021)	(0.021)	(0.022)	(0.021)
$(30°C, 35°C]$	-0.017*	-0.017*	-0.017*	-0.018**	-0.009	-0.023	-0.022	-0.020	-0.023	0.005	-0.001	0.002	0.004	0.002	-0.017*	-0.000	0.003	0.004	0.004	0.000
	(0.009)	(0.009)	(0.009)	(0.009)	(0.006)	(0.014)	(0.014)	(0.014)	(0.014)	(0.007)	(0.008)	(0.008)	(0.008)	(0.008)	(0.009)	(0.010)	(0.011)	(0.011)	(0.011)	(0.011)
$(35°C, 40°C]$	-0.050***	-0.046***	-0.047***	-0.045***	-0.019	-0.068**	-0.060**	-0.057**	-0.056**	0.008	-0.010	-0.003	-0.003	-0.004	-0.035*	0.001	0.004	0.006	0.006	0.003
	(0.017)	(0.017)	(0.017)	(0.017)	(0.013)	(0.026)	(0.025)	(0.026)	(0.025)	(0.016)	(0.017)	(0.017)	(0.017)	(0.017)	(0.018)	(0.019)	(0.019)	(0.020)	(0.020)	(0.020)
$(40°C, +\infty)$	-0.827***	-0.806***	-0.829***	-0.889***	-0.357**	-0.571**	-0.560**	-0.554**	-0.645**	-0.343*	-0.433**	-0.367**	-0.363*	-0.456**	-0.121	0.040	0.033	0.024	0.001	0.119
	(0.191)	(0.194)	(0.194)	(0.200)	(0.144)	(0.243)	(0.242)	(0.243)	(0.254)	(0.181)	(0.194)	(0.187)	(0.190)	(0.195)	(0.211)	(0.204)	(0.216)	(0.220)	(0.211)	(0.235)
Fixed Effects																				
Firm	✓	✓	✓	✓	✓	✓	✓	✓	✓	✓	✓	✓	✓	✓	✓	✓	✓	✓	✓	✓
Sector × Year	✓	✓	✓	✓	✓	✓	✓	✓	✓	✓	✓	✓	✓	✓	✓	✓	✓	✓	✓	✓
GR and SDC × Region	✓	✓	✓	✓	✓	✓	✓	✓	✓	✓	✓	✓	✓	✓	✓	✓	✓	✓	✓	✓
Controls																				
Rainfalls	✓	✓	✓	✓	✓	✓	✓	✓	✓	✓	✓	✓	✓	✓	✓	✓	✓	✓	✓	✓
Region Trends	✓	✓	✓	✓	✓	✓	✓	✓	✓	✓	✓	✓	✓	✓	✓	✓	✓	✓	✓	✓
Observations	4,463,602	4,685,250	4,603,410	4,394,813	3,653,159	4,463,602	4,685,250	4,603,410	4,394,813	3,653,159	4,463,602	4,685,250	4,603,410	4,394,813	3,653,159	4,463,602	4,685,250	4,603,410	4,394,813	3,653,159

Note. All dependent variables are in logs. Columns. Columns 1, 6, 11, and 16 provide estimates from the baseline specification in equation (25) excluding foreign firms. Columns 2, 7, 12, and 17 provide estimates from the baseline specification in equation (25) excluding listed firms. Columns 3, 8, 13, and 18 provide estimates from the baseline specification in equation (25) excluding firms reporting consolidated accounts. Columns 4, 9, 14, and 19 provide estimates from the baseline specification in equation (25) excluding firms with sales above top 5%. Columns 5, 10, 15, and 20 provide estimates from the baseline specification in equation (25) but the sample has been restricted to ensure consistency in number of observations across all variables. Rows 1-4 present the effect on the log of the dependent variable of adding an extra day in the given temperature range respectively (temperature bin coefficients). Standard errors are clustered at the grid-cell level and reported in parentheses. *, **, and *** denote 10, 5, and 1% statistical significance respectively.

Table C.8: Average Effect of Temperature on Revenue-Based Marginal Products of Inputs—Robustness II

Dependent Variable	**MRPM**					**MRPL**					**MRPK**				
	(1)	(2)	(3)	(4)	(5)	(6)	(7)	(8)	(9)	(10)	(11)	(12)	(13)	(14)	(15)
Temperature Bins															
$(-\infty, 0°C]$	-0.016	-0.018	-0.019	-0.021	0.015	0.005	0.008	0.009	0.014	0.010	-0.034	-0.030	-0.027	-0.025	-0.021
	(0.020)	(0.019)	(0.020)	(0.021)	(0.014)	(0.014)	(0.013)	(0.013)	(0.014)	(0.013)	(0.023)	(0.022)	(0.022)	(0.024)	(0.021)
$(30°C, 35°C]$	0.007	0.006	0.004	0.006	0.007	-0.010*	-0.012**	-0.012**	-0.011*	-0.013**	-0.012	-0.014	-0.014	-0.015	-0.009
	(0.007)	(0.008)	(0.008)	(0.008)	(0.006)	(0.006)	(0.006)	(0.006)	(0.006)	(0.005)	(0.010)	(0.010)	(0.010)	(0.011)	(0.010)
$(35°C, 40°C]$	0.014	0.011	0.007	0.009	0.014	-0.021	-0.021	-0.022*	-0.017	-0.025**	-0.046**	-0.045**	-0.048**	-0.048**	-0.026
	(0.015)	(0.014)	(0.015)	(0.015)	(0.011)	(0.013)	(0.013)	(0.013)	(0.014)	(0.013)	(0.020)	(0.021)	(0.022)	(0.022)	(0.021)
$(40°C, +\infty)$	-0.220	-0.206	-0.234	-0.217	-0.196	-0.016	-0.020	-0.017	0.001	-0.004	-0.638***	-0.579**	-0.583**	-0.604***	-0.482**
	(0.160)	(0.156)	(0.162)	(0.164)	(0.147)	(0.148)	(0.145)	(0.149)	(0.152)	(0.142)	(0.217)	(0.231)	(0.239)	(0.229)	(0.212)
Fixed Effects															
Firm	✓	✓	✓	✓	✓	✓	✓	✓	✓	✓	✓	✓	✓	✓	✓
Sector × Year	✓	✓	✓	✓	✓	✓	✓	✓	✓	✓	✓	✓	✓	✓	✓
GR and SDC × Region	✓	✓	✓	✓	✓	✓	✓	✓	✓	✓	✓	✓	✓	✓	✓
Controls															
Rainfalls	✓	✓	✓	✓	✓	✓	✓	✓	✓	✓	✓	✓	✓	✓	✓
Region Trends	✓	✓	✓	✓	✓	✓	✓	✓	✓	✓	✓	✓	✓	✓	✓
Observations	4,463,602	4,685,250	4,603,410	4,394,813	3,576,070	3,576,070	3,765,341	3,687,667	3,480,405	3,576,070	4,120,335	4,326,444	4,246,524	4,040,241	3,576,070

Note. All dependent variables are in logs. Columns provide estimates from the baseline specification in equation (25). Columns 1, 6, and 11 estimate from the baseline specification in equation (25) excluding foreign firms. Columns 2, 7, and 12 provide estimates from the baseline specification in equation (25) excluding listed firms. Columns 3, 8, and 13 provide estimates from the baseline specification in equation (25) excluding firms reporting consolidated accounts. Columns 4, 9, and 14 provide estimates from the baseline specification in equation (25) excluding firms with sales above top 5%. Columns 5, 10, and 15 provide estimates from the baseline specification in equation (25) but the sample has been restricted to ensure consistency in number of observations across all variables. Rows 1-4 present the effect on the log of the dependent variable of adding an extra day in the given temperature range respectively (temperature bin coefficients). Standard errors are clustered at the grid-cell level and reported in parentheses. *, **, and *** denote 10, 5, and 1% statistical significance respectively.

C.3 Additional Demand-Adjusted Productivity Results

Table C.9 presents sector-level losses in demand-adjusted productivity due to a 2-degree Celsius increase in temperature.

Table C.9: Sector-Level Demand-Adjusted Productivity Losses

Sector	NACE 1	Sector-level loss	α^K
Services	G-S	-0.35	0.05
Manufacturing	C	-0.37	0.07
Construction	F	-0.38	0.08
Mining and Quarrying	B	-0.46	0.21
Agriculture, Forestry and Fishing	A	-0.51	0.27

Note. Table C.9 presents sector-level losses in demand-adjusted productivity due to a 2-degree Celsius increase in temperature. Column 1 lists the sector names, Column 2 provides the corresponding NACE codes, Column 3 shows the loss levels, and Column 4 indicates the capital intensity.

To obtain these numbers, we applied equation (11) using our estimates from Tables 2 and 3, along with the sector-level production function elasticities as explained in Section 3. For conciseness, we report a single number summarizing the sector-level losses. This was done by applying the temperature bin-specific semiparametric losses for each sector to the homogeneous 2-degree Celsius temperature increase from our benchmark scenario explained in Section 6.1.1. Our losses are broadly in line with those reported in the literature, such as the high damages to agriculture and lower damages for manufacturing noted by Addoum et al. (2020) and Ponticelli et al. (2023).

D Aggregate Results

D.1 Counterfactual Temperature Distributions

This appendix describes the counterfactual distribution of days within temperature bins under different warming scenarios compared to the observed data. Table D.10 provides summary statistics of the distribution of days within temperature bins, while Table D.11 presents the changes in the distribution of days under each warming scenario.

Table D.10 summarizes the distribution of days within temperature bins for the observed data and various warming scenarios. The temperature bins are categorized from below 0 degrees Celsius to 40 degrees Celsius or higher, as explained in Section 3.2. The table includes statistical measures such as mean, median, minimum, and maximum values for each temperature bin.

Table D.10: Summary Statistics of Counterfactual Distribution of Days Within Temperature Bins

		Temperature Bins				
		$(-\infty, 0°C]$	$(0°C, 30°C]$	$(30°C, 35°C]$	$(35°C, 40°C]$	$(40°C, +\infty)$
Warming Scenario	*Variable*					
1999-2013	Mean	1.90	316.10	41.87	5.08	0.04
	Median	0	317	44	3	0
	Min	0	201	0	0	0
	Max	164	365	95	56	10
1°C	Mean	1.14	304.04	50.38	9.31	0.13
	Median	0	304	51	6	0
	Min	0	212	0	0	0
	Max	153	365	105	64	17
2°C	Mean	0.66	291.22	57.53	15.18	0.41
	Median	0	289	59	11	0
	Min	0	221	0	0	0
	Max	140	365	105	70	32
4°C	Mean	0.23	265.02	65.142	32.06	2.55
	Median	0	264	65	31	1
	Min	0	198	0	0	0
	Max	111	365	117	87	52
RCP4.5	Mean	0.83	298.21	57.89	16.37	0.7
	Median	0	289	59	11	0
	Min	0	208	0	0	0
	Max	142	365	113	74	37
RCP8.5	Mean	0.30	265.37	64.46	31.92	2.95
	Median	0	266	65	30	0
	Min	0	190	0	0	0
	Max	104	365	122	92	58

Note. Table D.10 summarizes the distribution of days within temperature bins in the data and under different warming scenarios. It includes statistics such as mean, median, minimum, and maximum values for each temperature bin. The temperature bins range from below 0 degrees Celsius to 40 degrees Celsius or higher as defined in Section 3.2.

The first four rows present the distribution of days within each temperature bin in the data for the period 1999-2013. The second four rows present the distribution of days within each temperature bin for the 1-degree Celsius temperature increase counterfactual scenario. The third four rows present the distribution of days within each temperature bin for the 2-degree Celsius temperature increase counterfactual scenario. The fourth four rows present the distribution of days within each temperature bin for the 4-degree Celsius temperature increase counterfactual scenario. The fifth four rows present the distribution of days within each temperature bin for the RCP4.5 counterfactual scenario. The sixth four rows present the distribution of days within each temperature bin for the RCP8.5 counterfactual scenario. Overall, we see that the more extreme the counterfactual warming scenario, the larger the shift in the number of days toward higher temperatures.

Table D.11 presents the changes in the distribution of days within temperature bins under different warming scenarios. The values indicate the deviation in the number of days

Table D.11: Summary Statistics of Counterfactual Change in Distribution of Days Within Temperature Bins

		Temperature Bins				
		$(-\infty, 0°C]$	$(0°C, 30°C]$	$(30°C, 35°C]$	$(35°C, 40°C]$	$(40°C, +\infty)$
1°C	Mean	-0.76	-12.07	8.51	4.23	0.09
	Median	0	-12	9	3	0
	Min	-27	-33	-21	-2	0
	Max	0	27	33	25	10
2°C	Mean	-1.24	-24.88	15.66	10.10	0.37
	Median	0	-251	17	8	0
	Min	-56	-64	-31	-10	0
	Max	0	56	57	39	22
4°C	Mean	-1.67	-51.09	23.27	26.98	2.51
	Median	0	-52	24	27	1
	Min	-84	-100	-48	-15	0
	Max	0	84	86	71	44
RCP4.5	Mean	-1.07	-26.89	16.02	11.28	0.66
	Median	0	-24	16	8	0
	Min	-71	-79	-41	-10	0
	Max	0	71	70	57	35
RCP8.5	Mean	-1.60	-50.82	22.59	26.83	2.91
	Median	0	-51	23	25	0
	Min	-100	-120	-49	-22	0
	Max	0	101	100	85	56

Note. Table D.11 presents the changes in the distribution of days within temperature bins under various warming scenarios. It provides statistical measures such as mean, median, minimum, and maximum values for each temperature range. The values indicate the deviation in the number of days compared to the data. Negative values indicate a decrease, while positive values represent an increase in the number of days.

compared to the observed data. Negative values represent a decrease, while positive values indicate an increase in the number of days.

The first four rows present the change relative to the data in the distribution of days within each temperature bin for the 1-degree Celsius temperature increase counterfactual scenario. The second four rows present the change relative to the data in the distribution of days within each temperature bin for the 2-degree Celsius temperature increase counterfactual scenario. The third four rows present the change relative to the data in the distribution of days within each temperature bin for the 4-degree Celsius temperature increase counterfactual scenario. The fourth four rows present the change relative to the data in the distribution of days within each temperature bin for the RCP4.5 counterfactual scenario. The fifth four rows present the change relative to the data in the distribution of days within each temperature bin for the RCP8.5 counterfactual scenario. Overall, we see that the more extreme the counterfactual warming scenario, the larger the increase in the number of days with higher temperatures and the decline in the number of days with lower temperatures.

D.2 Additional Robustness Main Results

Table D.12: Climate Change Impact on Aggregate Productivity With Adaptation

	Aggregate Productivity Loss	
	Without Adaptation	*With Adaptation*
1°C	0.77%	0.60%
4°C	6.82%	5.51%
RCP4.5	1.64%	1.32%
RCP8.5	5.35%	4.18%

Note. Column 1 reports the aggregate productivity losses without adaptation for the scenarios in the robustness exercises in Table 7. Column 2 reports the effect of adding adaptation effects to each of these scenarios.

Table D.12 presents the impact of controlling for adaptation on the scenarios used as robustness exercises in Section 6.1.2. Introducing adaptation in the 1-degree Celsius scenario reduces productivity losses to 0.60, and in the 4-degree Celsius scenario, it decreases losses to 5.51. Finally, adaptation reduces productivity losses from the RCP4.5 and RCP8.5 scenarios to 1.32 and 4.18, respectively. Overall, we find that adaptation lowers the aggregate productivity losses of the different scenarios by an average of 20 percent.

Aggregation with a Representative firm: Following Zhang et al. (2018), we use a representative firm to compute the aggregate effects. First, we calculate the firm-specific predicted changes in the number of days in each temperature bin for a 2°C temperature rise scenario. These firm-specific differences in weather variables are then averaged to create a representative firm. Next, we multiply these predicted differences by the relevant estimated regression coefficients to determine the impacts of climate change on output for the average firm in the sample. We find that revenues for representative firms decrease by 1.02%, while total factor productivity (TFP) declines by 0.5%. The differences can be attributed to the fact that the aggregate of a nonlinear function leads to different outcomes than the averages due to the Jensen Inequality. These biases grow with the skewness of the productivity distribution. Further, due to the absence of the allocative efficiency channel, the losses are smaller in the representative firm approach.

D.3 Regional Heterogeneity

This appendix section explores the impact of climate change on productivity losses at the province level (NUTS 3) in Italy, examining four alternative warming scenarios: a 1-degree Celsius increase, a 4-degree Celsius increase, and increases according to the RCP4.5 and

RCP8.5 scenarios. Moreover, we explore the role of adaptation for regional economic losses. We employ the methodology described in Section 2 and apply the same approach used in Section 6.3 to assess productivity losses for each province under these different warming scenarios.

Figure D.2: Regional Productivity Losses for Alternative Warming Scenarios

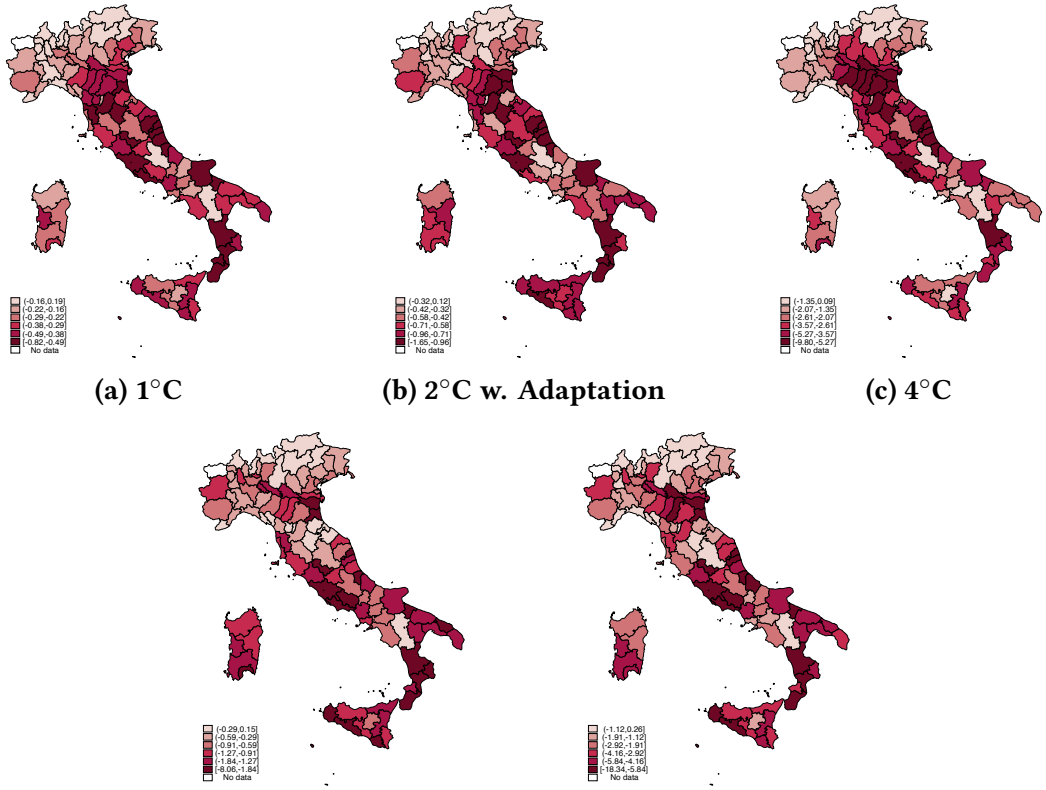

(a) 1°C **(b) 2°C w. Adaptation** **(c) 4°C**

(d) RCP4.5 **(e) RCP8.5**

Note. Figure D.2a shows the productivity losses across NUTS 3 regions due to a 1-degrees Celsius increase in temperature, calculated using equation (19), adjusted with the ratio of gross output to value added. Figure D.2b shows the productivity losses across NUTS 3 regions due to the 2-degrees Celsius increase in temperature but in the presence of adaptation, calculated using equation (19), adjusted with the ratio of gross output to value added. Figure D.2c shows the productivity losses across NUTS 3 regions due to a 4-degrees Celsius increase in temperature, calculated using equation (19), adjusted with the ratio of gross output to value added. Figure D.2d shows the productivity losses across NUTS 3 regions due to the RCP4.5 scenario, calculated using equation (19), adjusted with the ratio of gross output to value added. Figure D.2e shows the productivity losses across NUTS 3 regions due to the RCP8.5 scenario, calculated using equation (19), adjusted with the ratio of gross output to value added. Productivity losses are in percent, and darker colors represent larger losses.

Figures D.2a, D.2c, D.2d, D.2e, and D.2b display regional productivity changes under various warming scenarios. In the 1-degree Celsius warming scenario (D.2a), Italian provinces show diverse outcomes, with some experiencing gains of up to 0.19 percent and others facing losses of up to 0.82 percent. Under the 4-degree Celsius scenario (D.2c), variations are even more pronounced, ranging from slight increases of 0.09 percent to severe reductions of up to

9.80 percent. The RCP4.5 and RCP8.5 scenarios (D.2d, D.2e) also exhibit varying degrees of change, with some provinces seeing gains and others facing losses, particularly severe under RCP8.5, reaching -13.23 percent. The RCP4.5 and RCP8.5 scenarios exhibit the most significant regional variations due to the non-uniform distribution of temperature increases, predicting larger in southern regions compared to the north. In the 2-degree Celsius warming scenario with adaptation (D.2b), regional differences persist, with increases of 1.55 percent in the least affected areas and decreases of 2.80 percent in the most affected ones.

The relationship between GDP per capita in our sample and future productivity losses is depicted in Figure D.3. With the exception of the 4-degree Celsius scenario, which shows no significant relation, all other scenarios predict increasing inequality due to climate change.

Figure D.3: Correlation Between Regional Losses and GDP Per Capita

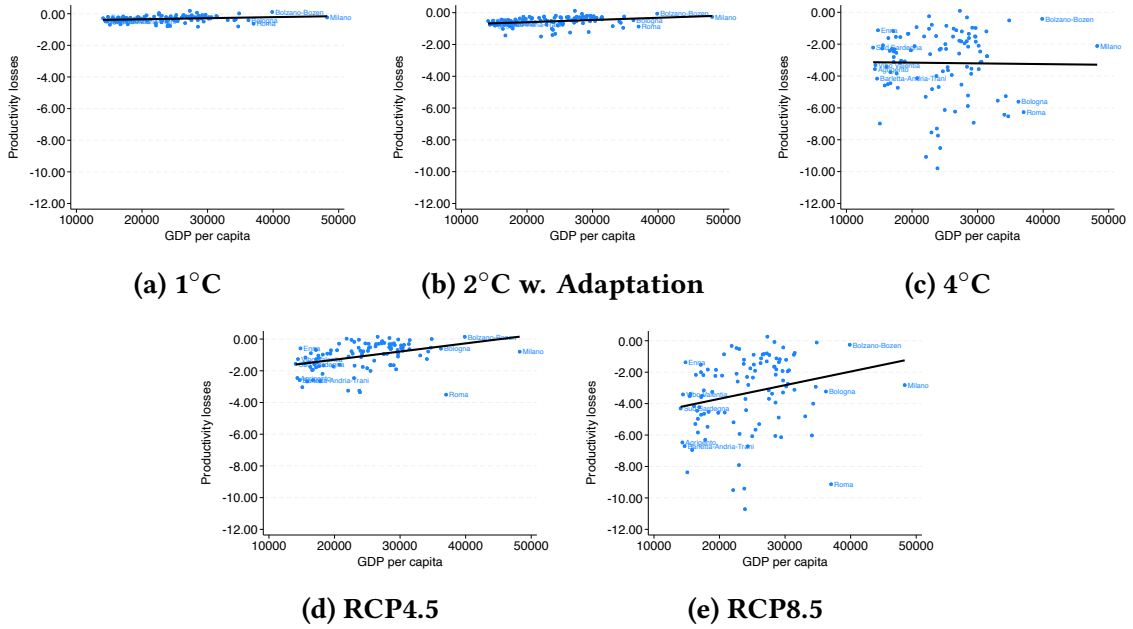

(a) 1°C **(b) 2°C w. Adaptation** **(c) 4°C**

(d) RCP4.5 **(e) RCP8.5**

Note. Figure D.3a scatters the productivity losses across NUTS 3 regions due to a 1-degrees Celsius increase in temperature against GDP per capita in the data. Figure D.3b shows the productivity losses across NUTS 3 regions due to a 2-degrees Celsius increase in temperature in the presence of adaptation against GDP per capita in the data. Figure D.3c scatters the productivity losses across NUTS 3 regions due to a 4-degrees Celsius increase in temperature against GDP per capita in the data. Figure D.3d scatters the productivity losses across NUTS 3 regions due to a the RCP4.5 scenario against GDP per capita in the data. Figure D.3e scatters the productivity losses across NUTS 3 regions due to the RCP8.5 scenario against GDP per capita in the data. Light blue dots are NUTS 3 regions and the black line represents the best fit.

Acknowledgements

We thank Matteo Alpino, Lint Barrage, Andrew Bernard, Douglas Gollin, Banu Demir, Maarten De Ridder, Dave Donaldson, Farid Farrokhi, Stephie Fried, Kerem Cosar, Jeremy Majerovitz, Asier Mariscal, Eduardo Morales, Ishan Nath, Michael Peters, Sophie Piton, Stephen Redding, Richard Rogerson, Federico Rossi, Karthik Sastry, Anant Sudarshan, Lucian Taylor, Rick Van Der Ploeg, John Van Reenen, Christopher Woodruff, and the conference participants of the Finpro-CEPR Rome, BSE Summer Forum, ENRI meeting in Luxembourg, EEA, London Junior Macro, LSE Environment Week, Lancaster Climate Change and Global Economy, Tilburg Growth International Finance and Trade, University of Mannheim conference and seminar participants at CREST-ENSAI, Princeton, Duke, ESADE, Illinois Urbana-Champaign, Oxford, CREI, Houston, Virginia, University of Barcelona, ETH CEPE, IMF, San Francisco Fed, New York Fed, CERGE-EI, University of Oslo, NYU Abu Dhabi for useful comments and suggestions. We thank Robert Wojciechowski for his excellent research assistance. We thank Antoine Gervais for sharing his tradability data with us. We acknowledge financial support from the EIBURS grant on “Intangibles, Technology Diffusion and Public Policies: Implications for Firm Investment, Market Structure and Aggregate Productivity”.

Andrea Caggese
Universitat Pompeu Fabra, Barcelona, Spain; Barcelona School of Economics, Barcelona, Spain; Centre de Recerca en Economia Internacional, Barcelona, Spain; email: andrea.caggese@upf.edu

Andrea Chiavari
University of Oxford, oxford, United Kingdom; email: andrea.chiavari@economics.ox.ac.uk

Sampreet Singh Goraya
Stockholm School of Economics, Stockholm, Sweden; email: sampreet.goraya@hhs.se

Carolina Villegas-Sanchez
ESADE Business School, Barcelona, Spain; Universitat Ramon Llull, Barcelona, Spain; European Central Bank, Frankfurt am Main, Germany; Centre for Economic Policy Research, London, United Kingdom; email: carolina.villegas@esade.edu

Postal address 60640 Frankfurt am Main, Germany
Telephone +49 69 1344 0
Website www.ecb.europa.eu

PDF ISBN 978-92-899-7408-0 ISSN 1725-2806 doi:10.2866/5686477 QB-01-25-181-EN-N